Laser-driven plasma wakefield acceleration

(LWFA)

Lecture overview

- What is a laser-driven plasma wakefield accelerator?
- Fundamentals of plasma waves
  - 1D fluid description of laser generated plasma waves
  - Energy gain in the wakefield
  - Relativistic effects
  - Particle trapping
- Full 3D description
  - Particle-in-cell simulations
  - High intensity plasma wakefields – the bubble regime
  - Plasma optics in a wakefield
  - Self-injection in the bubble regime
  - Controlled injection techniques
- Measurements of electron bunch properties
- LWFA as a photon source
  - Plasma wiggler radiation
  - Inverse Compton scattering
  - Applications in quantum electrodynamics

- Plasma has been considered for particle acceleration since **1956** [1]
- Plasma waves generated with laser using beat-wave mechanism in **1972** [2]
- Seminal paper in **1979** [3] suggesting GV/cm acceleration would be possible with a short intense laser pulse
- Beat-wave (**1993**) [4] and self-modulated (**1995**) [5] laser pulses used to accelerate electrons
- Narrow energy spread beams observed in experiments (**2004**) [6] using short laser pulses
- Electron beam energies now demonstrated in excess of 4 GeV (**2014**) [7]

1. Veksler V.I. Proc. CERN Symp. Pp. 80–83. (1956).
2. Rosenbluth, M. N. & Liu, C. S. Phys. Rev. Lett. 29, 701–705 (1972).
3. Tajima, T. & Dawson, J. M.. Phys. Rev. Lett. 43, 267–270 (1979).
4. Clayton, C. E. et al. Phys. Rev. Lett. 70, 37–40 (1993).
5. Modena, A. et al. Nature 377, 606–608 (1995).
6. Mangles, S. P. D. et al. Nature 431, 535–8 (2004). Faure, J. et al. Nature 431, 541–544 (2004). Geddes, C. G. R. et al. Nature 431, 538–41 (2004).
7. Leemans, W. P. et al. Phys. Rev. Lett. 113, 245002 (2014).

Maximum electron energy roughly scales with laser power

Each point is a published experimental result

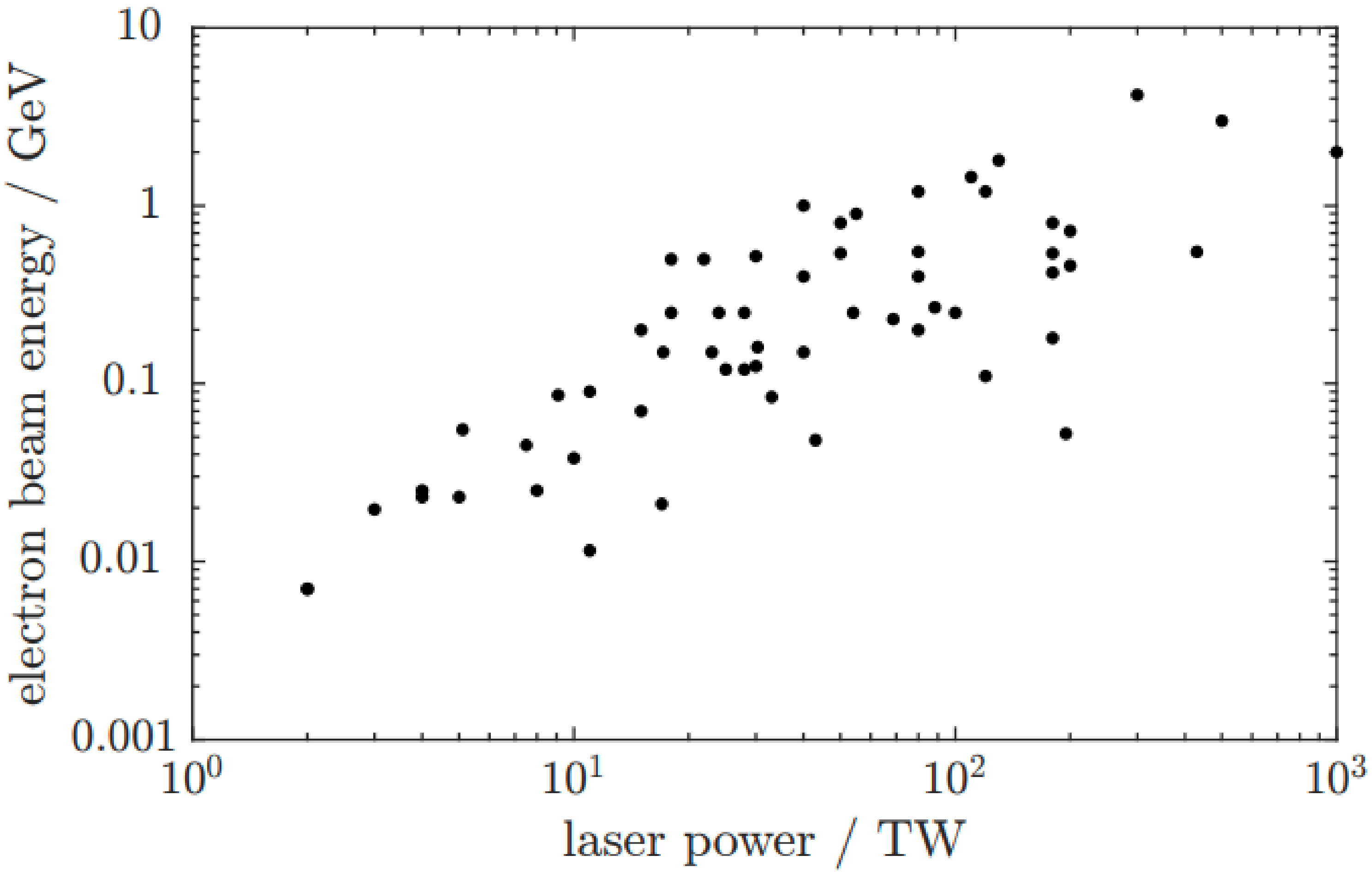

1. Stuart Mangles, Alegro workshop 2018

Plasma wave generation by a laser pulse

- Laser fields drive the electron motion of the plasma wave

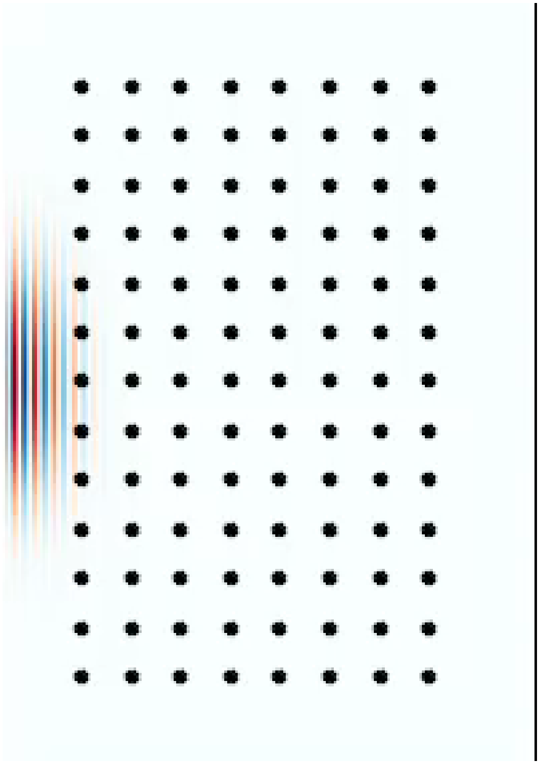

$a_0 = 1$

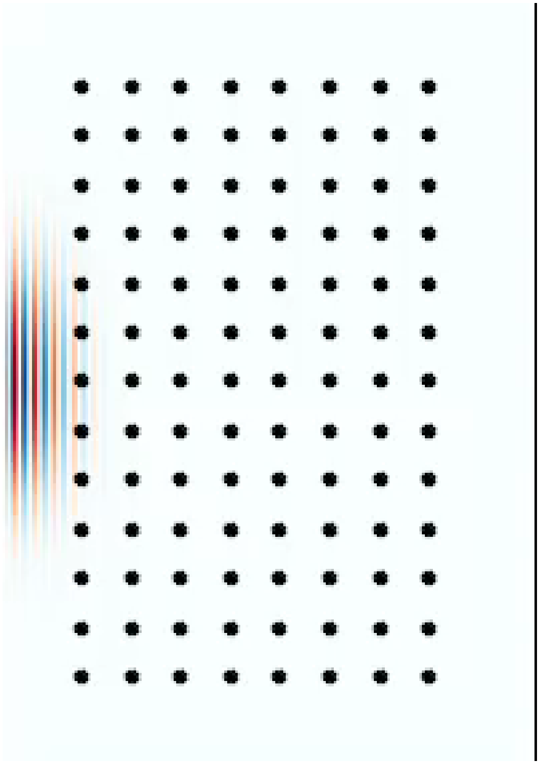

$a_0 = 2$

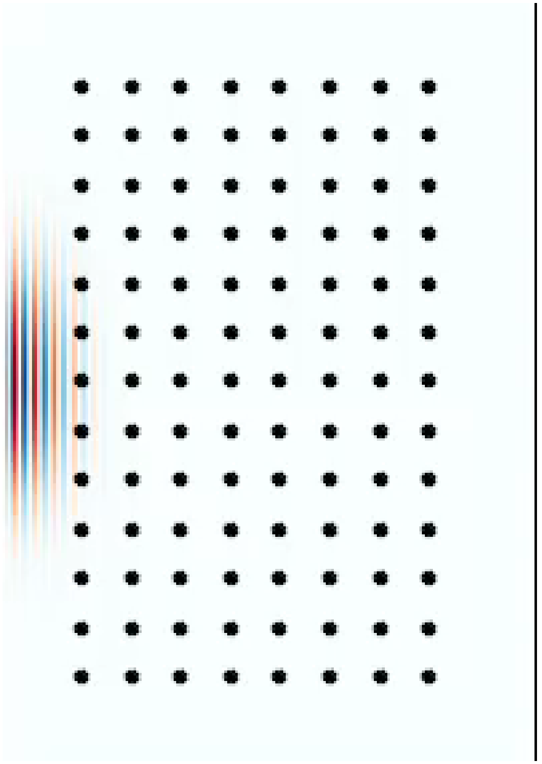

$a_0 = 4$

Increasing the laser intensity changes the wakefield structure

LWFA in the co-moving frame $\xi = z - ct$

- Laser pulse slowly evolves compared to the plasma period
- Self focusing occurs relatively quickly until a matched spot size is reached
- Increase in intensity causes changes in the plasma wake structure
- The laser pulse compresses longitudinally, further increasing the intensity

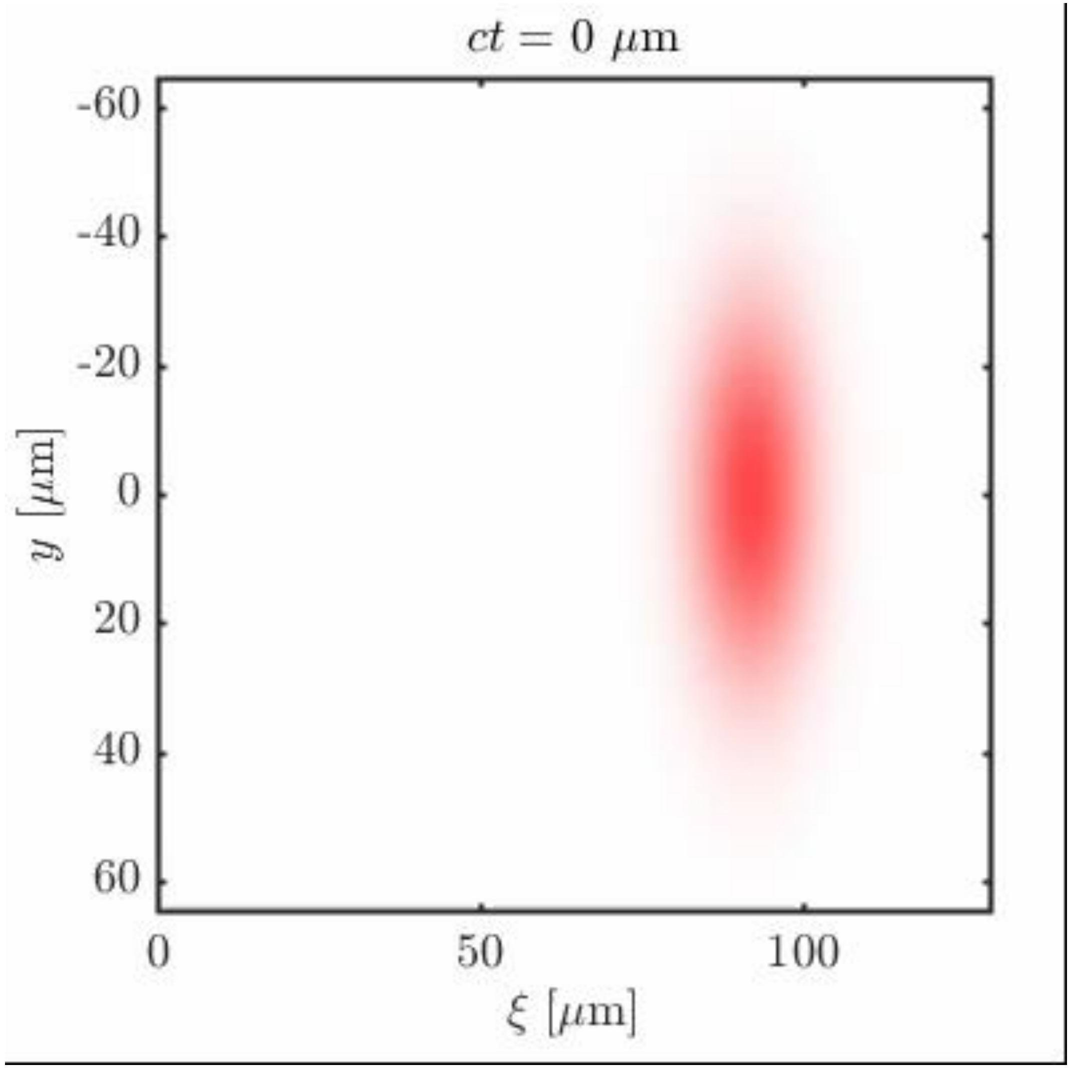

Plasma wave fundamentals

- A(n electron) plasma wave is due to displacement of electrons from their equilibrium position
- In 1D Gauss' law gives an electric field $$E_x = \frac{e n_e D(x)}{\epsilon_0}$$
- The equation of motion is therefore $$\frac{\mathrm{d}^2}{\mathrm{d}t^2} D(x) = -{\omega_p}^2 D(x)$$
- With a solution of the form $$D(x) = D_0 \sin(\omega_p t - k_p x)$$
- Therefore, $D_0 = 1/k_p$ is the maximum displacement, at which the particle velocities equal the speed of light and particle trajectories cross.
- This defines the critical electric field at the threshold of wavebreaking

$$E_{\text{crit}} = \omega_p m_e c / e$$

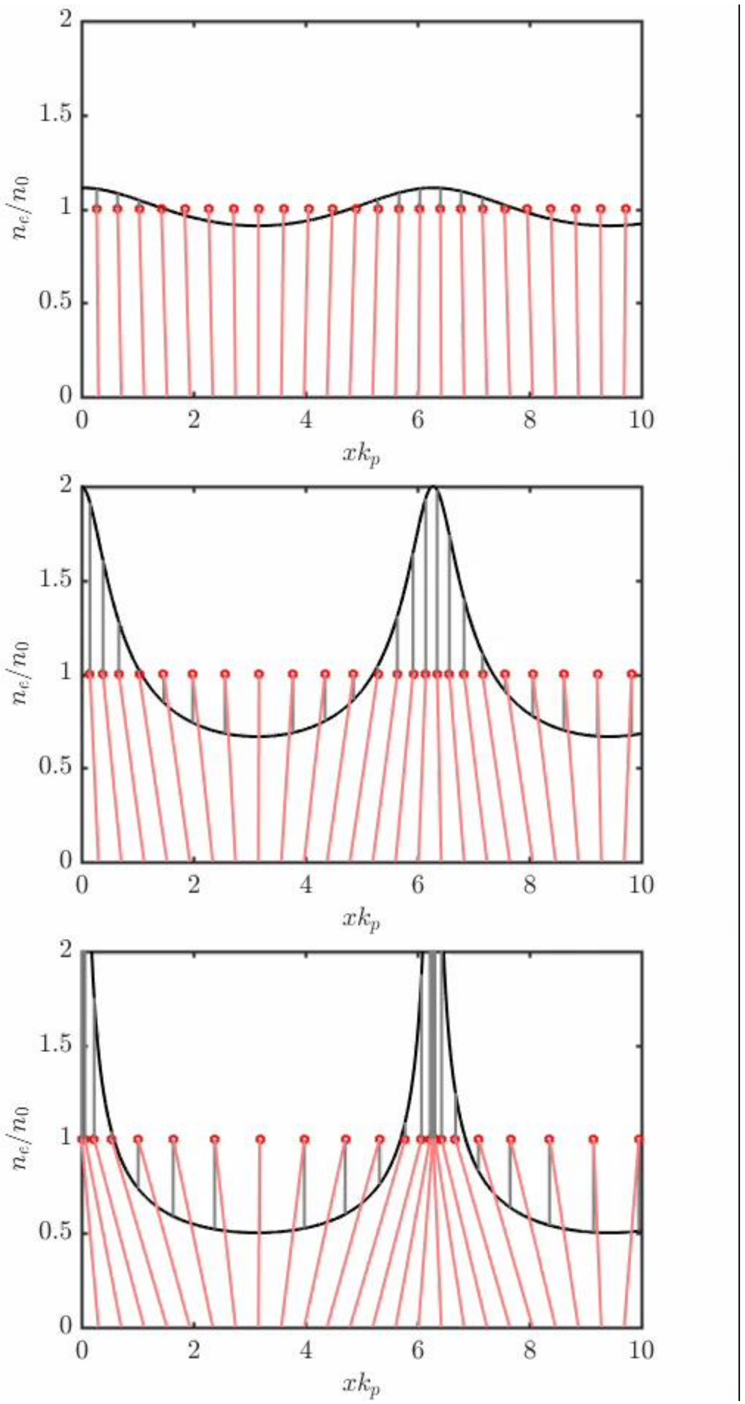

Plasma wave generation by a laser pulse

- 1D(*) Fluid equations for $v \ll c$

$$m_e \left[\frac{\partial \mathbf{v}}{\partial t} + (\mathbf{v} \cdot \nabla) \mathbf{v} \right] = -e \left(\mathbf{E} + \mathbf{v} \times \mathbf{B} \right)$$ Lorentz force

$$\nabla \cdot (n_e \mathbf{v}) = -\frac{\partial n_e}{\partial t}$$ Conservation equation

$$\nabla \cdot \mathbf{E} = -\frac{e \left(n_e - n_i \right)}{\epsilon_0}$$ Gauss' law

(*) 1D means quantities only vary in one dimension vectors (e.g. fields and momenta) can point in all three

Plasma wave generation by a laser pulse

- 1D(*) Fluid equations for $v \ll c$

$$m_e \left[\frac{\partial \mathbf{v}}{\partial t} + (\mathbf{v} \cdot \nabla)\,\mathbf{v}\right] = -e\left(\mathbf{E} + \mathbf{v} \times \mathbf{B}\right)$$

$$\nabla \cdot (n_e \mathbf{v}) = -\frac{\partial n_e}{\partial t}$$

$$\nabla \cdot \mathbf{E} = -\frac{e\,(n_e - n_i)}{\epsilon_0}$$

Linearise with

$$v_\perp = a/c$$

$$n_i = n_0$$

$$n_e = n_0 + \delta n_e$$

$$\longrightarrow$$

$$m_e \frac{\partial v}{\partial t} + eE = -\frac{1}{2} m_e c^2 \frac{\partial a^2}{\partial x}$$

$$n_0 \frac{\partial v}{\partial x} = -\frac{\partial \delta n_e}{\partial t}$$

$$\frac{\partial E}{\partial x} = -\frac{e \delta n_e}{\epsilon_0}$$

(*) 1D means quantities only vary in one dimension vectors (e.g. fields and momenta) can point in all three

Plasma wave generation by a laser pulse

- 1D(*) Fluid equations for $v \ll c$

$$m_e \frac{\partial v}{\partial t} + eE = -\frac{1}{2} m_e c^2 \frac{\partial a^2}{\partial x}$$
$$n_0 \frac{\partial v}{\partial x} = -\frac{\partial \delta n_e}{\partial t}$$
$$\frac{\partial E}{\partial x} = -\frac{e \delta n_e}{\epsilon_0}$$

(*) 1D means quantities only vary in one dimension vectors (e.g. fields and momenta) can point in all three

Plasma wave generation by a laser pulse

- 1D(*) Fluid equations for $v \ll c$

$$m_e \frac{\partial v}{\partial t} + eE = -\frac{1}{2} m_e c^2 \frac{\partial a^2}{\partial x}$$
$$n_0 \frac{\partial v}{\partial x} = -\frac{\partial \delta n_e}{\partial t}$$
$$\frac{\partial E}{\partial x} = -\frac{e \delta n_e}{\epsilon_0}$$

Take derivatives and rearrange $\longrightarrow$

$$m_e \frac{\partial^2 v}{\partial xt} + e \frac{\partial E}{\partial x} = -\frac{1}{2} m_e c^2 \frac{\partial^2 a^2}{\partial x^2}$$
$$m_e \frac{\partial^2 v}{\partial xt} = -\frac{m_e}{n_0} \frac{\partial^2 \delta n_e}{\partial t^2}$$
$$e \frac{\partial E}{\partial x} = -\frac{e^2 \delta n_e}{\epsilon_0}$$

(*) 1D means quantities only vary in one dimension vectors (e.g. fields and momenta) can point in all three

Plasma wave generation by a laser pulse

- 1D(*) Fluid equations for $v \ll c$

$$m_e \frac{\partial^2 v}{\partial xt} + e\frac{\partial E}{\partial x} = -\frac{1}{2} m_e c^2 \frac{\partial^2 a^2}{\partial x^2}$$

$$m_e \frac{\partial^2 v}{\partial xt} = -\frac{m_e}{n_0}\frac{\partial^2 \delta n_e}{\partial t^2}$$

$$e\frac{\partial E}{\partial x} = -\frac{e^2 \delta n_e}{\epsilon_0}$$

(*) 1D means quantities only vary in one dimension vectors (e.g. fields and momenta) can point in all three

Plasma wave generation by a laser pulse

- 1D(*) Fluid equations for $v \ll c$

$$m_e \frac{\partial^2 v}{\partial xt} + e\frac{\partial E}{\partial x} = -\frac{1}{2}m_e c^2 \frac{\partial^2 a^2}{\partial x^2}$$

$$m_e \frac{\partial^2 v}{\partial xt} = -\frac{m_e}{n_0}\frac{\partial^2 \delta n_e}{\partial t^2}$$

$$e\frac{\partial E}{\partial x} = -\frac{e^2 \delta n_e}{\epsilon_0}$$

Substitute into first equation

$$\frac{m_e}{n_0}\frac{\partial^2 \delta n_e}{\partial t^2} + \frac{e^2 \delta n_e}{\epsilon_0} = \frac{1}{2}m_e c^2 \frac{\partial^2 a^2}{\partial x^2}$$

Rearrange

$$\left(\frac{\partial^2}{\partial t^2} + {\omega_p}^2\right)\delta n_e = \frac{n_0 c^2}{2}\frac{\partial^2 a^2}{\partial x^2}$$

Hence, density modulation is a harmonic oscillation driven by the gradient of the ponderomotive potential

(*) 1D means quantities only vary in one dimension vectors (e.g. fields and momenta) can point in all three

Plasma wave generation by a laser pulse

- 1D(*) Fluid equations for $v \ll c$

$$\left(\frac{\partial^2}{\partial t^2} + {\omega_p}^2\right)\delta n_e = \frac{n_0 c^2}{2}\frac{\partial^2 a^2}{\partial x^2}$$

- We can apply the quasi-static approximation, which states that in the co-moving frame the travelling wave appears static (i.e. changes gradually in time compared to the spatial scale)

New coordinates and derivatives

$$\xi = x - ct$$

$$\tau = t$$

$$\frac{\partial}{\partial t} = -c\frac{\partial}{\partial \xi} + \cancel{\frac{\partial}{\partial \tau}}$$

(quasi-static)

$$\frac{\partial}{\partial x} = \frac{\partial}{\partial \xi}$$

1D fluid equation in quasi-static approximation

$$\left(\frac{\partial^2}{\partial \xi^2} + {k_p}^2\right)\delta n_e = \frac{n_0}{2}\frac{\partial^2 a^2}{\partial \xi^2}$$

(*) 1D means quantities only vary in one dimension vectors (e.g. fields and momenta) can point in all three

Plasma wave generation by a laser pulse

1D fluid equation in quasi-static approximation

$$\left(\frac{\partial^2}{\partial \xi^2} + {k_p}^2\right)\delta n_e = \frac{n_0}{2}\frac{\partial^2 a^2}{\partial \xi^2}$$

For a driving pulse $a^2 = \exp(-\xi^2/{\sigma_\xi}^2)$

The driver is resonant for $k_p \sigma_\xi = \sqrt{2}$

In units of time : $\sigma_t = \sqrt{2}/\omega_p$

$k_p \sigma_\xi = \sqrt{2}$

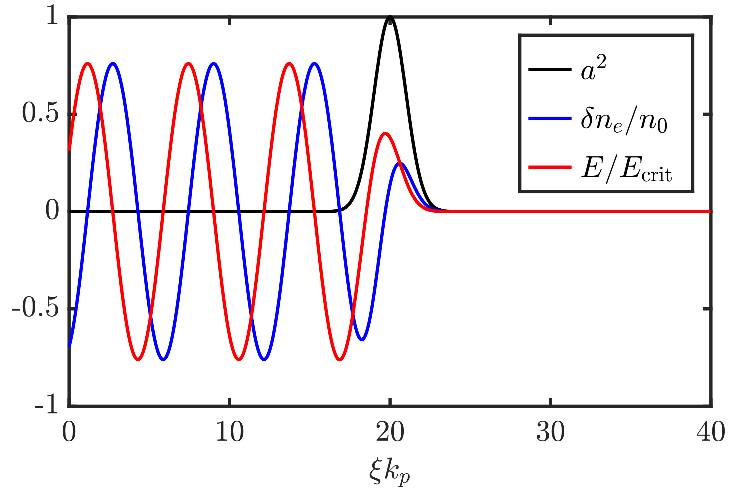

$k_p \sigma_\xi = 3\sqrt{2}$

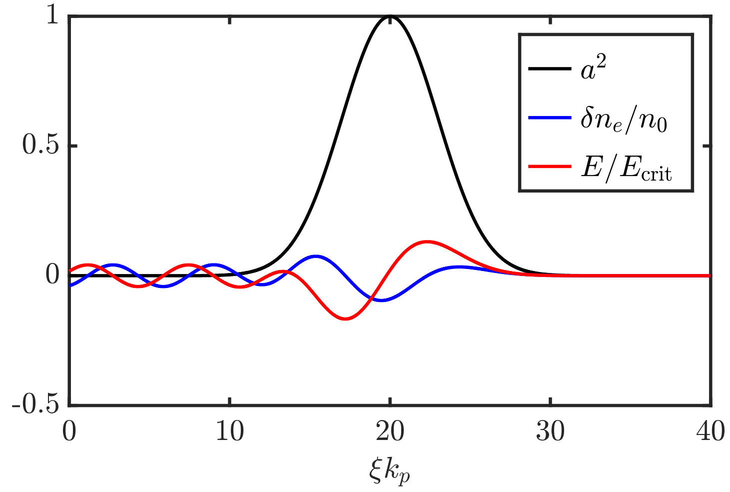

Maximum energy gain limited by dephasing

Phase velocity of the wakefield structure is set by the laser group velocity

$$v_g = c\sqrt{1-(\omega_p/\omega_0)^2}$$

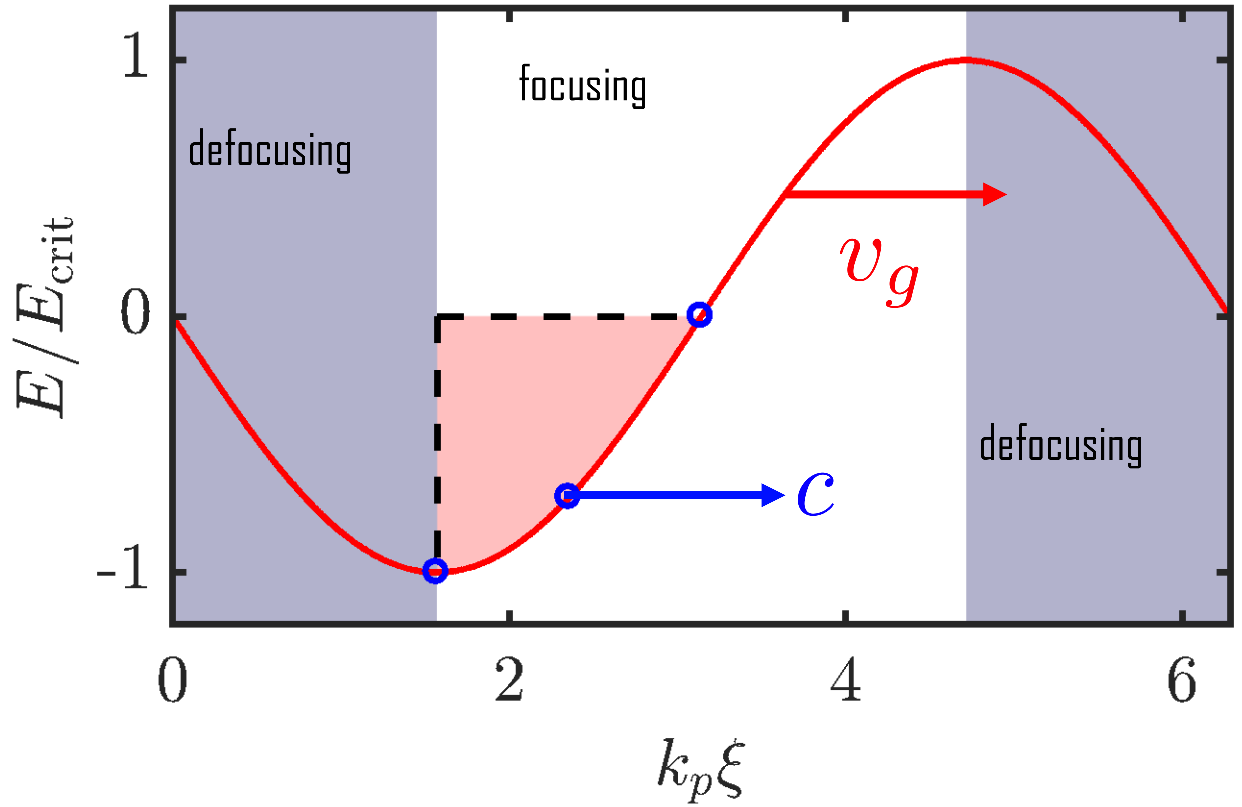

Therefore, a relativistic particle will outrun the accelerating field, after the dephasing length

$$L_{\mathrm{dph}} = c\frac{\Delta x}{\Delta v} = c\frac{\lambda_p}{4c(1-\sqrt{1-(\omega_p/\omega_0)^2})}$$

$$\approx \frac{\lambda_p}{2(\omega_p/\omega_0)^2} = \frac{{\lambda_p}^3}{2{\lambda_0}^2}$$

Assuming $v_e = c$ and $\omega_0 \gg \omega_p$

The maximum energy gain is therefore

$$W_{\max} = \int -eEdx$$

$$= e\frac{2E_{\mathrm{crit}}}{\pi}L_{\mathrm{dph}}$$

$$= 2\frac{{\omega_0}^2}{{\omega_p}^2}m_ec^2 = \frac{2m_e\epsilon_0}{e}\frac{{\omega_0}^2}{n_e}m_ec^2$$

$$= 2{\gamma_\phi}^2m_ec^2$$

Relativistic 1D fluid model

A full relativistic derivation of the 1D fluid model, using a hamiltonian approach results in [1],

$$\frac{\delta n_e}{n_0} = \frac{\partial^2 \Phi}{\partial \xi^2} = {\gamma_\phi}^2 {k_p}^2 \left(\beta_\phi \left[1 - \frac{1 + a^2}{{\gamma_\phi}^2 \left(1 + \Phi\right)^2} \right]^{-1/2} - 1 \right)$$

$$\mathcal{H}(\xi, \gamma) = \gamma(1 - \beta_\phi \beta) - \Phi(\xi)$$

$$\Phi = \phi \frac{e}{m_e c^2}$$

$$\gamma^2 = \left(1 - \beta^2\right)^{-1}$$

$$E = \frac{\mathrm{d}\phi}{\mathrm{d}\xi}$$

$$\gamma_\phi = \left(1 - {\beta_\phi}^2\right)$$

$$\beta_\phi = \sqrt{1 - (\omega_p / \omega_0)^2}$$

1. Esarey, E. & Pilloff, M. "Trapping and acceleration in nonlinear plasma waves"
   Phys. Plasmas 2, 1432–1436 (1995).
   Esarey, E., Schroeder, C. & Leemans, W. "Physics of laser-driven plasma-based electron accelerators"
   Rev. Mod. Phys. 81, 1229–1285 (2009).

Relativistic 1D fluid model

With the assumption $\gamma_\phi \gg 1$

$$\frac{\delta n_e}{n_0} = {k_p}^{-2}\frac{\partial^2 \Phi}{\partial \xi^2} = \frac{1+a^2}{2\left(1+\Phi\right)^2} - \frac{1}{2}$$

In general this must be solved numerically, but allows us to study plasma waves for $a \sim 1$

As well as increasing the plasma wave amplitude, we also see an increase in plasma wavelength due to relativistic effects

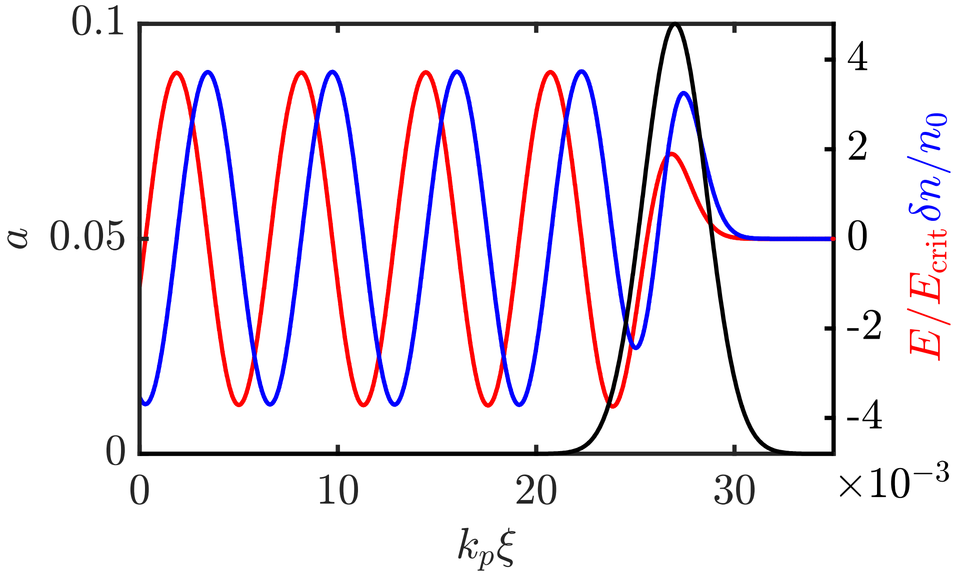

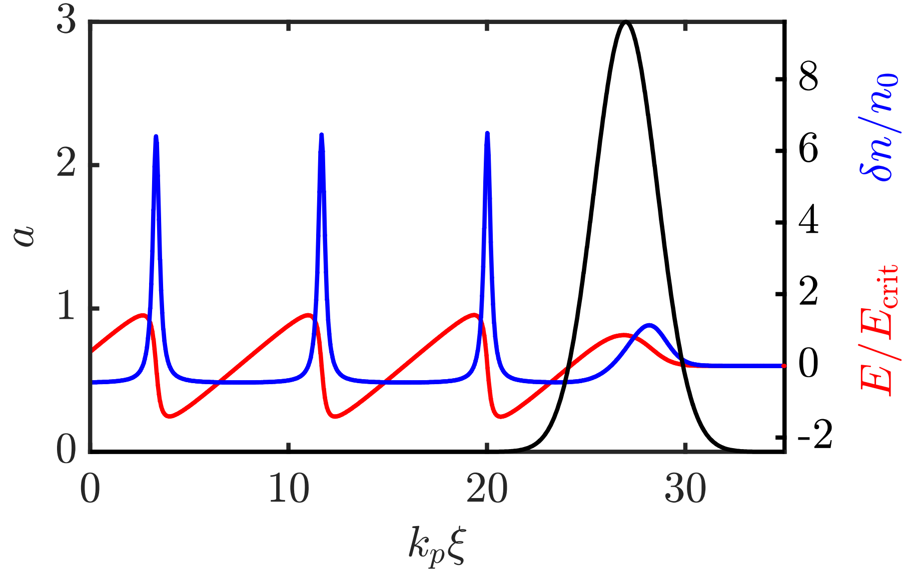

1. Esarey, E., Schroeder, C. & Leemans, W. Physics of laser-driven plasma-based electron accelerators. Rev. Mod. Phys. 81, 1229–1285 (2009).

LWFA fields as a function of laser a_0

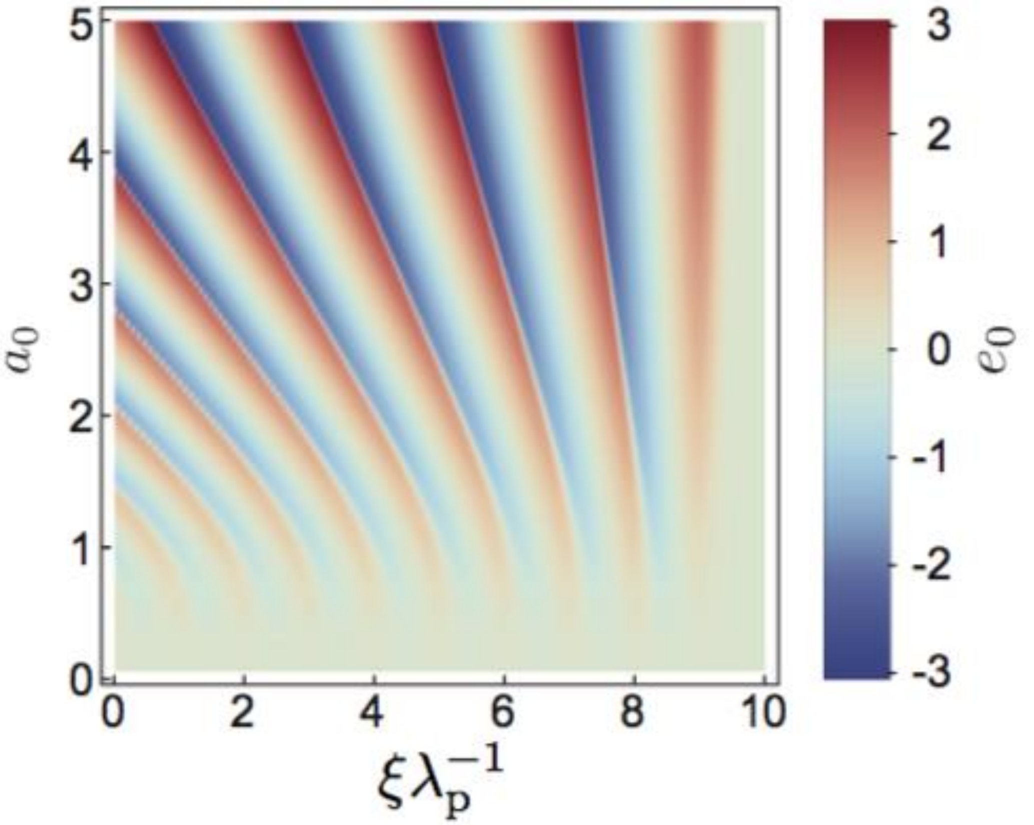

Figure 1.4.3 – The scale lengths of longitudinal plasma oscillations deviate for relativistic intensities from the non-relativistic plasma wavelength λ_p. These calculations again assume a Gaussian pulse (see figure 1.4.1).

1. Jens Osterhoff, PhD thesis 2009

Particle trapping in 1D plasma wave

The particle trajectories can be analysed using the hamiltonian:

$$\mathcal{H}(\xi, \gamma) = \gamma(1 - \beta_\phi \beta) - \Phi(\xi) = \text{constant}$$

And assuming the particle is initialized ahead of the plasma wave with initial conditions

$$\Phi(\infty) = 0, \gamma(\infty) = \gamma_0$$

Then the particle trajectory is described by

$$\gamma_0 - \beta_\phi \sqrt{\gamma_0^2 - 1} = \gamma - \beta_\phi \sqrt{\gamma^2 - 1} - \Phi(\xi)$$

Particle trapping in 1D plasma wave

Trajectories for $a_0 = 0.1, n_0 = 5 \times 10^{18}\ \mathrm{cm}^{-3}$
for various initial forward momenta.

Minimum momentum required for trapping can be found by setting particle velocity equal to the phase velocity at the point of minimum potential (trajectory in red opposite)

$$\Phi_0 - \Phi_{\mathrm{min}} = \gamma_0(1 - \beta_0\beta_\phi) - \gamma_\phi(1 - {\beta_\phi}^2)$$

In this case with $\gamma_\phi = 18.7$, a particle must have initially to become trapped and accelerated.

$\gamma_m > 12.9$

Higher amplitude waves can trap stationary electrons but then the fluid model has problems.

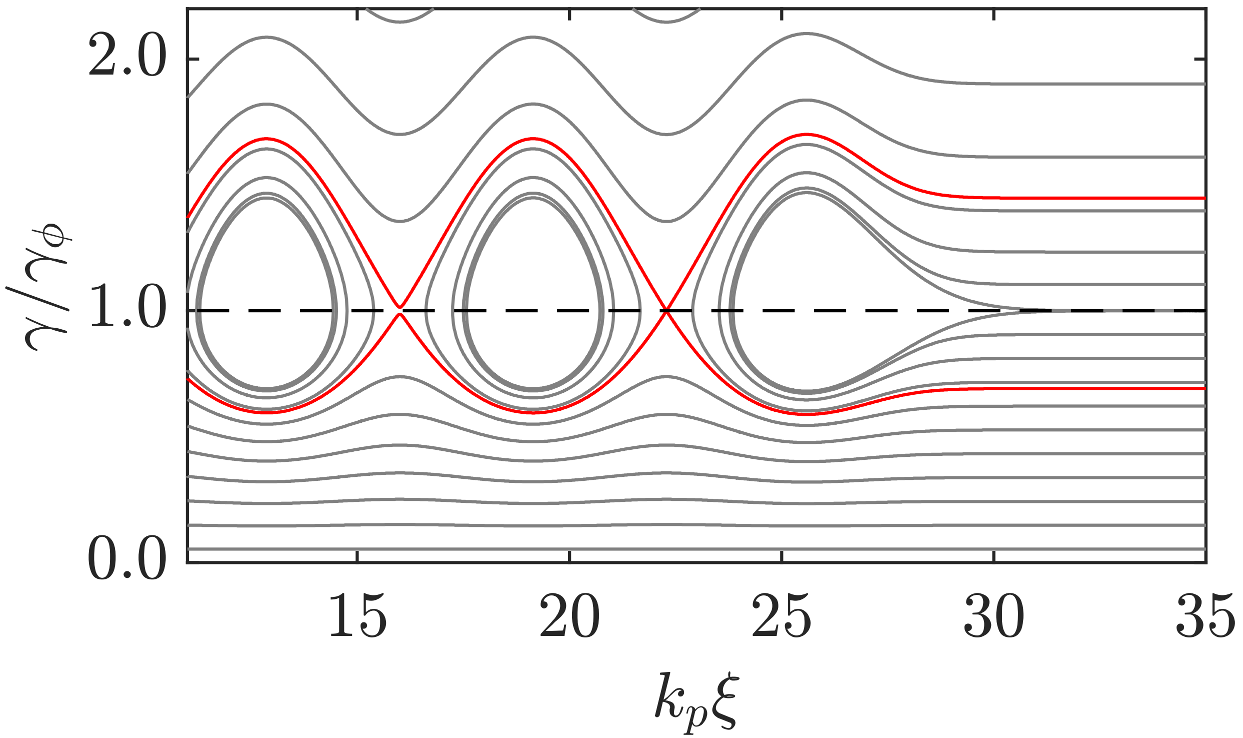

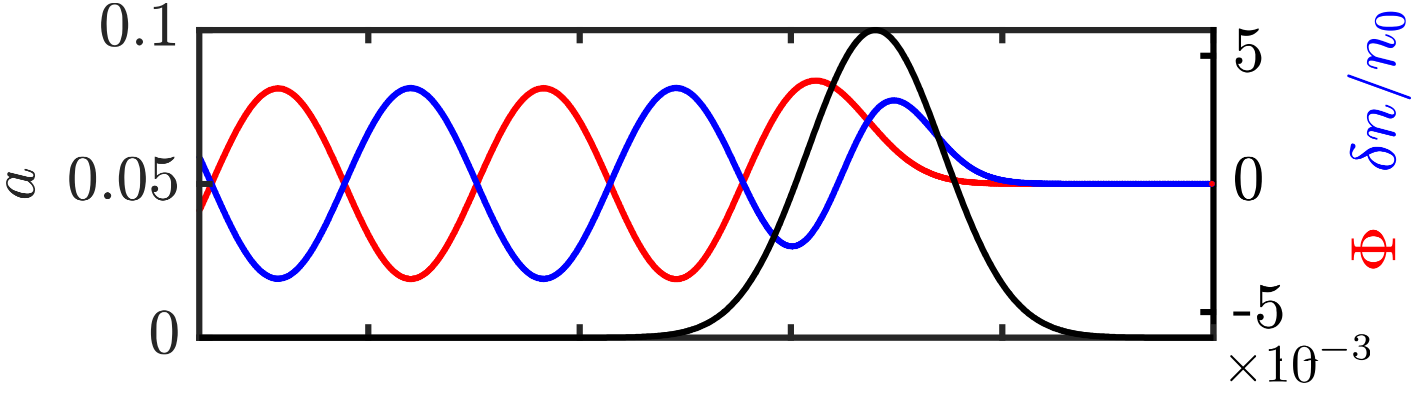

Particle trapping in 1D plasma wave

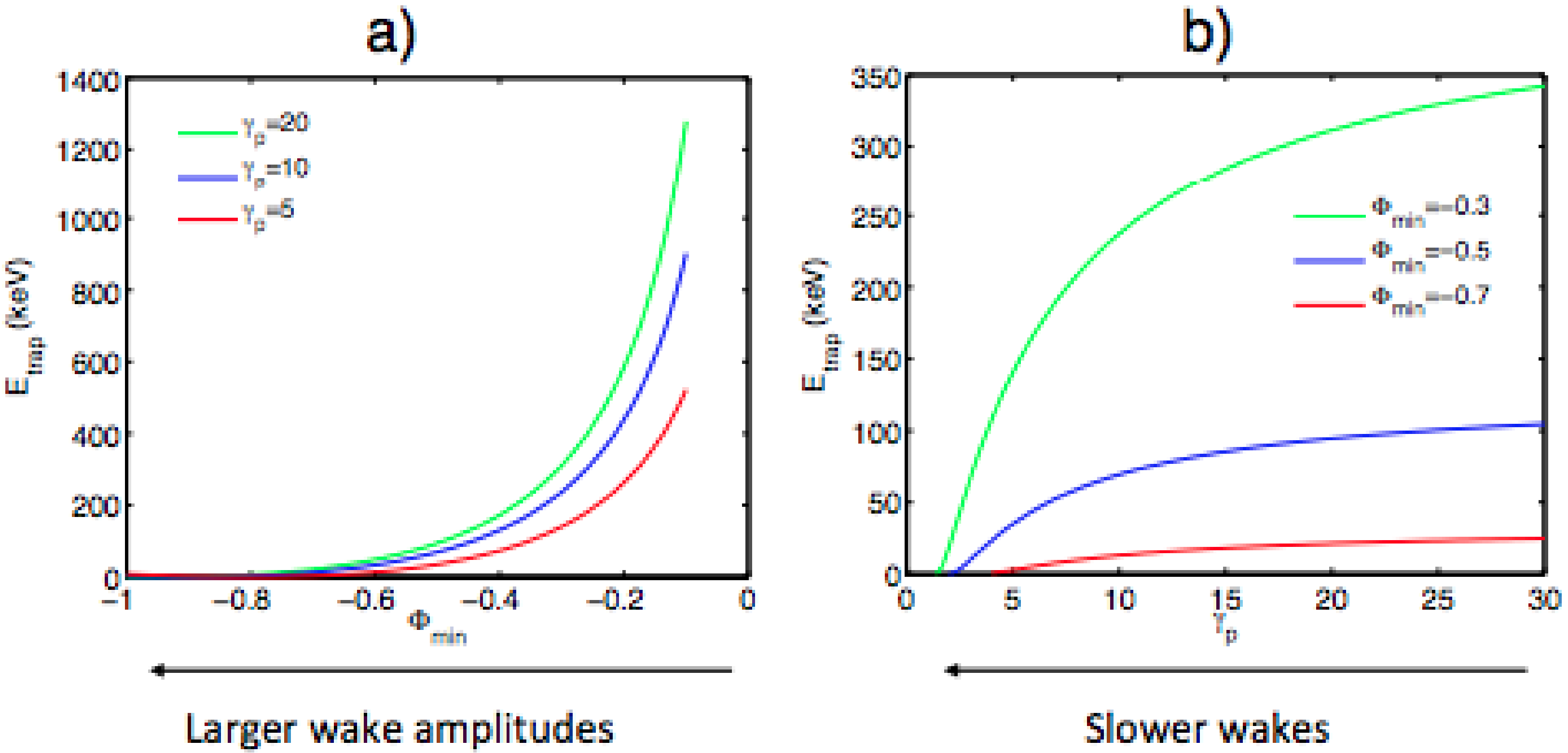

Fig. 3: (a) Trapping thresholds plotted as a function of wake amplitude (where ϕ_{min} represents the minimum of the wake potential), for three different wake phase velocities. (b) Trapping thresholds plotted as a function of γ_p, the Lorentz factor associated with the wakefield velocity, for three different wake amplitudes.

1. Faure J. https://arxiv.org/abs/1705.10542 2017

Full 3D description requires particle in cell simulations

Solves plasma properties and fields in discrete time steps

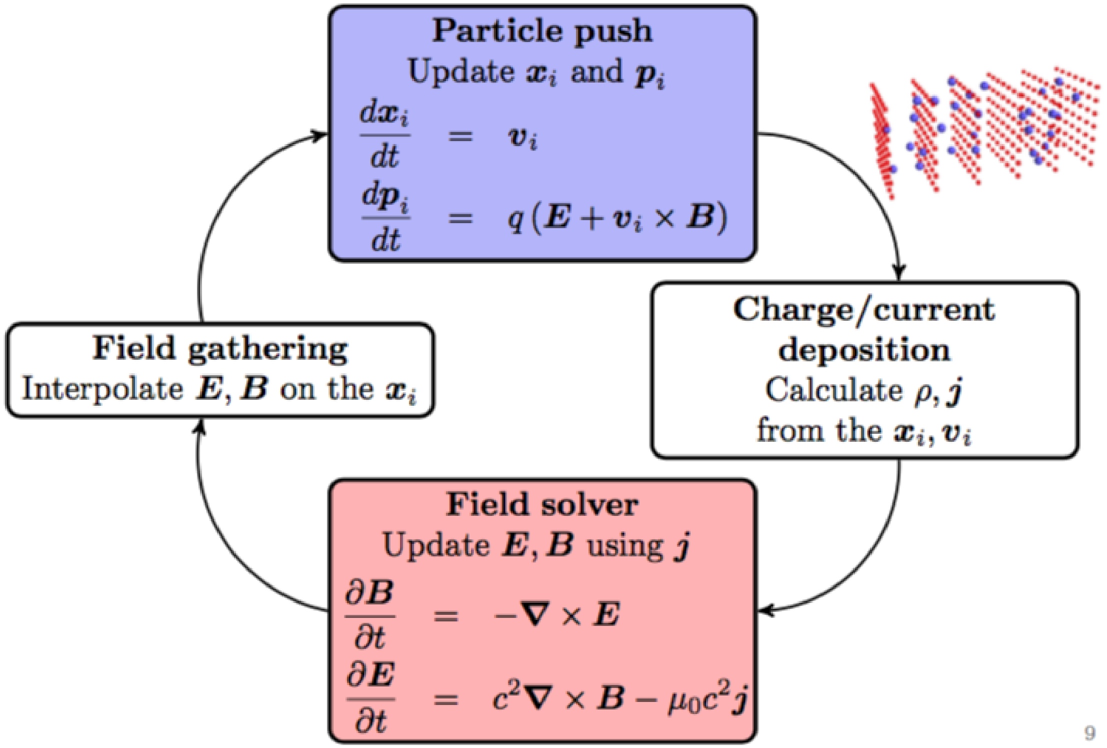

Plasma particles are grouped into macro-particles
Fields are calculated on the cell and then interpolated onto macro-particle positions

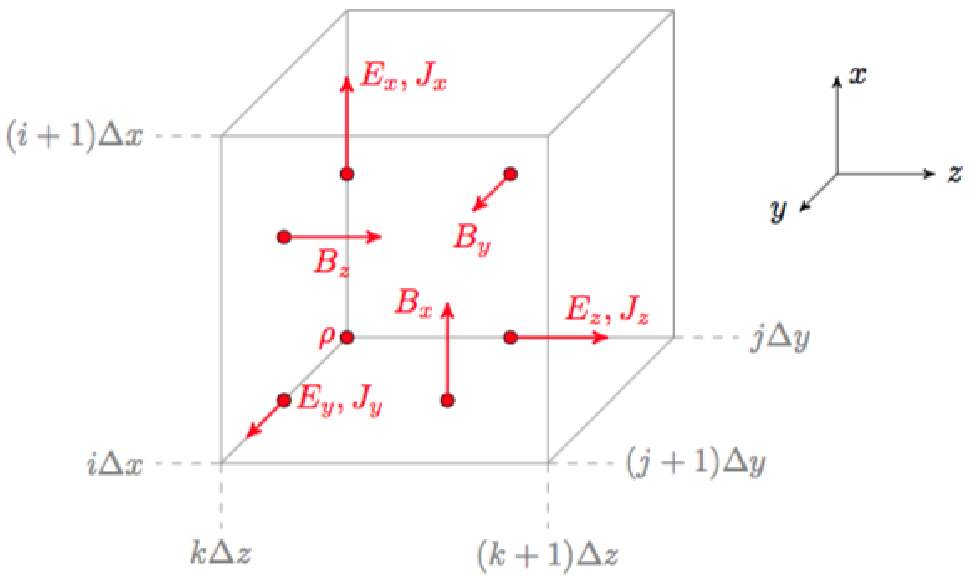

1. Remi Lehe “Self-Consistent Simulations of Beam and Plasma Systems”
   US Particle Accelerator School (USPAS) Summer Session 13-17 June, 2016

Full 3D description requires particle in cell simulations

Many different methods are used and many different codes are available.
A couple of freely available examples…
EPOCH http://www.ccpp.ac.uk/codes.html, https://cfsa-pmw.warwick.ac.uk/
Extendable PIC Open Collaboration project to develop a UK community advanced relativistic EM PIC code.
FBPIC https://fbpic.github.io/index.html
Fourier-Bessel Particle-In-Cell code for relativistic plasma physics using spectral cylindrical representation. Can do simple 3D simulations on a laptop due to its reduced geometry.

Most codes can be parallelized to make use of high performance computer clusters – needed for full 3D simulations.

For LWFA simulations it is common to use a moving window – to only look at the plasma around the laser pulse – similar to the quasi-static picture.

Full 3D description requires particle in cell simulations

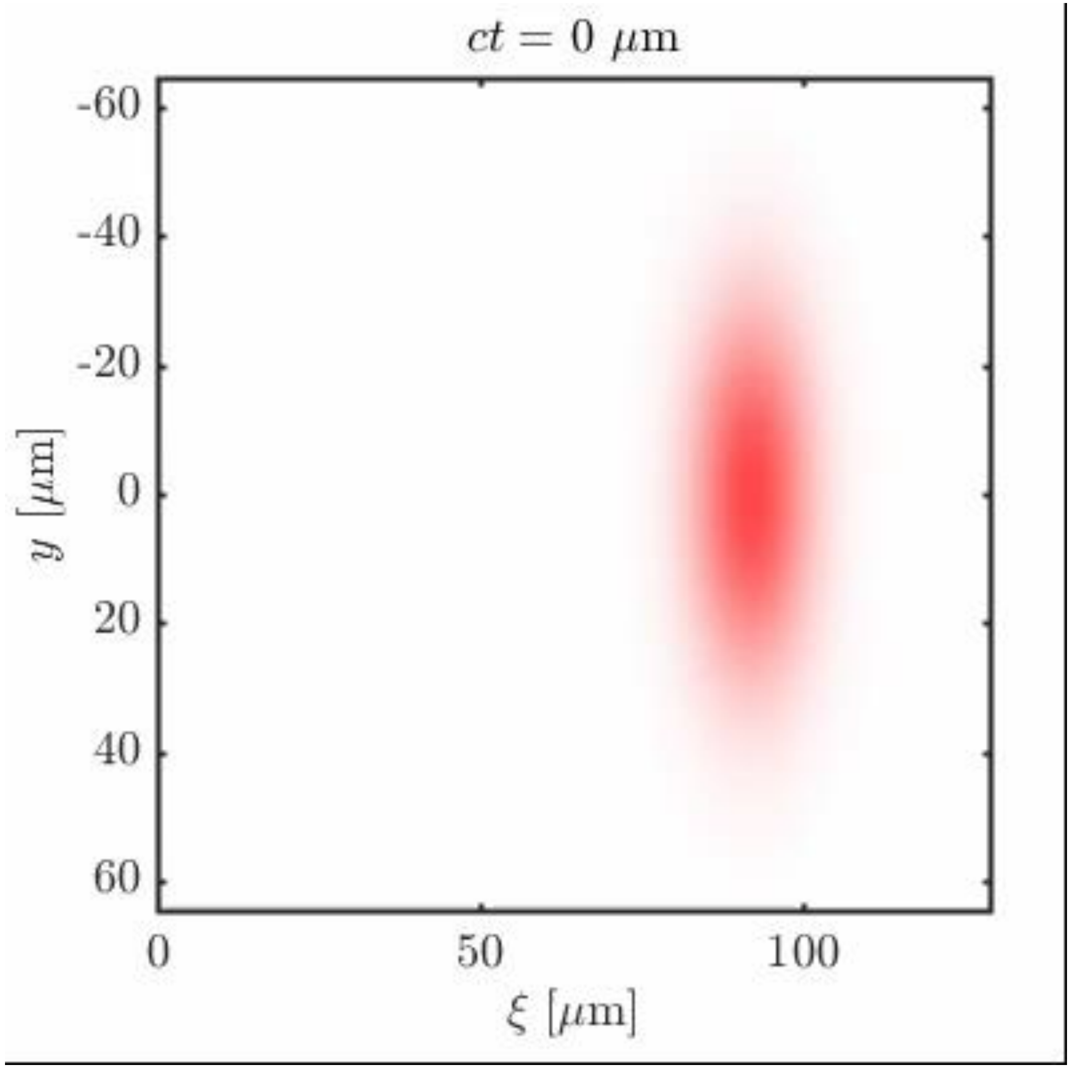

Full 3D description requires particle in cell simulations

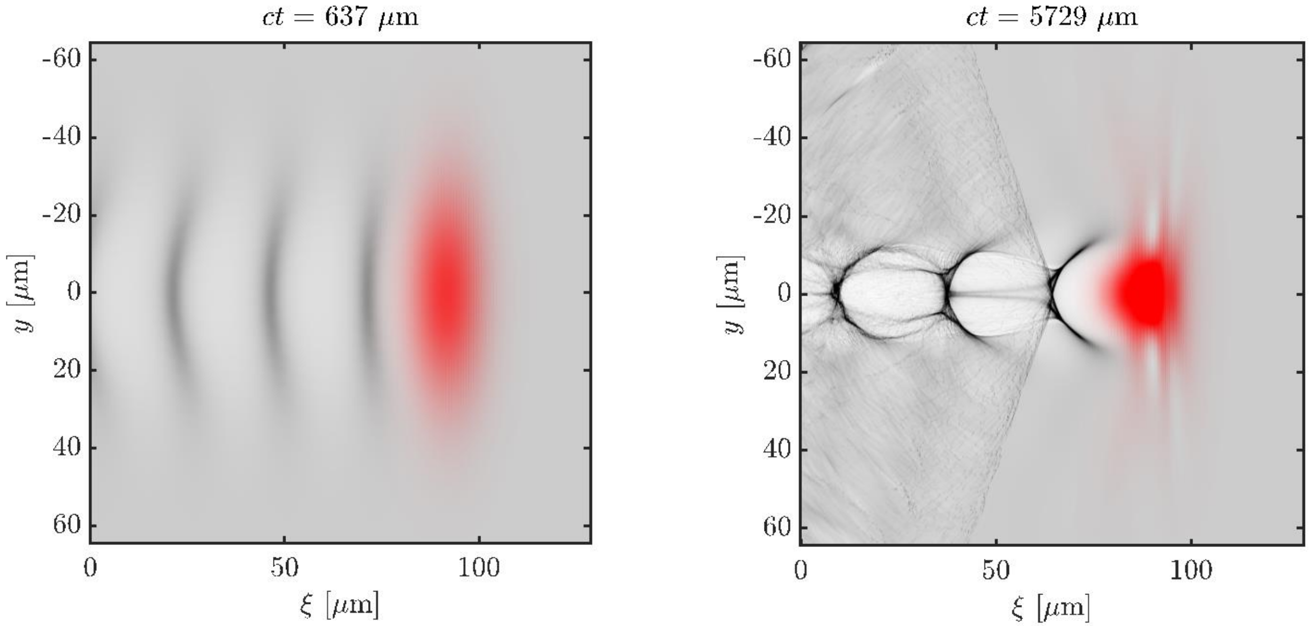

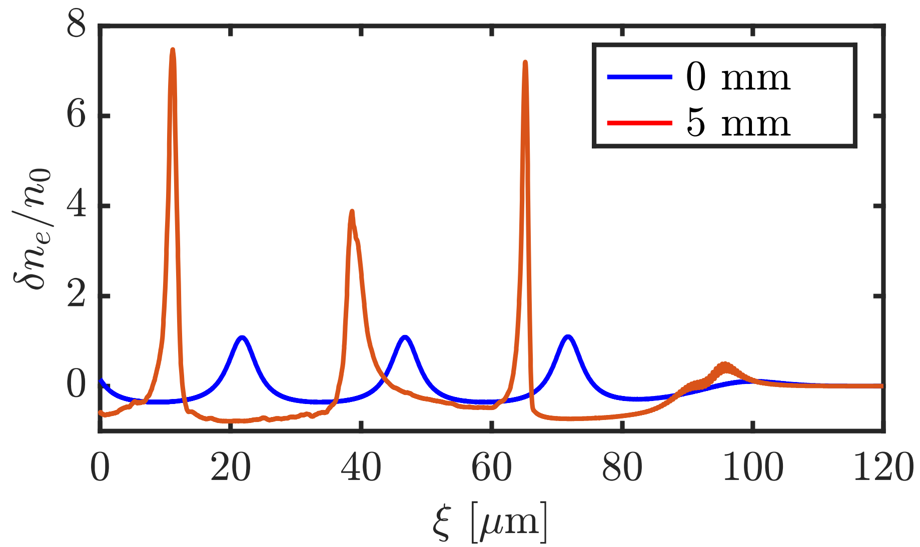

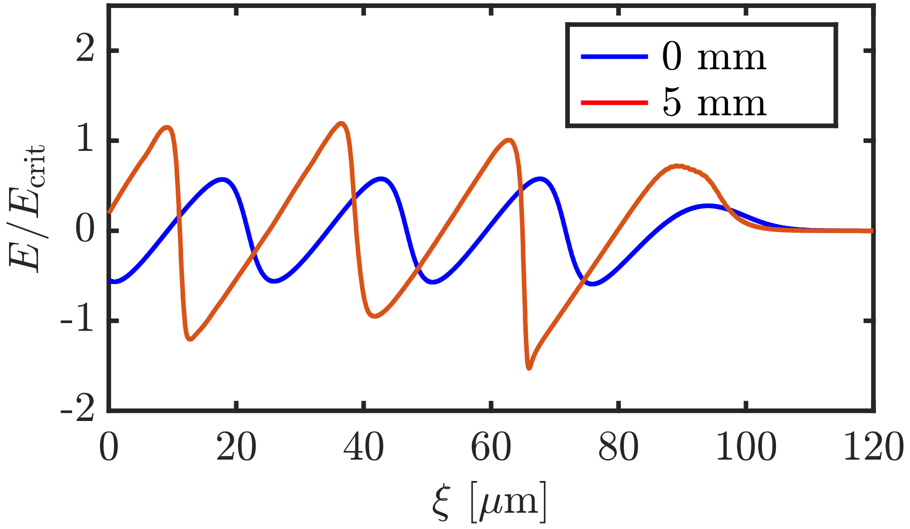

Evolution of the laser pulse changes the wakefield structure from slightly non-linear to cavitated "bubble" or "blowout" regime

Ion cavity forms behind the driving laser pulse and the wave breaks after a few periods

But the wake fields are very strong and have linear longitudinal and transverse gradients

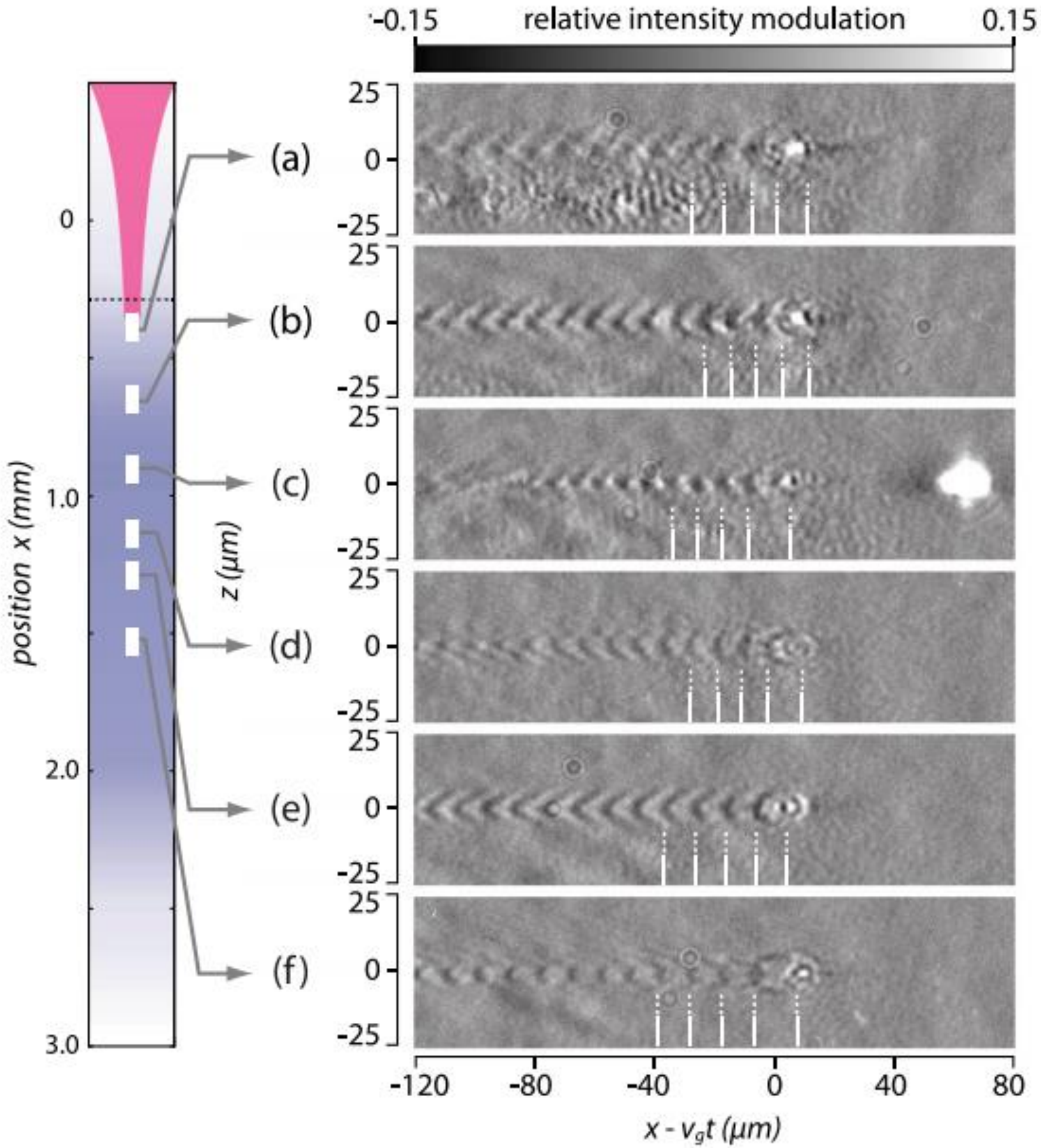

Probing of laser driven plasma wakefields matches the simulation behavior

1. Sävert, A. *et al.* Direct Observation of the Injection Dynamics of a Laser Wakefield Accelerator Using Few-Femtosecond Shadowgraphy. *Phys. Rev. Lett.* **115,** 55002 (2015).

LWFA in the bubble regime

First seen to in PIC simulations by Pukhov *et al.* [1]
Laser pulse used was 12J in 33fs with $a_0 = 10$

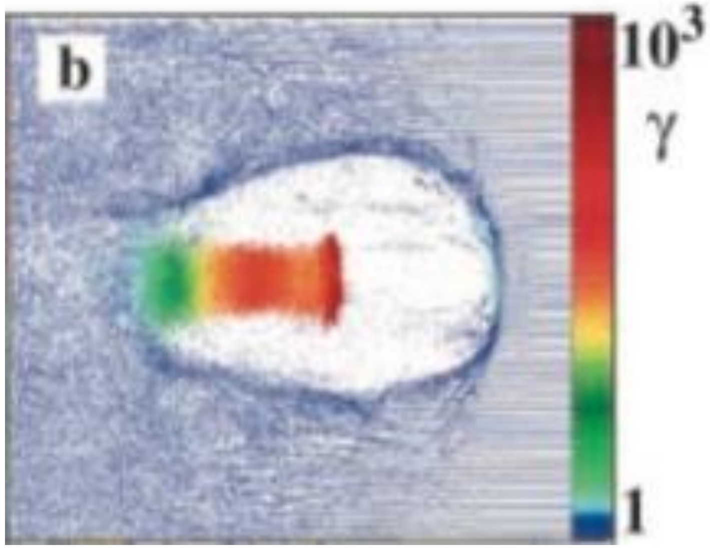

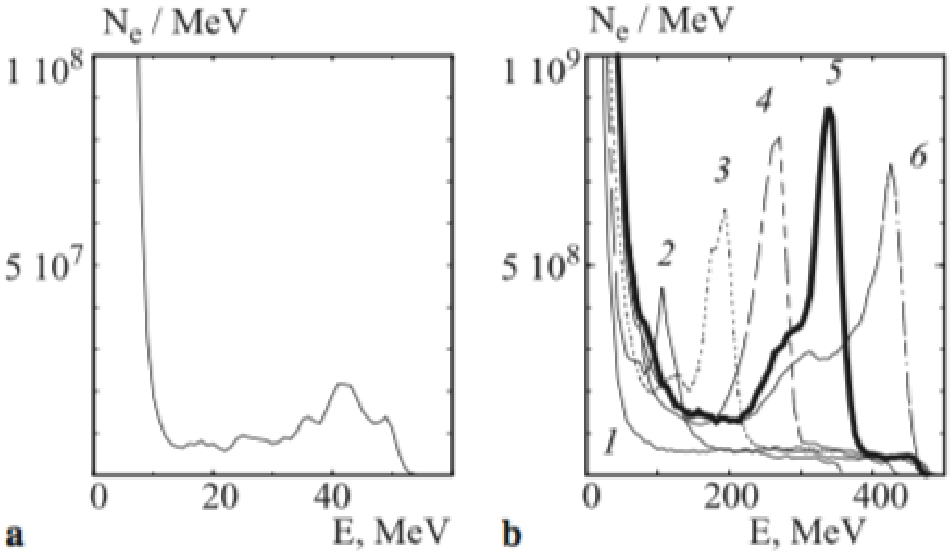

FIGURE 2 Spectra of accelerated electrons: **a** final spectrum of the case of Fig. 1; **b** the case of the 33-fs, 12-J laser pulse, time evolution of the energy spectrum: (1) $ct/\lambda = 350$, (2) $ct/\lambda = 450$, (3) $ct/\lambda = 550$, (4) $ct/\lambda = 650$, (5) $ct/\lambda = 750$ corresponding to Figs. 3, 4, and 5, (6) $ct/\lambda = 850$

1. Pukhov, A. & Meyer-ter-Vehn, J. Laser wake field acceleration: the highly non-linear broken-wave regime. *Appl. Phys. B Lasers Opt.* **74,** 355–361 (2002).

LWFA in the bubble regime

Experiments first saw narrow energy spread beams in 2004 [1], with 500mJ lasers in 40fs

$a_0 \approx 1$

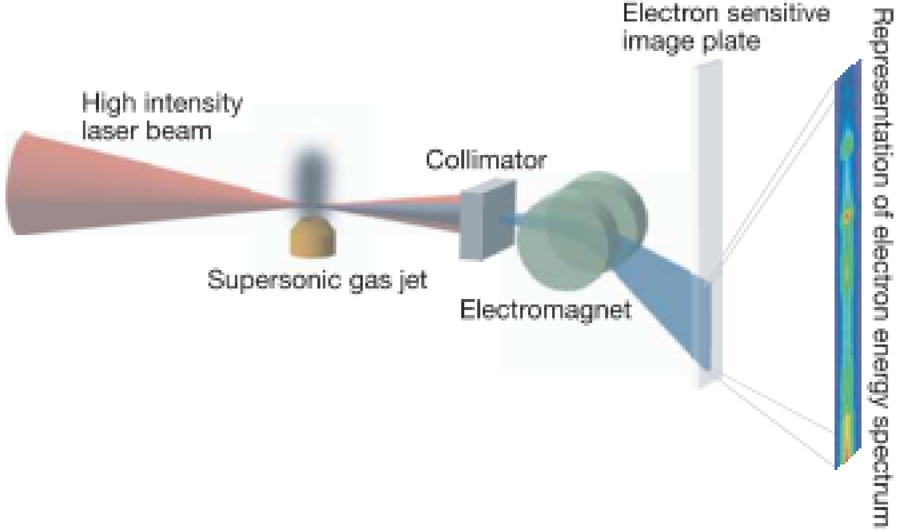

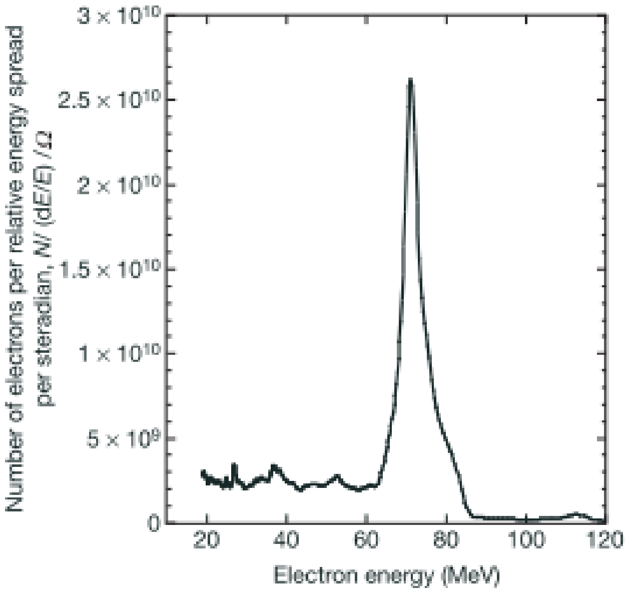

Figure 3 Measured electron spectrum at a density of 2×10^{19} cm^{-3}. Laser parameters: $E = 500$ mJ, $\tau = 40$ fs, $I \approx 2.5 \times 10^{18}$ W cm^{-2}. The energy spread is $\pm 3\%$. The energy of this monoenergetic beam fluctuated by ~30%, owing to variations in the laser parameters.

1. Mangles, S. P. D. *et al. Nature* **431,** 535–8 (2004).
Faure, J. *et al. Nature* **431,** 541–544 (2004).
Geddes, C. G. R. *et al. Nature* **431,** 538–41 (2004).

LWFA in the bubble regime

- Why do we get narrow energy spread beams in the bubble regime?
- How do we see this in experiments with ? $a_0 \approx 1$

Although these questions are hard to answer with general formula, simulation and experimental results reveal the phenomena that lead to this behaviour

Plasma optics in a wakefield accelerator

- Refractive index in a plasma is given by:
  (always less than 1 for a plasma)

$$\eta = \sqrt{1 - \left(\frac{\omega_p}{\omega_0}\right)^2}$$

- The plasma frequency is modified if the electron motion becomes relativistic

$$\omega_p = \sqrt{\frac{n_e e^2}{\langle\gamma\rangle m_e \epsilon_0}}$$

- So the relativistic refractive index (averaged over a laser cycle) is:

$$\eta = \sqrt{1 - \frac{n_e}{\langle\gamma\rangle n_c}} \qquad n_c = \frac{m_e \epsilon_0 {\omega_0}^2}{e}$$

- Therefore the refractive index is larger (closer to 1) in regions of high laser intensity.
  Approximating for $a_0 \ll 1$ gives

$$\langle\gamma\rangle \approx 1 + \frac{{a_0}^2}{2}$$

Self-guiding of a laser pulse in a plasma

- For a gaussian laser pulse, the wavefronts are curved around focus and the pulse naturally diffracts

$$w(z) = \sigma_r \sqrt{1 + \left(\frac{z}{z_r}\right)^2}, \quad \text{where} \;\; z_r = \pi {\sigma_r}^2/\lambda$$

$$\frac{\partial^2 w}{\partial z^2} = \frac{4c^2}{{\omega_0}^2 {\sigma_r}^3}$$

- For small divergence angles $\quad \sin(\theta) \approx \theta = \frac{\mathrm{d}w}{\mathrm{d}z}$

- The radial profile for a gaussian laser pulse is

$$a(r) = a_0 \exp(-r^2/(2{\sigma_r}^2))$$

$$\frac{\mathrm{d}a^2}{\mathrm{d}r} \simeq -a_0^2/\sigma_r$$

- And the phase velocity in a plasma as a function of radius is

$$v_\phi(r) = c\left[1 - \frac{n_e}{(1 + a^2/2)n_c}\right]^{-1/2}$$

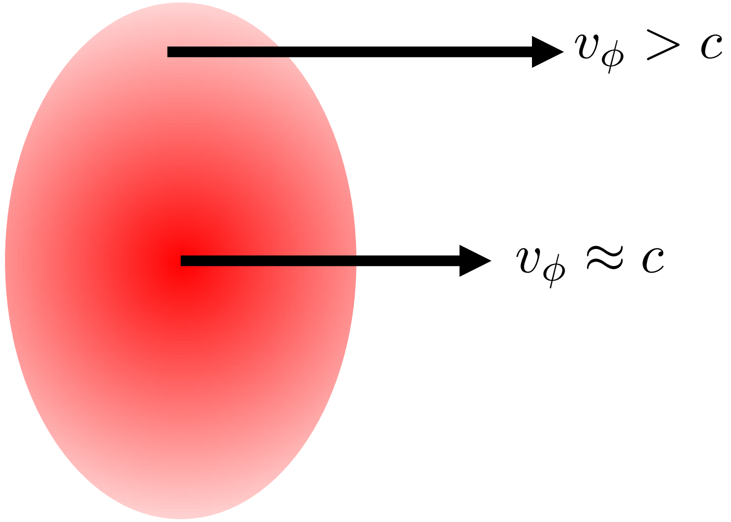

Self-guiding of a laser pulse in a plasma

- For guiding we want the pulse waist to stay the same, so we require the radial dependence of the phase velocity to balance the natural divergence

$$\frac{\mathrm{d}w}{\mathrm{d}z} = \frac{\mathrm{d}v_\phi}{\mathrm{d}r}\Delta t$$

- Differential with respect to t and taking

$$\frac{\mathrm{d}}{\mathrm{d}z} = \frac{1}{c}\frac{\mathrm{d}}{\mathrm{d}t}$$

$$\frac{\mathrm{d}^2 w}{\mathrm{d}z^2} = \frac{1}{c}\frac{\mathrm{d}v_\phi}{\mathrm{d}r}$$

$$\frac{\mathrm{d}^2 w}{\mathrm{d}z^2} = \frac{\mathrm{d}}{\mathrm{d}r}\left(1 - \frac{n_e}{(1+a^2/2)n_c}\right)^{-\frac{1}{2}}$$

$$\frac{\mathrm{d}^2 w}{\mathrm{d}z^2} \approx -\frac{\mathrm{d}a^2}{\mathrm{d}r}\frac{n_e}{8n_c} = \frac{{a_0}^2}{\sigma_r}\frac{n_e}{8n_c}$$

Self-guiding of a laser pulse in a plasma

- Substituting in the divergence expression $\frac{\partial^2 w}{\partial z^2} = \frac{4c^2}{{\omega_0}^2 {\sigma_r}^3}$ gives:

$$\frac{4c^2}{{\omega_0}^2 {\sigma_r}^3} = \frac{{a_0}^2}{\sigma_r} \frac{n_e}{8 n_c}$$

$${a_0}^2 {\sigma_r}^2 = \frac{32c^2}{{\omega_p}^2}$$

- The quantity ${a_0}^2 {\sigma_r}^2$ is proportional to the pulse power and so we can define a critical pulse power for which self-guiding occurs

$$P_{\text{crit}} \simeq 17 \frac{n_c}{n_e} \; [GW]$$ For a spot radius given by $$\sigma_r = \frac{4\sqrt{2}}{a_0} \frac{c}{\omega_p}$$

- So as long as the pulse power exceeds the critical power for self-guiding, the laser will self-focus to a matched spot size which will be maintained for orders of magnitude longer than the Rayleigh range.
- This is required for long acceleration lengths and high energy electron beams from LWFA.

External guiding of a laser pulse in a plasma waveguide

- Alternatively, a plasma waveguide can be used to balance divergence through a radial dependence of the plasma density

$$\delta n_e(r) = \Delta n_e \frac{r^2}{{r_0}^2}$$

$$v_\phi(r) = c\left[1 - \frac{n_e}{(1+a^2/2)n_c}\right]^{-1/2}$$

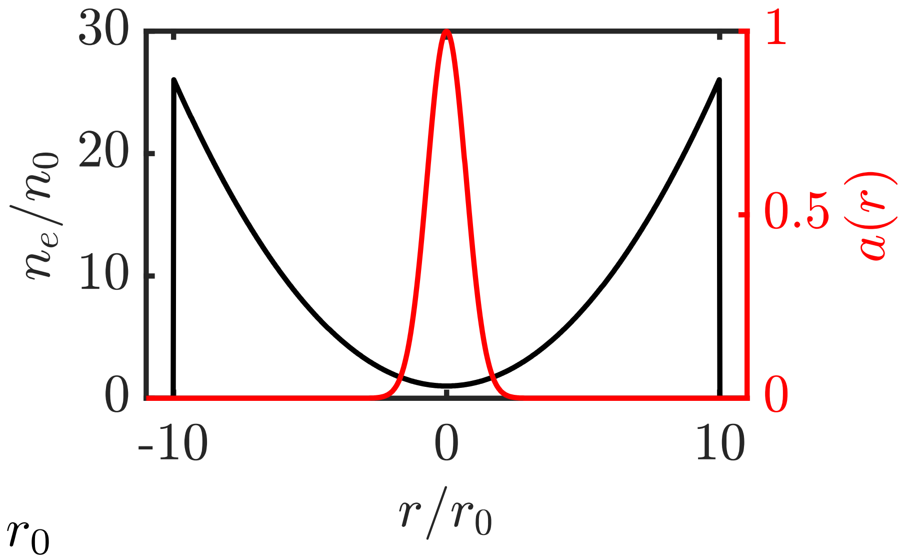

- For $a_0 = 0$, $\Delta n_c = \frac{1}{\pi r_e {r_0}^2}$ will guide a pulse with $\sigma_r = r_0$
- In practise for LWFA $a_0 \gtrsim 1$ and so self-guiding will also occur so the optimal guiding profile will differ

External guiding of a laser pulse in a plasma waveguide

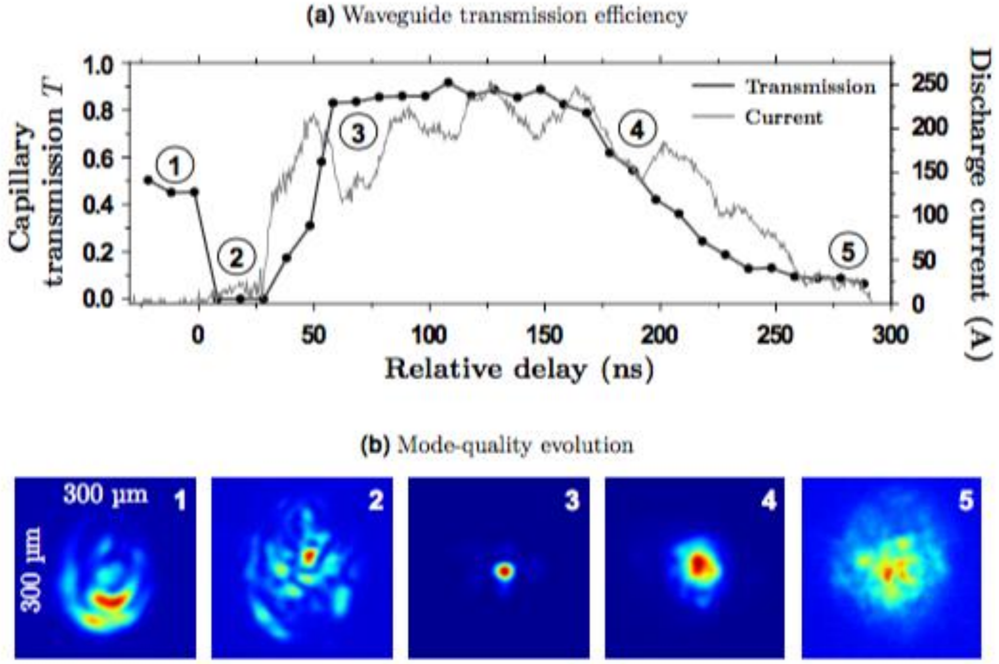

Figure 3.3.1 – (a) The waveguide transmission efficiency T and the discharge current as functions of the timing delay between the onset of the high-voltage breakdown and the arriving laser pulse. (b) Mode quality at the output of the channel in false-colors pertaining to regions 1 to 5. Each image is normalized to its maximum. The color-scale is equivalent to the one used in figure 3.3.3.

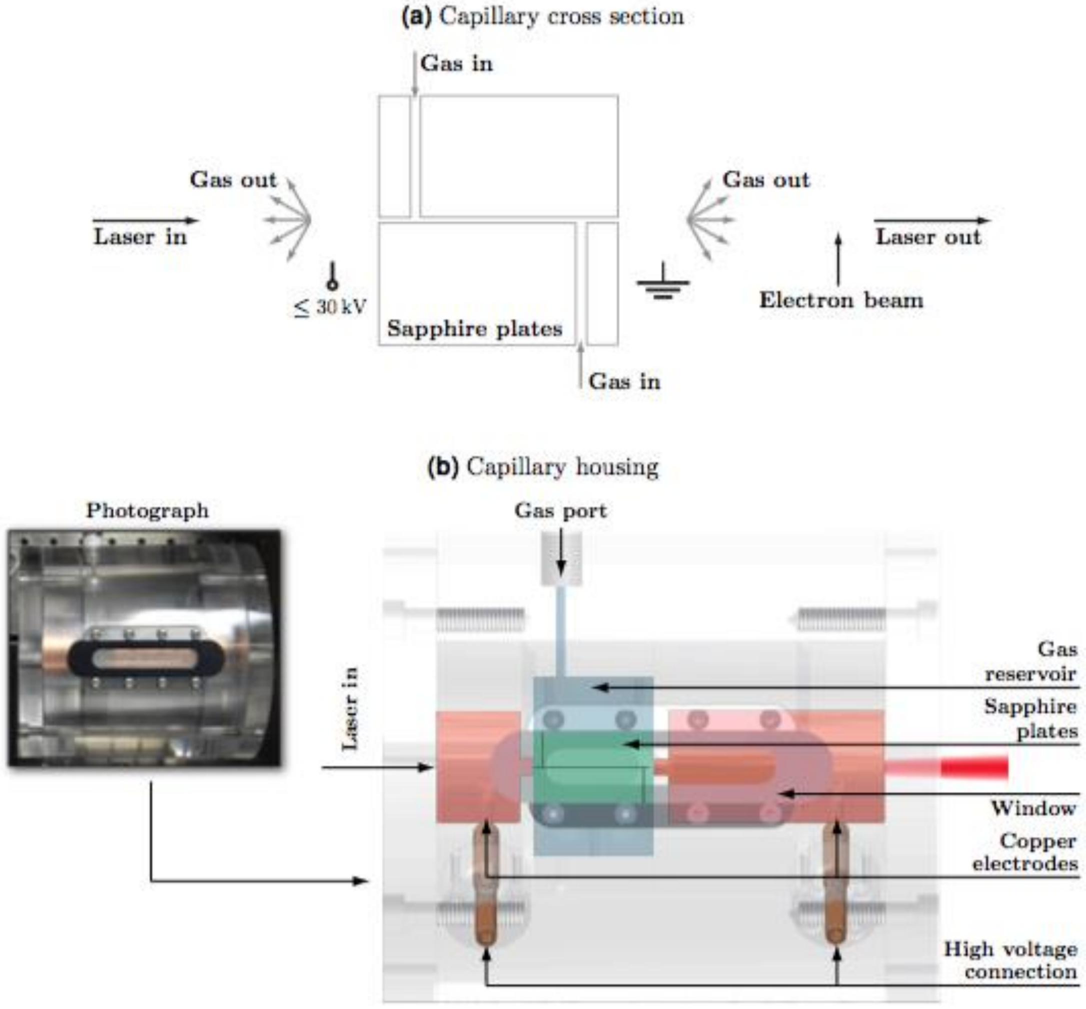

Figure 3.1.1 – (a) Cross section of a capillary discharge waveguide and (b) layout of the Perspex enclosure with high voltage connections and gas port.

1. Jens Osterhoff, PhD thesis 2009

Frequency shifts and pulse compression of the driving laser pulse

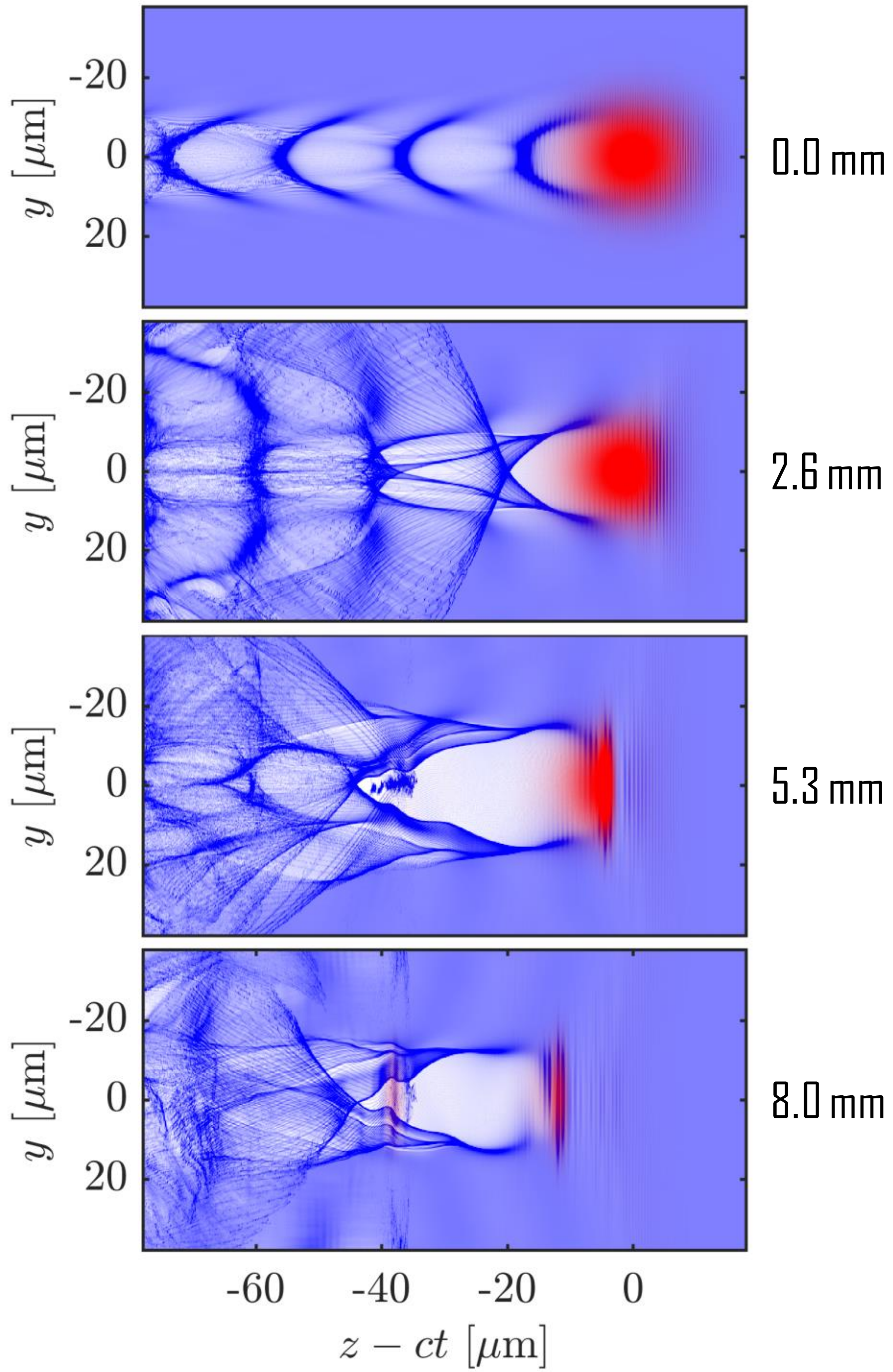

Simulations and experiments show pulse compression in LWFA with short pulses

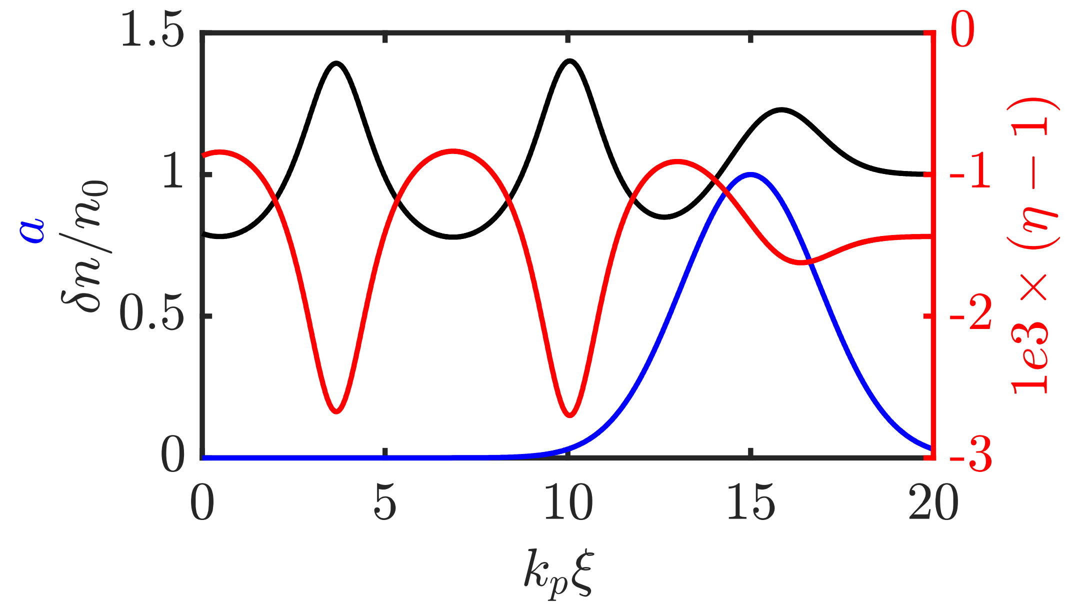

$$v_g = c\eta$$
$$v_\phi = c\eta^{-1}$$

There is a co-moving refractive index profile that caused group velocity dispersion and frequency shift of the driving pulse

Photon acceleration due to co-moving refractive index gradients

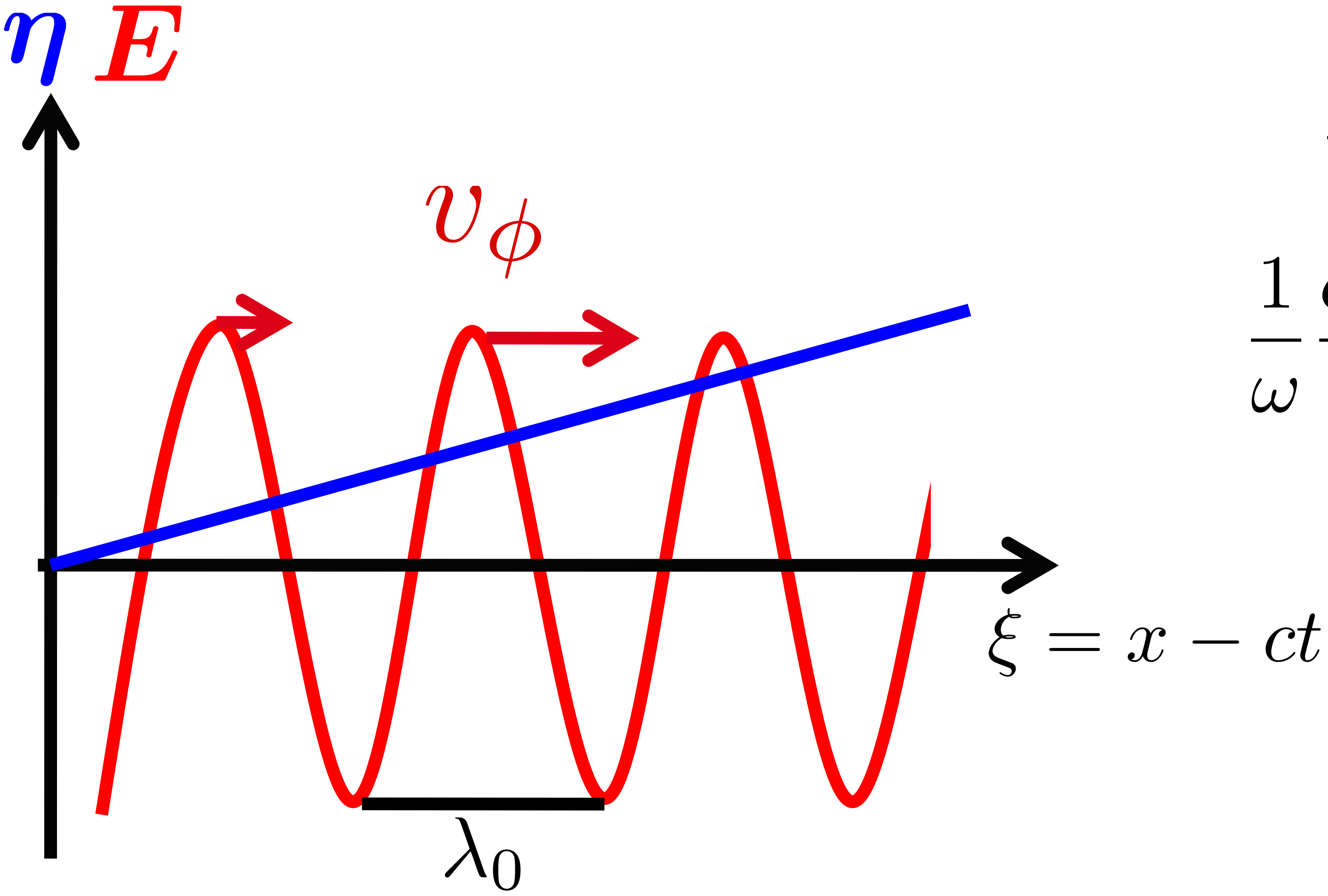

$$\frac{\mathrm{d}\lambda}{\mathrm{d}t} = c\lambda \frac{\partial}{\partial \xi} \eta^{-1}$$

$$\frac{1}{\omega}\frac{\partial \omega}{\partial t} = \frac{c}{\eta^2}\frac{\partial \eta}{\partial \xi}$$

Traffic analogy for refraction and photon acceleration

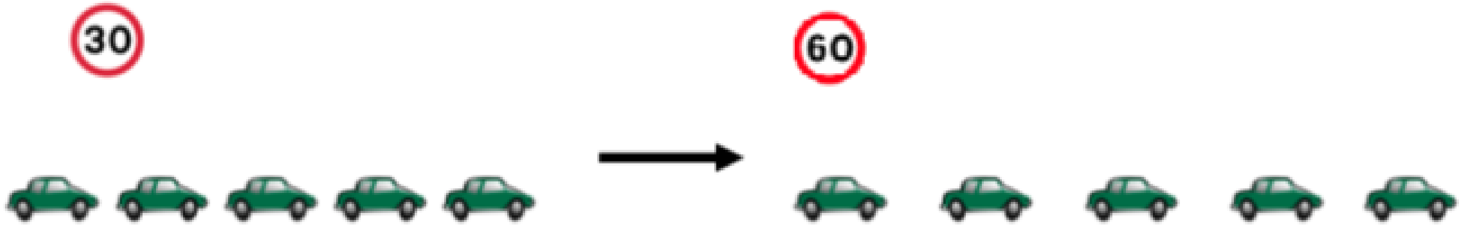

Normal refraction:
The cars each speed up as they reach the sign
Cars/time stays constant, but spatial separation between cars increases

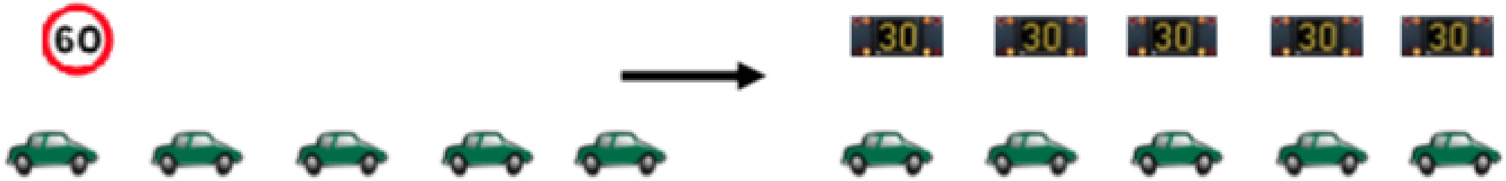

Photon acceleration:
The cars each speed up simultaneously
Now the spatial separation is constant but the cars/time has reduced -> frequency is lower

1. Chris Murphy, PhD thesis 2007

Redshift occurs at the front of the laser pulse

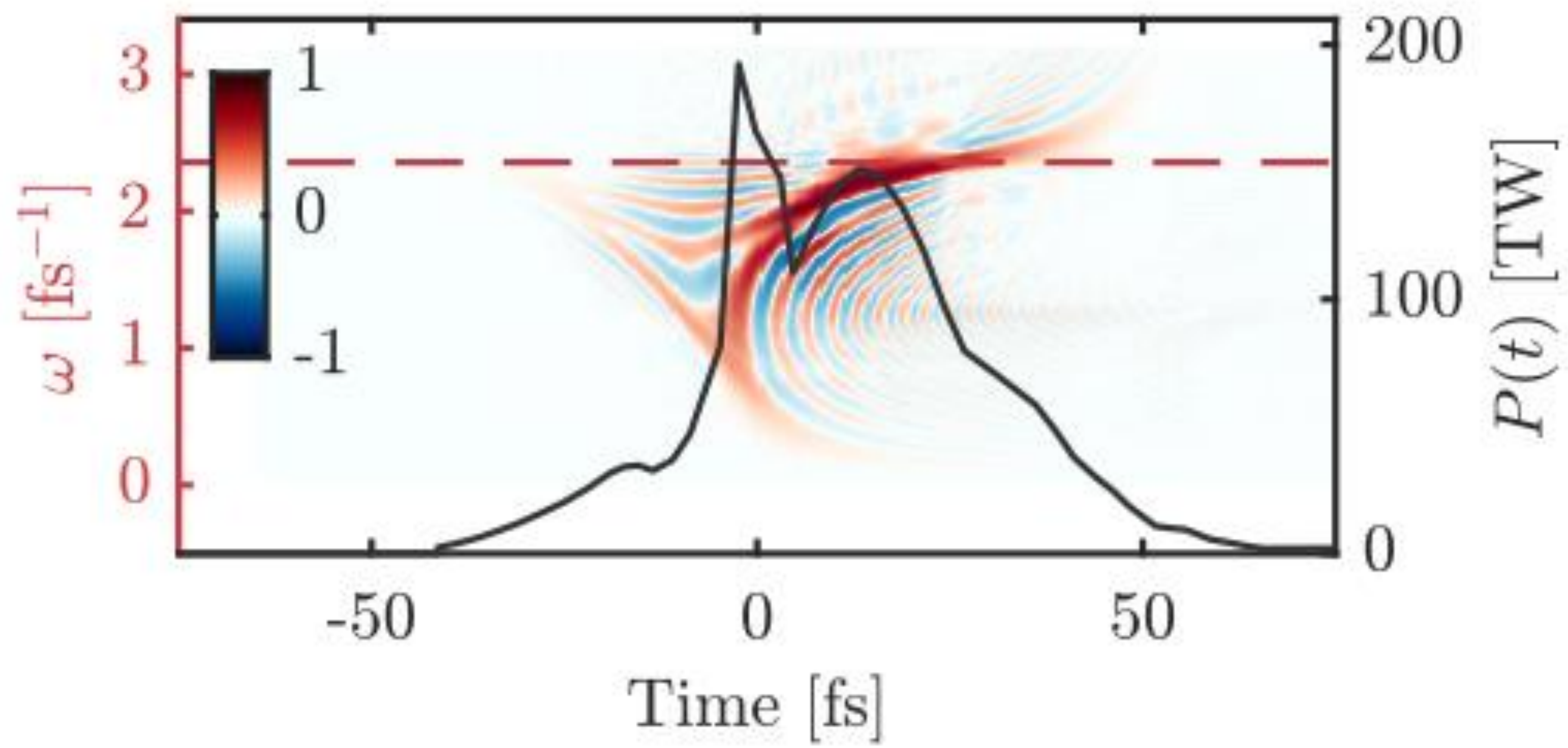

Typically we observe red-shifting at the front of the pulse. This is also the mechanism by which energy is coupled in the plasma wave. The redshifted photons slip backwards as their group velocity is lower and this leads to a sharp rising edge.

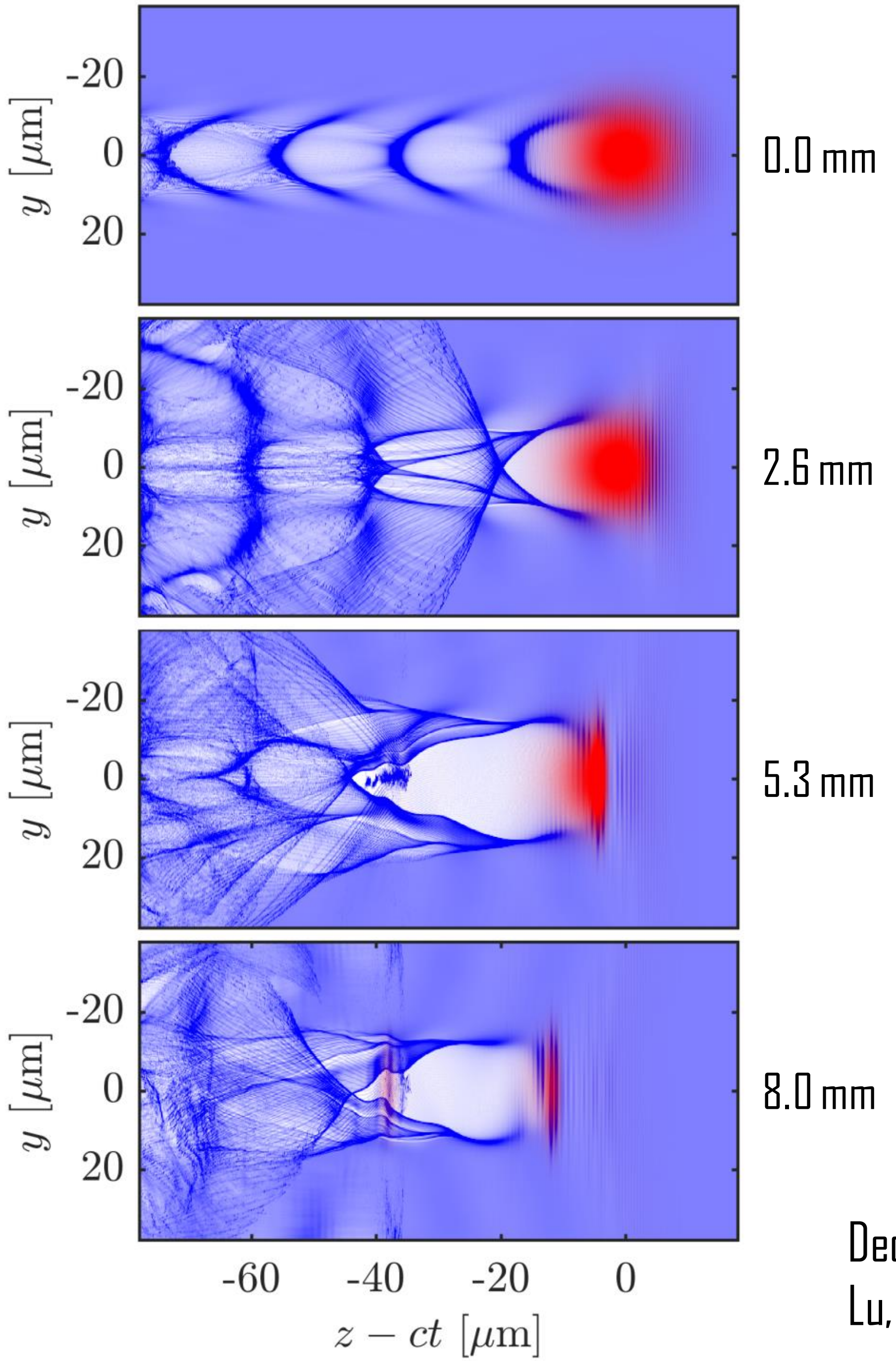

Depletion of the laser pulse occurs locally at the front

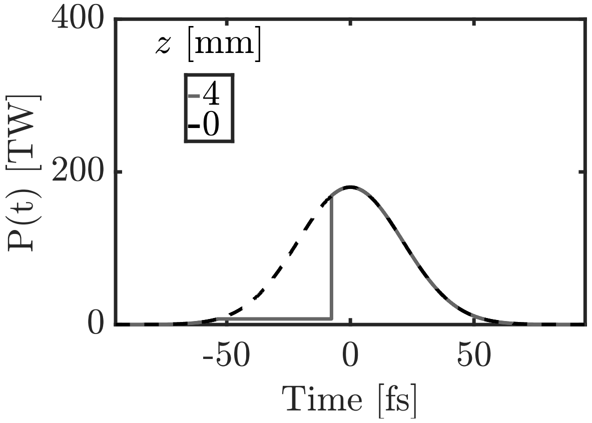

Pulse front etching model:

$$v_{\mathrm{etch}} = \left(\frac{\omega_0}{\omega_p}\right)^2 c$$

$$v_g = v_{g0} - v_{\mathrm{etch}}$$

Depletion length $$L_{\mathrm{dp}} \approx \left(\frac{\omega_0}{\omega_p}\right)^2 \sigma_t c$$

Dephasing length $$L_{\mathrm{d}} \approx \frac{2}{3}\left(\frac{\omega_0}{\omega_p}\right)^2 \lambda_p$$

Decker, C. D. *et al., Phys. Plasmas* **3,** 2047 (1996).
Lu, W. *et al., Phys. Rev. Spec. Top. - Accel. Beams* **10,** 61301 (2007).

Group velocity dispersion can compress the driving laser pulse

Difference in group velocity along pulse leads to changes in the temporal profile of the pulse.

The rear of the pulse travels in the ion cavity, where the plasma density is lower and so catches up the front of the pulse leading to compression

A more complete description must include the frequency shifts due to photon acceleration, which also affect the group velocity

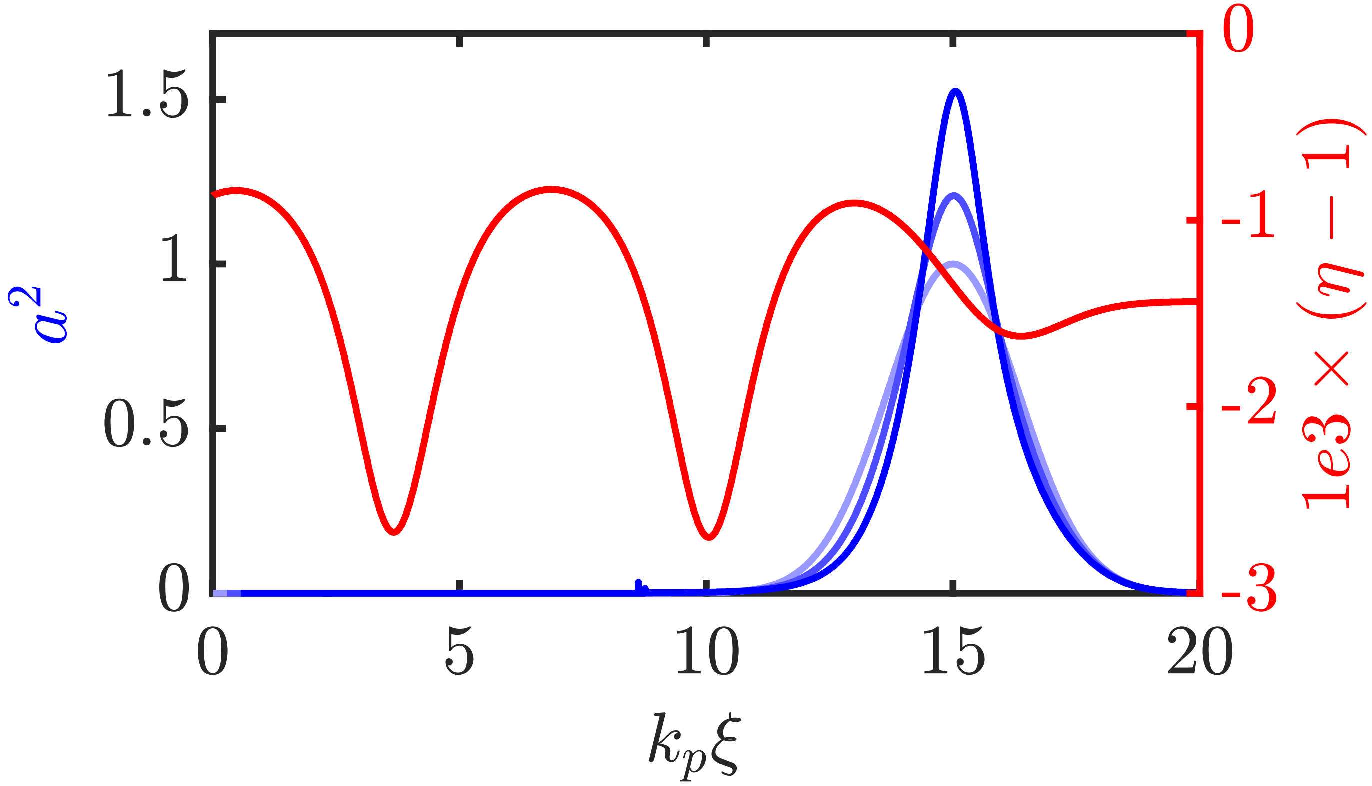

Lower limit on redshifted photons that drift back faster than the etching velocity

$$v_g(1) = v_g(0) - v_{\text{etch}}$$

$$c\sqrt{1-\frac{{\omega_p}^2}{{\omega_1}^2}} = c\sqrt{1-\frac{{\omega_p}^2}{{\omega_0}^2}} - \frac{{\omega_p}^2}{{\omega_0}^2}$$

$$\omega_1 = \frac{\omega_0}{\sqrt{3}}$$

These photons drift backwards and contribute to field behind the depletion region

Pulse front etching model

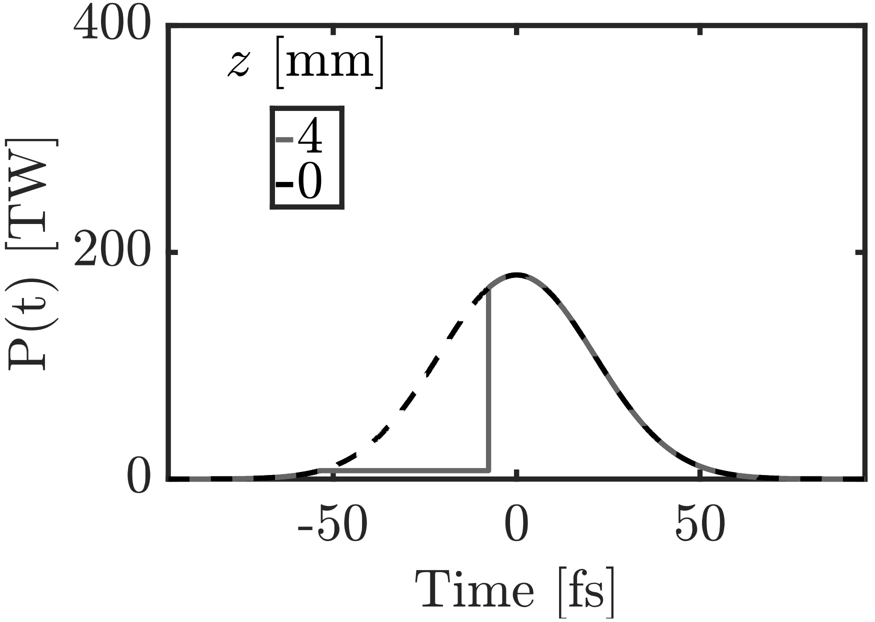

Model with group velocity dispersion

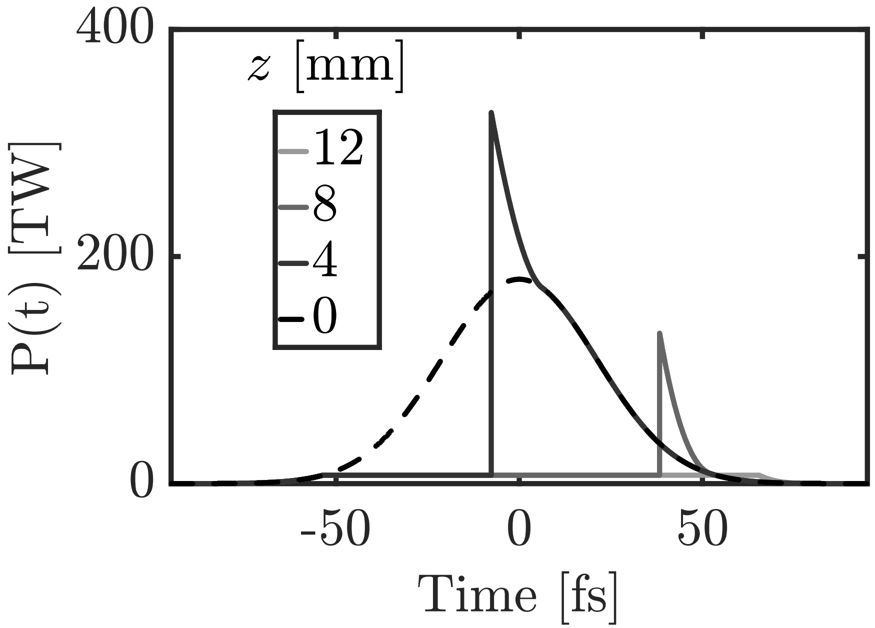

Pre-Injection Pulse Evolution length

For a gaussian pulse=:

$$L_{\text{evol}} \approx \sigma_t c \left(\frac{2}{3}\frac{{\omega_0}^2}{{\omega_p}^2}\right)\sqrt{\frac{1}{2}\ln\left(\frac{P_0}{P_c}\right)}$$

$$L_{\text{dp}} \approx 2L_{\text{evol}}$$

https://arxiv.org/abs/1710.05740

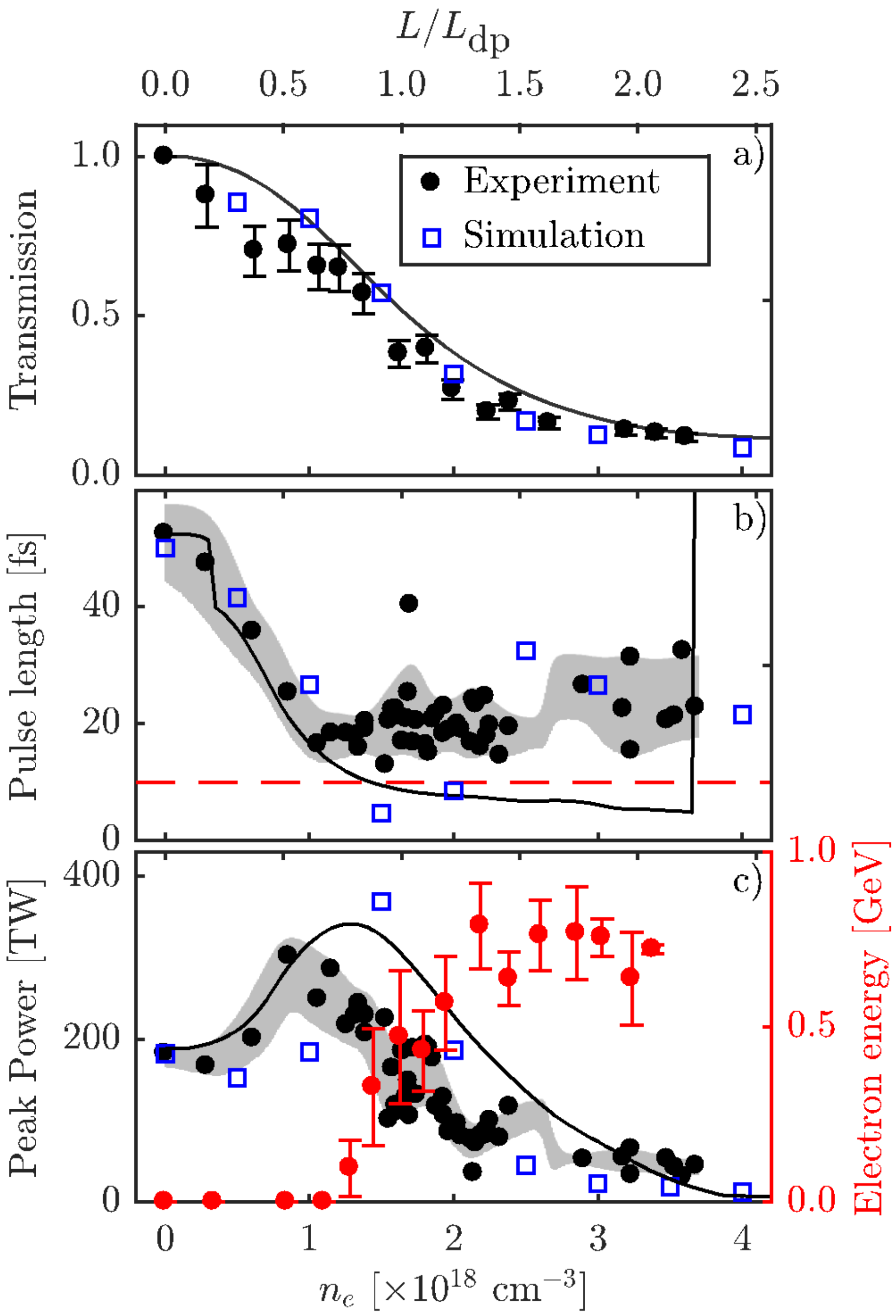

Pulse evolution due to depletion, photon acceleration and group velocity dispersion

Trapping and acceleration in the bubble regime

Phenomenological[1] and kinetic[2] theories have examined the field structure and particle trajectories in the bubble/blowout regime

Simplest model is a sphere of positive charge with a thin sheath of electrons around the edge moving at the laser group velocity

$$E_x = \frac{k_p \xi}{2} E_{\mathrm{crit}} \ , \ \ B_x = 0$$

$$E_y = -cB_z = \frac{k_p y}{4} E_{\mathrm{crit}}$$

$$E_z = cB_y = \frac{k_p z}{4} E_{\mathrm{crit}}$$

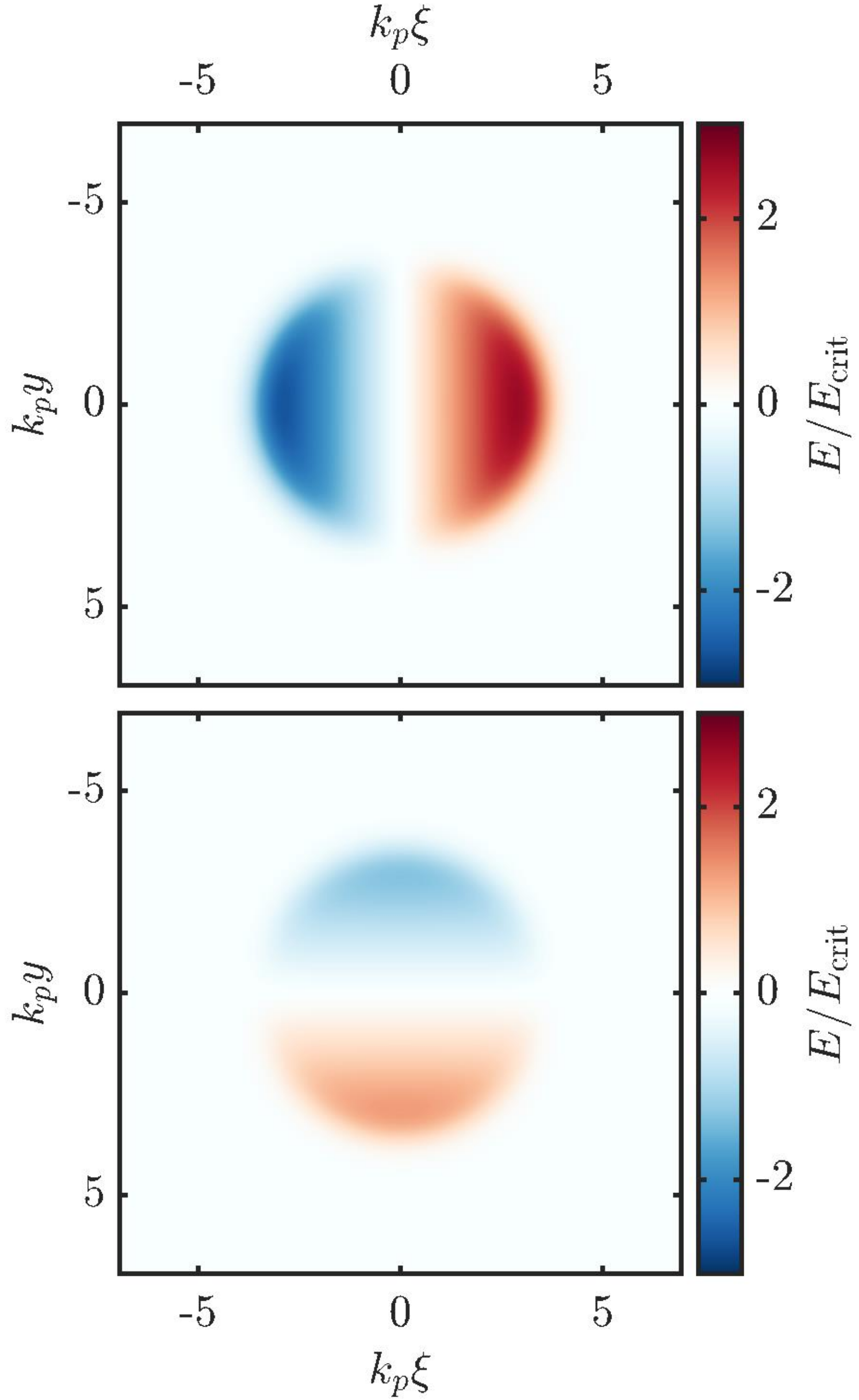

1. Kostyukov, I., Pukhov, A. & Kiselev, S. Phenomenological theory of laser-plasma interaction in 'bubble' regime. Phys. Plasmas 11, 5256 (2004).
   Gordienko, S. & Pukhov, A. Scalings for ultrarelativistic laser plasmas and quasimonoenergetic electrons. Phys. Plasmas 12, 43109 (2005).
2. Lu, W. et al. A nonlinear theory for multidimensional relativistic plasma wave wakefields. Phys. Plasmas 13, 56709 (2006).

Trapping and acceleration in the bubble regime

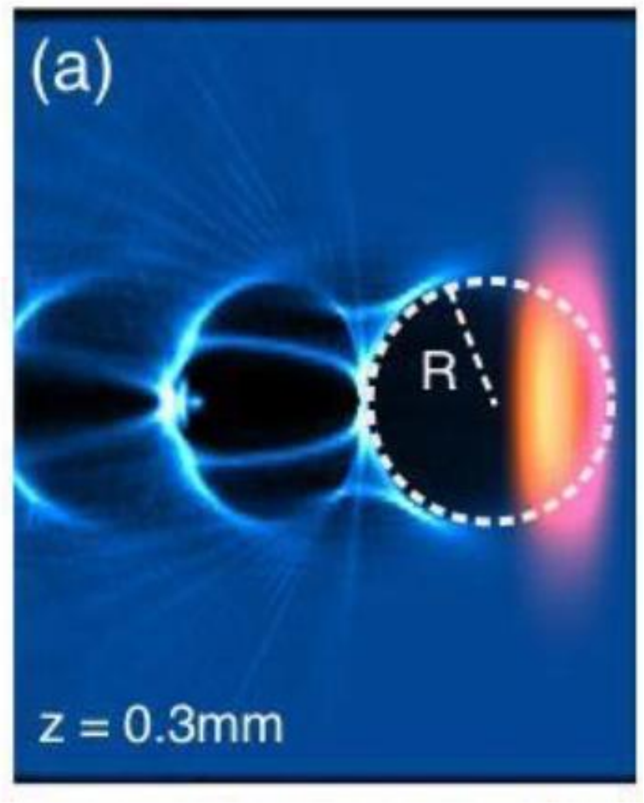

- Empirical match to plasma bubble radius from PIC simulations

$$r_b = \frac{2\sqrt{a_0}}{k_p} \quad \text{therefore} \quad E_{x,\max} = \sqrt{a_0} E_{\mathrm{crit}}$$

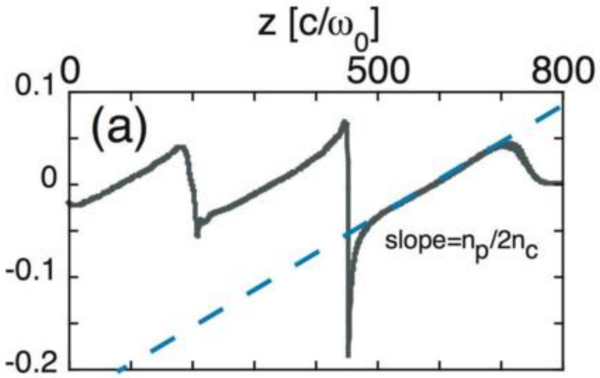

- The minimum electron field has a spike at the crossing point at the back of the bubble
- The field structure moves at the reduced group velocity due to pulse front etching

$$v_g = c\left[\sqrt{1-\left(\frac{\omega_p}{\omega_0}\right)^2}\right] - v_{\mathrm{etch}}$$

$$= c\left[\sqrt{1-\left(\frac{\omega_p}{\omega_0}\right)^2} - \left(\frac{\omega_p}{\omega_0}\right)^2\right]$$

$$v_g \approx c\left[1 - \frac{3}{2}\left(\frac{\omega_p}{\omega_0}\right)^2\right]$$

1. Lu, W. et al. Generating multi-GeV electron bunches using single stage laser wakefield acceleration in a 3D nonlinear regime. Phys. Rev. Spec. Top. - Accel. Beams 10, 61301 (2007).

Trapping and acceleration in the bubble regime

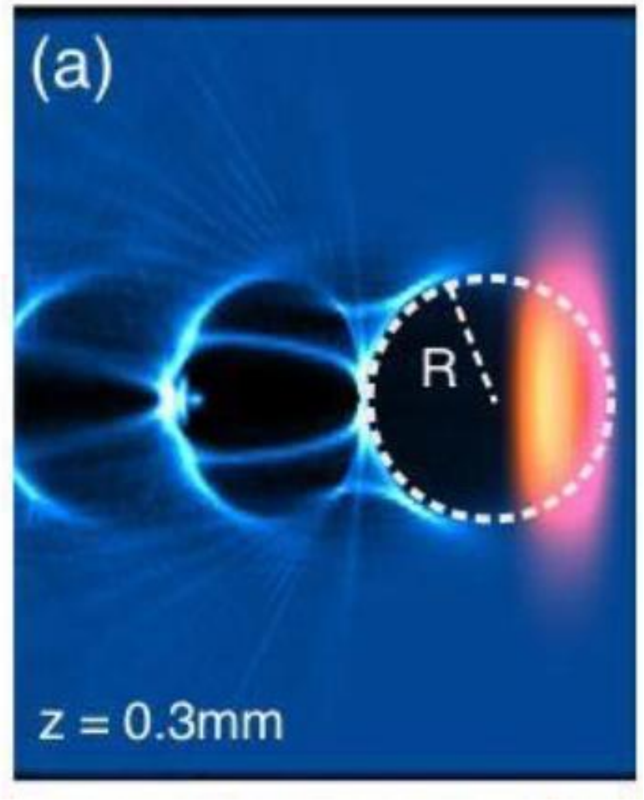

- In this regime the depletion and dephasing lengths are:

$$L_{dp} = \frac{{\omega_0}^2}{{\omega_p}^2}\sigma_t c \qquad L_d = \frac{4\sqrt{a_0}}{3}\frac{{\omega_0}^2}{{\omega_p}^3}c$$

- Acceleration for $a_0 = 3 \quad n_e = 10^{18}\ \mathrm{cm}^{-3}$

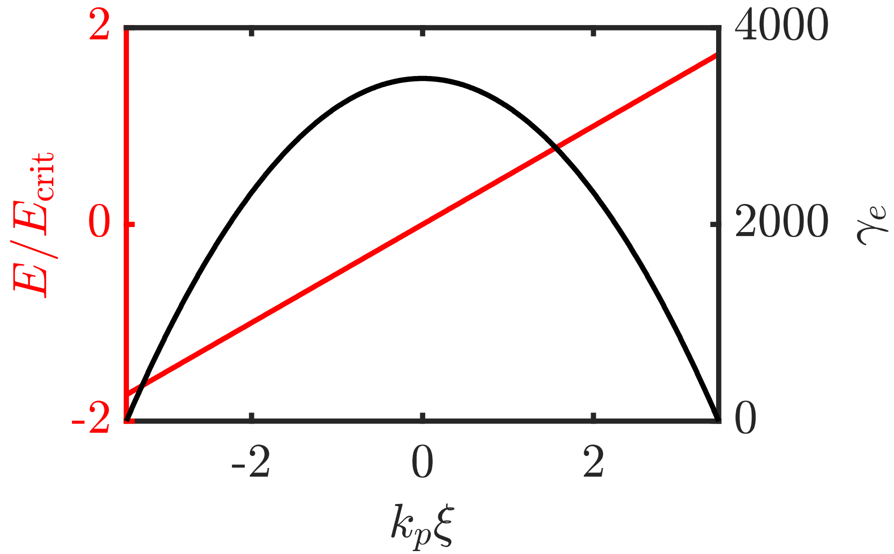

$$W_{\max} = \frac{2a_0}{3}\frac{{\omega_0}^2}{{\omega_p}^2}m_e c^2$$

1. Lu, W. et al. Generating multi-GeV electron bunches using single stage laser wakefield acceleration in a 3D nonlinear regime. Phys. Rev. Spec. Top. - Accel. Beams 10, 61301 (2007).

Trapping and acceleration in the bubble regime

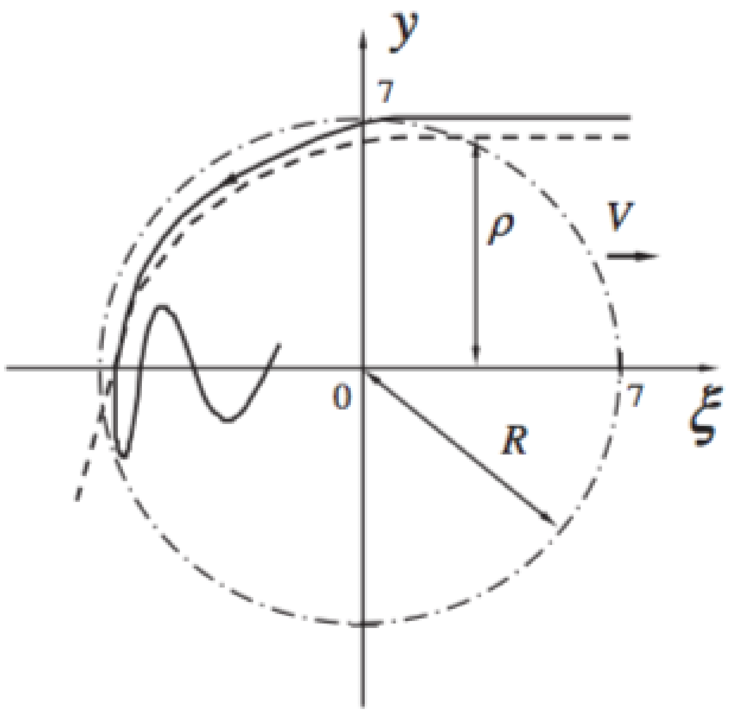

FIG. 1. Trajectory of the trapped (solid line) and untrapped electron (dashed line) calculated by numerical solution of Eqs. (1) and (2) and the bubble border (dashed circle). The coordinates are given in c/ω_p.

- Electrons are injected at the rear of the bubble with a large transverse momentum.
- Injected electrons originate from an annulus of plasma.
- This simple model shows how electrons can be injected – although it does not match the observed thresholds in simulations or experiments

1. Kostyukov, I., Pukhov, A. & Kiselev, S. Phenomenological theory of laser-plasma interaction in 'bubble' regime. Phys. Plasmas 11, 5256 (2004).

Trapping and acceleration in the bubble regime

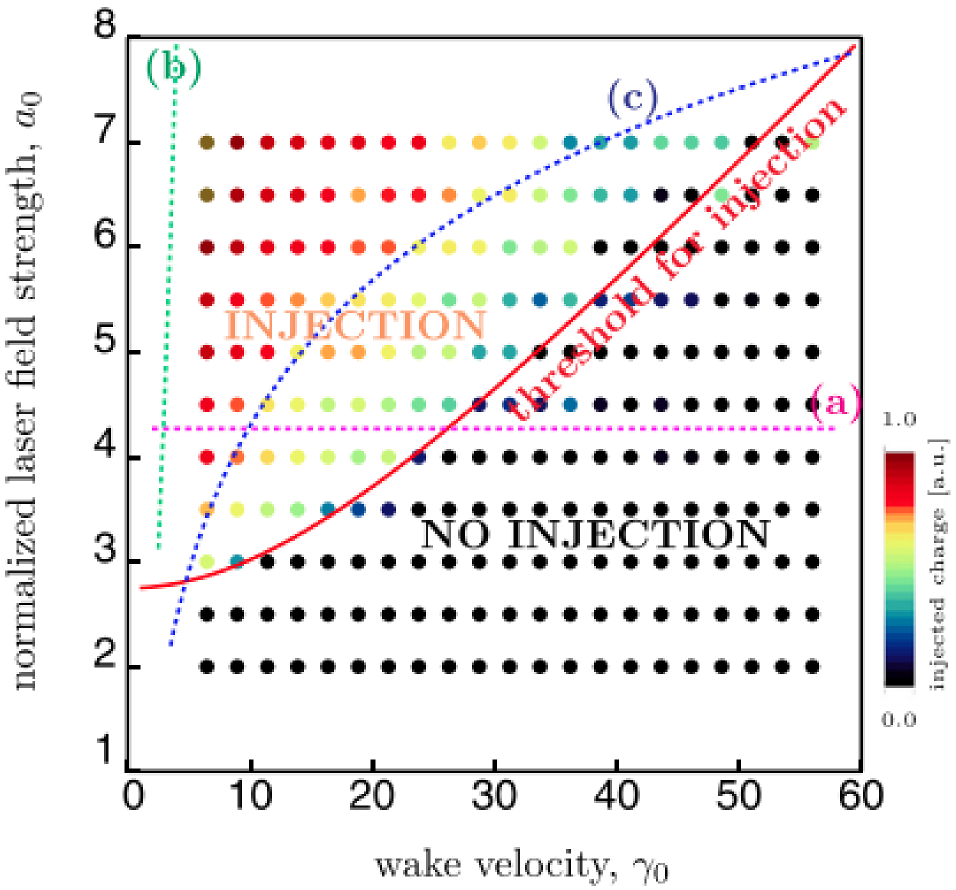

Self-injection threshold based on PIC results [1]

$$a_0 \geq 2.75\sqrt{1+\left(\frac{\gamma_\phi}{22}\right)^2 2}$$

Best performing analytical model [2]

$$a_0 \gtrsim \ln\left[2{\gamma_\phi}^2\right]-1$$

In reality pulse evolution needs to be taken into account.

1. Benedetti, C., Schroeder, C. B., Esarey, E., Rossi, F. & Leemans, W. P. Numerical investigation of electron self-injection in the nonlinear bubble regime. Phys. Plasmas 20, 103108 (2013).
2. Thomas, A. G. R. Scalings for radiation from plasma bubbles. Phys. Plasmas 17, 56708 (2010).

Controlled injection methods: density down ramp

A negative density gradient reduces the phase velocity of the wake as the bubble expands as it propagates

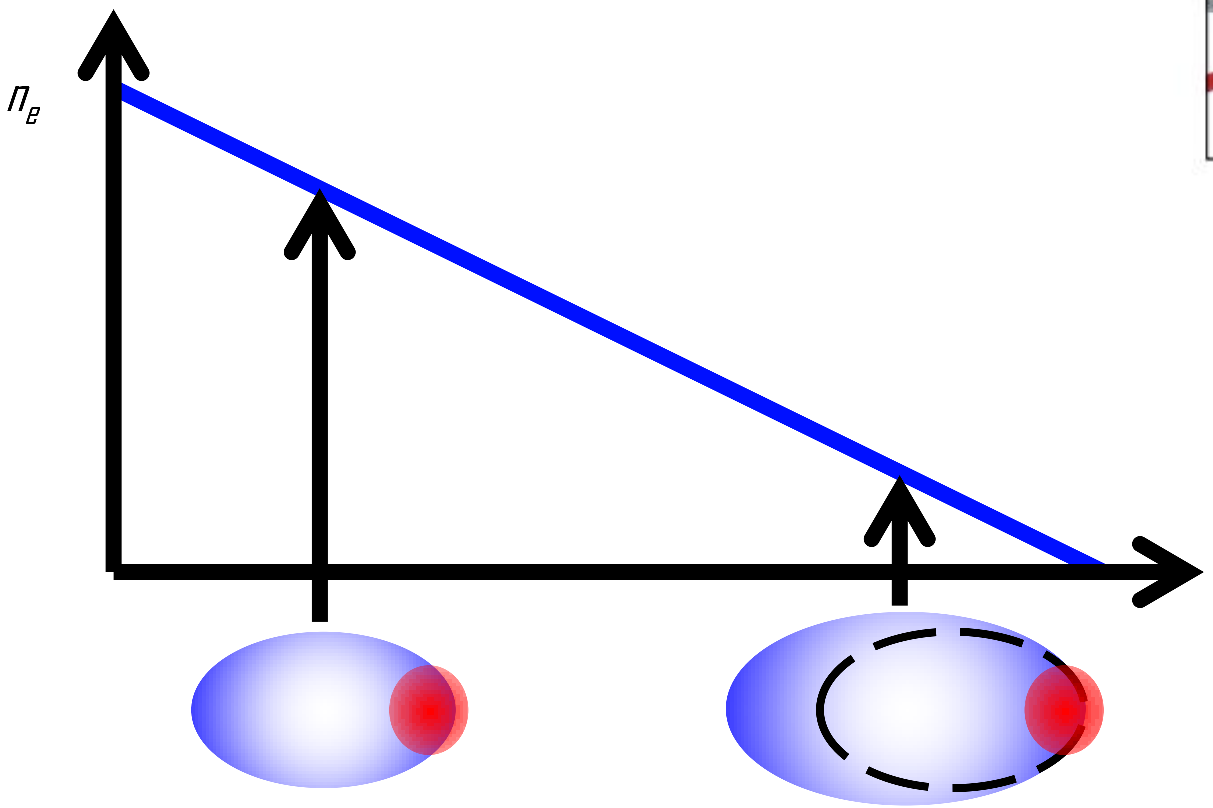

$$r_b = \frac{2\sqrt{a_0}}{k_p} = \frac{2\sqrt{a_0 m_e \epsilon_0}c}{e}{n_e}^{-1/2}$$

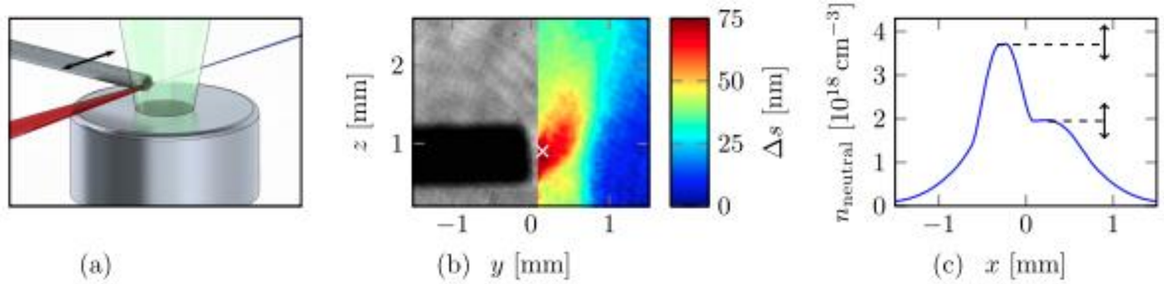

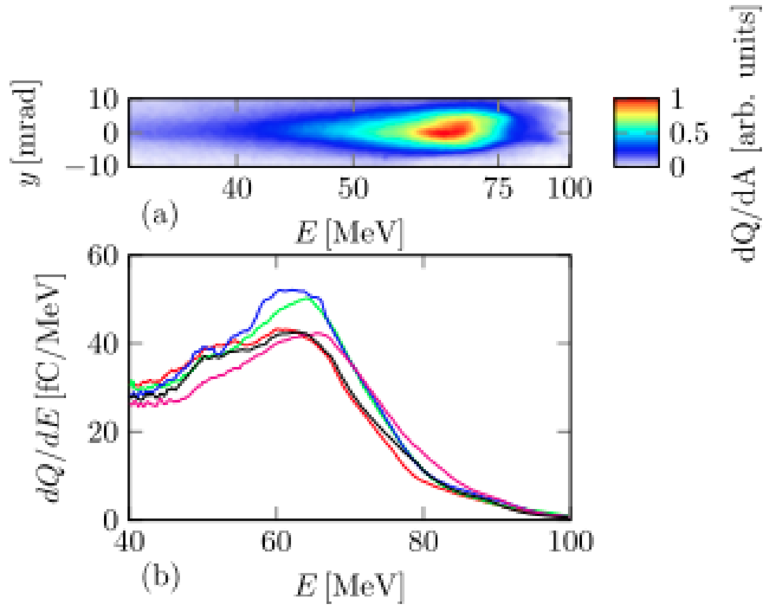

1. Hansson, M. et al. Phys. Rev. Spec. Top. - Accel. Beams 18, 71303 (2015).

Controlled injection methods: density down ramp

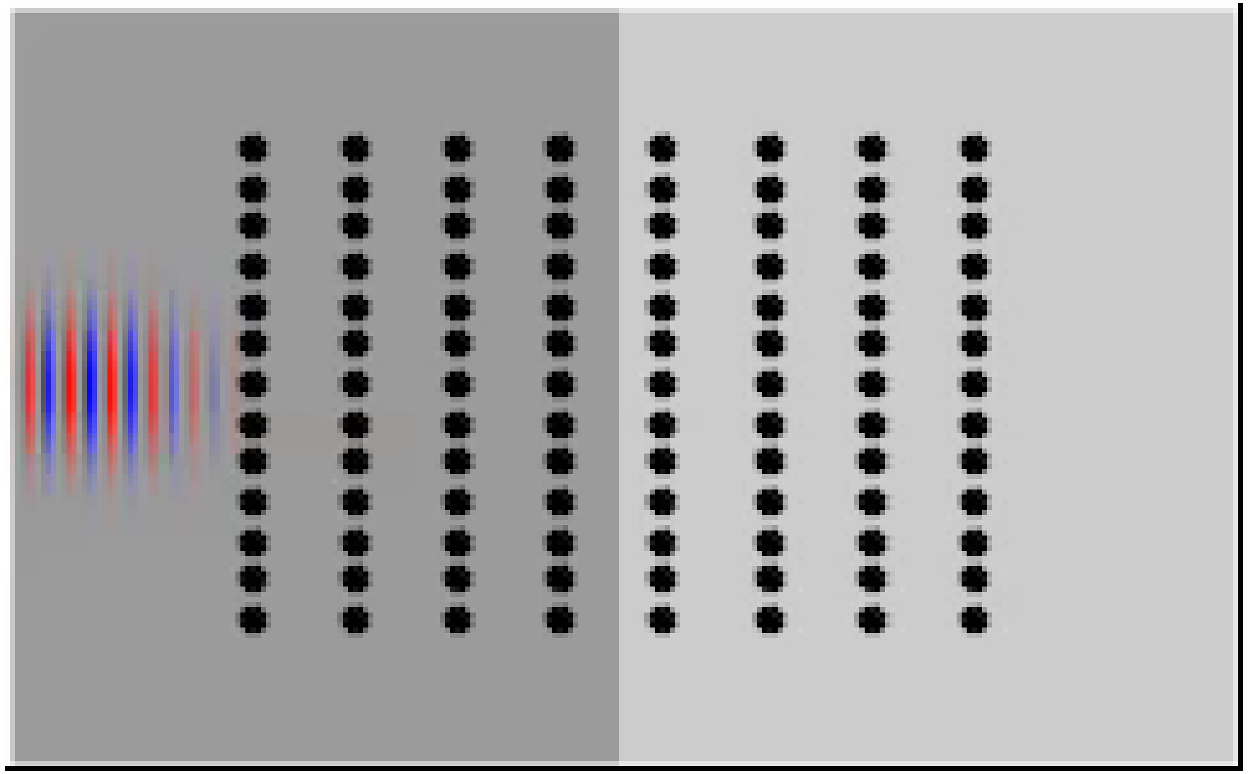

Plasma particle oscillations with a density step

Controlled injection methods: ionization injection

- For $a_0 \sim 1$ the low Z gasses we normally use are ionized far ahead of the peak of the laser pulse
- We can dope the low Z gas with a high Z gas so that some ionization levels are close to the peak of the laser

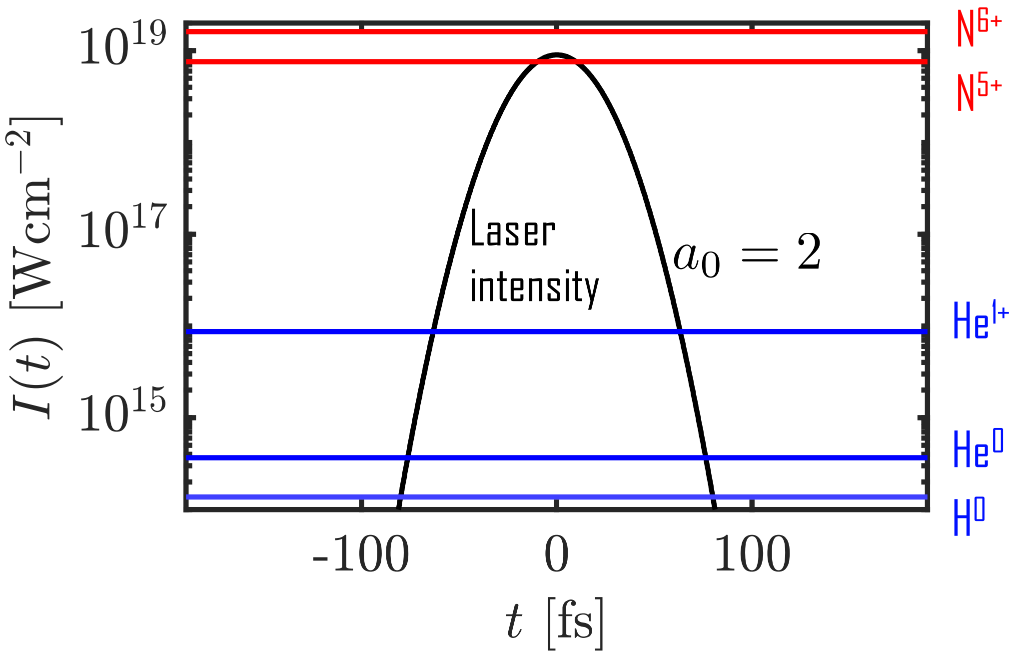

$$I_{\mathrm{app}} = \frac{c\mathcal{E}_b{}^4\pi^2\epsilon_0^3}{2e^6Z^2}$$

Appearance intensity for BSI [1]

Controlled injection methods: ionization injection

- By ionizing close the laser peak we can access trajectories that can not be reached by self-injection of plasma electrons

Minimum trapped trajectory for $a_0 = 2$

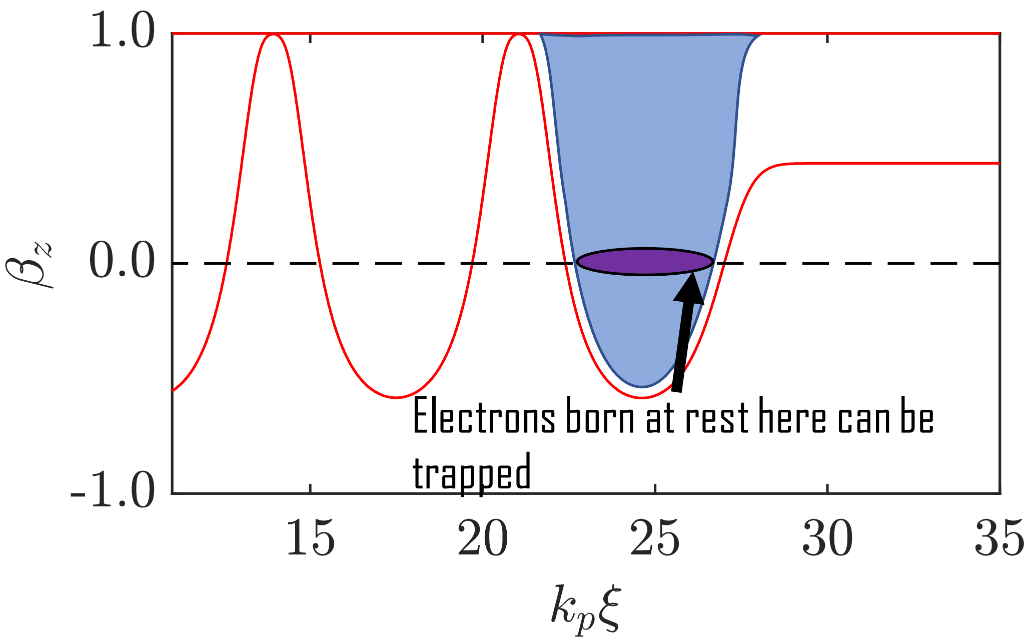

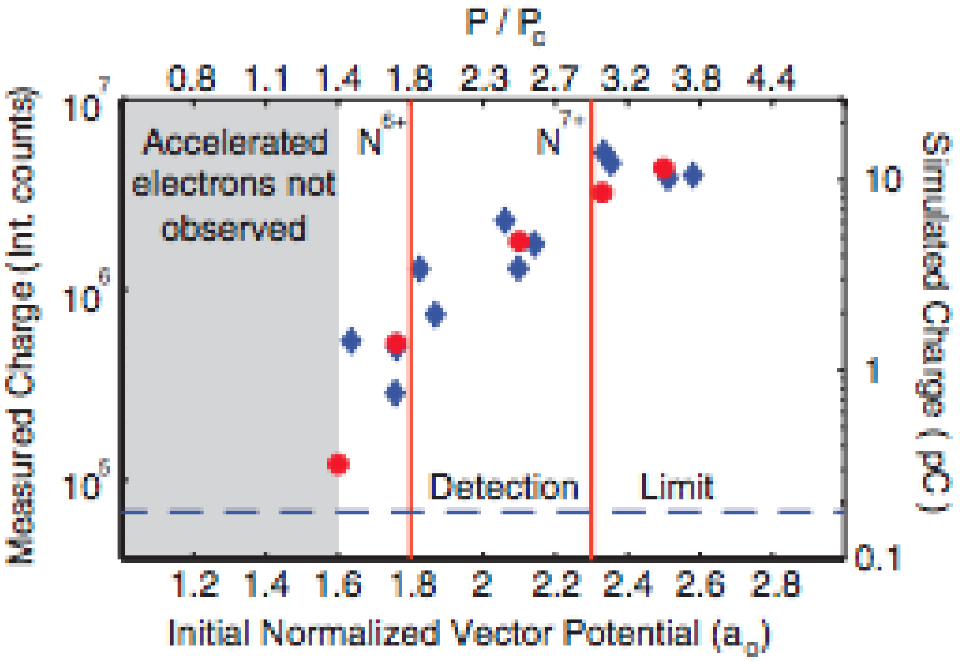

1. Pak, A. et al. Injection and Trapping of Tunnel-Ionized Electrons into Laser-Produced Wakes. Phys. Rev. Lett. 104, 25003 (2010).

Controlled injection methods: ionization injection

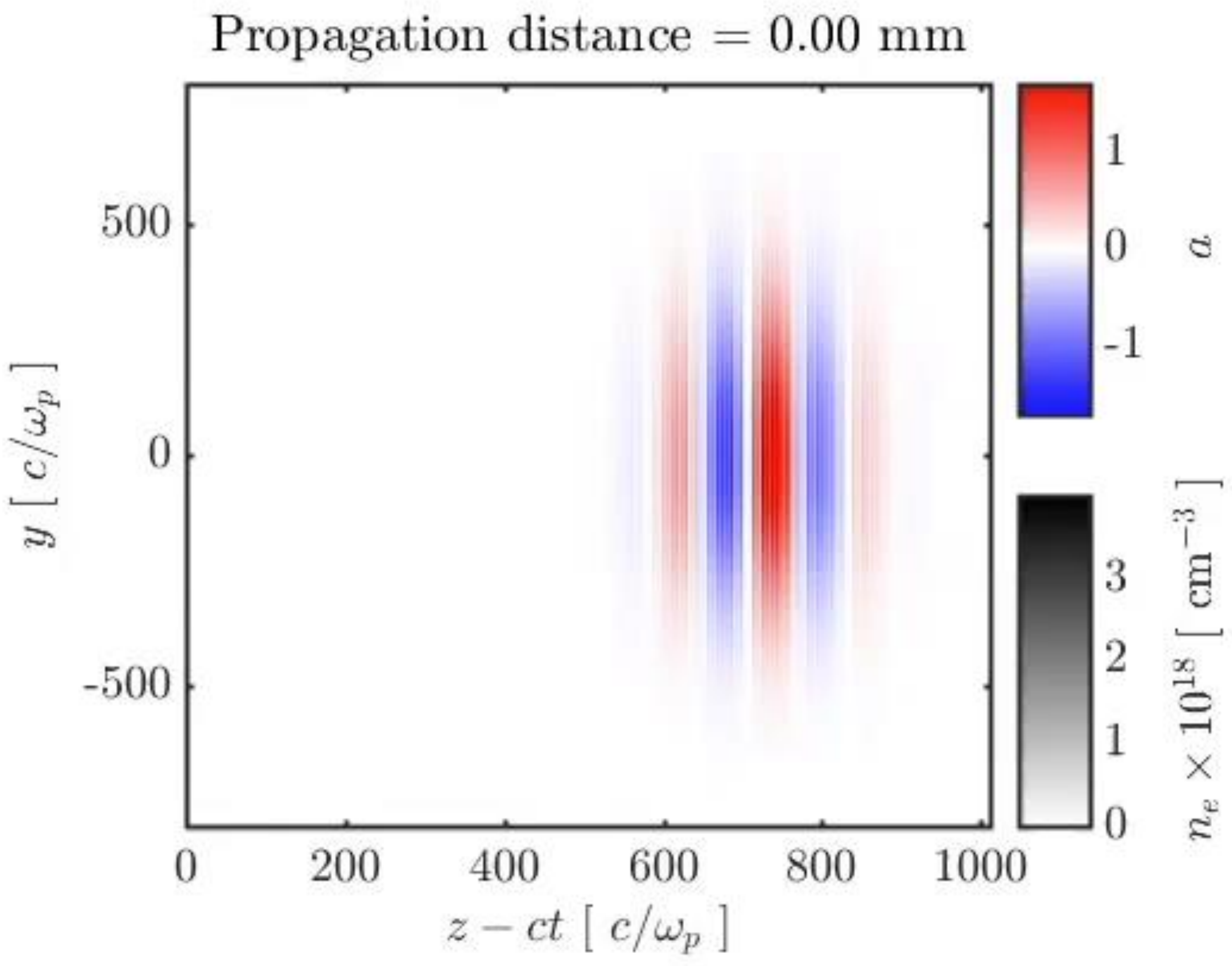

Controlled injection methods: colliding pulse injection

- One [1] or two [2] additional laser pulses can be used to collide inside the plasma wave to modify the energy of the electrons.
- A beat wave between the two colliding lasers can move electrons into trapped orbits

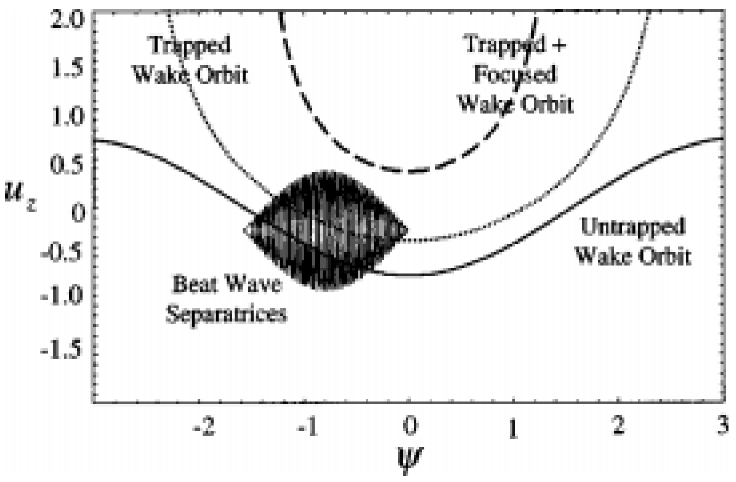

FIG. 4. Phase space (ψ, u_z) showing the beat wave separatrices, an untrapped plasma wake orbit (solid line), a trapped plasma wake orbit (dotted line), and a trapped and focused plasma wake orbit (dashed line).

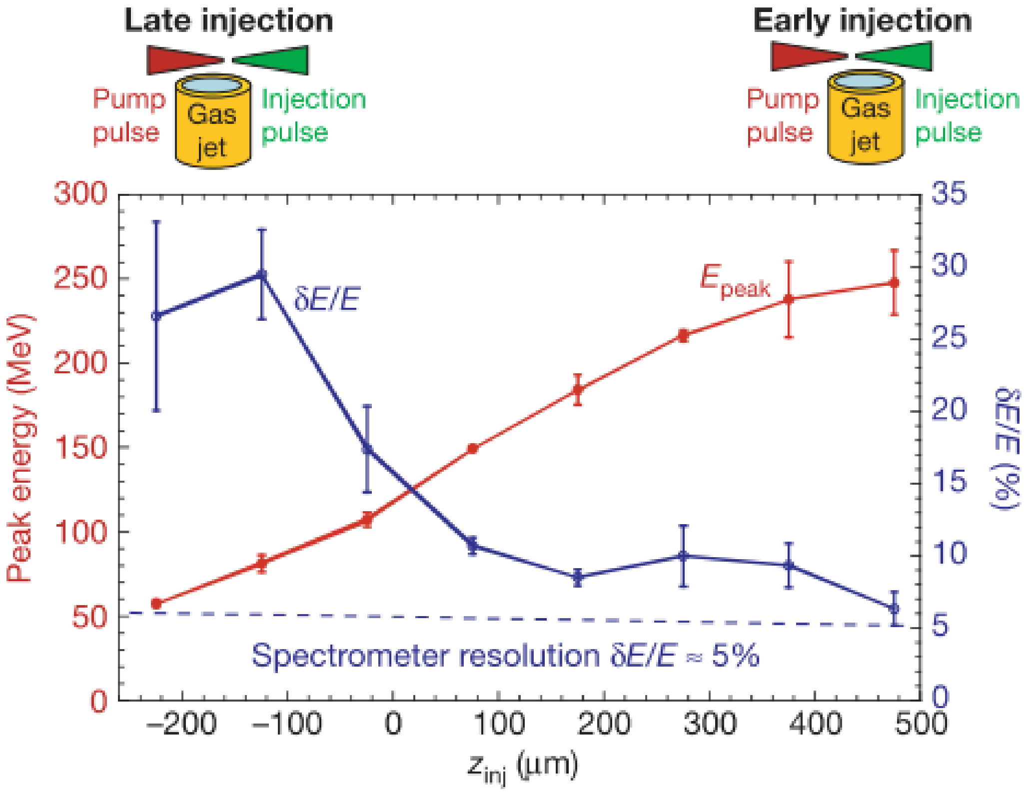

1. Fubiani, G., Esarey, E., Schroeder, C. B. & Leemans, W. P. Beat wave injection of electrons into plasma waves using two interfering laser pulses. Phys. Rev. E 70, 16402 (2004).
2. Esarey, E., Hubbard, R. F., Leemans, W. P., Ting, A. & Sprangle, P. Electron Injection into Plasma Wakefields by Colliding Laser Pulses. Phys. Rev. Lett. 79, 2682–2685 (1997).
3. Faure, J. et al. Controlled injection and acceleration of electrons in plasma wakefields by colliding laser pulses. Nature 444, 737–9 (2006).

Electron beam properties: Spectrum

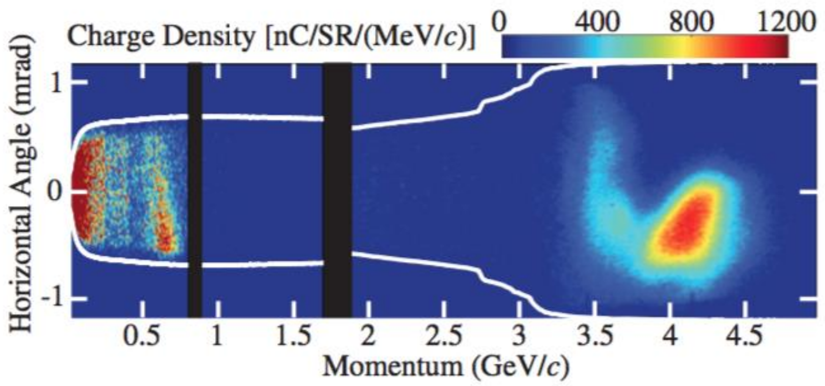

FIG. 5 (color). Energy spectrum of a 4.2 GeV electron beam measured using the broadband magnetic spectrometer. The plasma conditions closely match those in Fig. 2(c). The white lines show the angular acceptance of the spectrometer. The two black vertical stripes are areas not covered by the phosphor screen.

- Maximum energy limited by dephasing and depletion
- Chirp occurs due to extended injection process
- Slice energy spread due to phase area of trapped electrons
- Injected charge depends on mechanism
- Beam loading can occur for high charge bunches which can flatten the fields
- Lowest projected energy spreads on the order of 1%

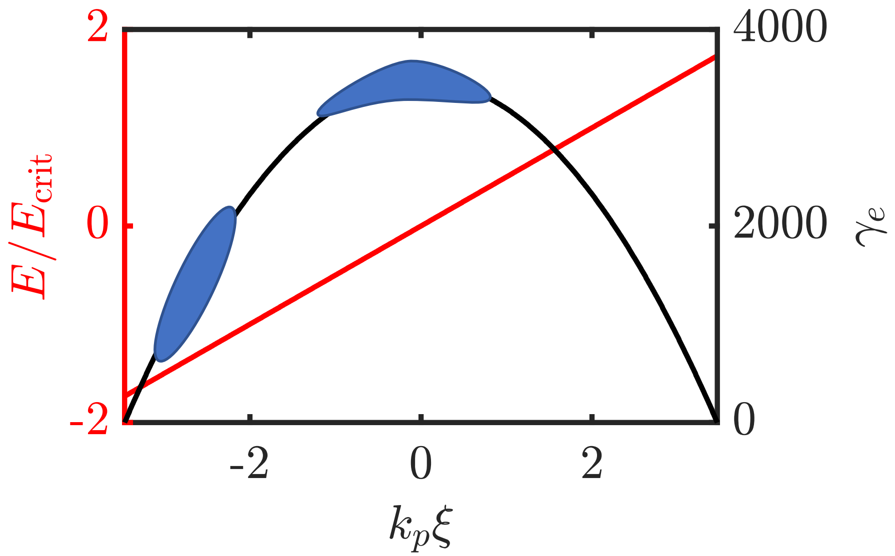

1. Leemans, W. P. et al. Multi-GeV Electron Beams from Capillary-Discharge-Guided Subpetawatt Laser Pulses in the Self-Trapping Regime. Phys. Rev. Lett. 113, 245002 (2014).

Electron beam properties: Bunch length

Transition radiation measurements used to estimate bunch duration

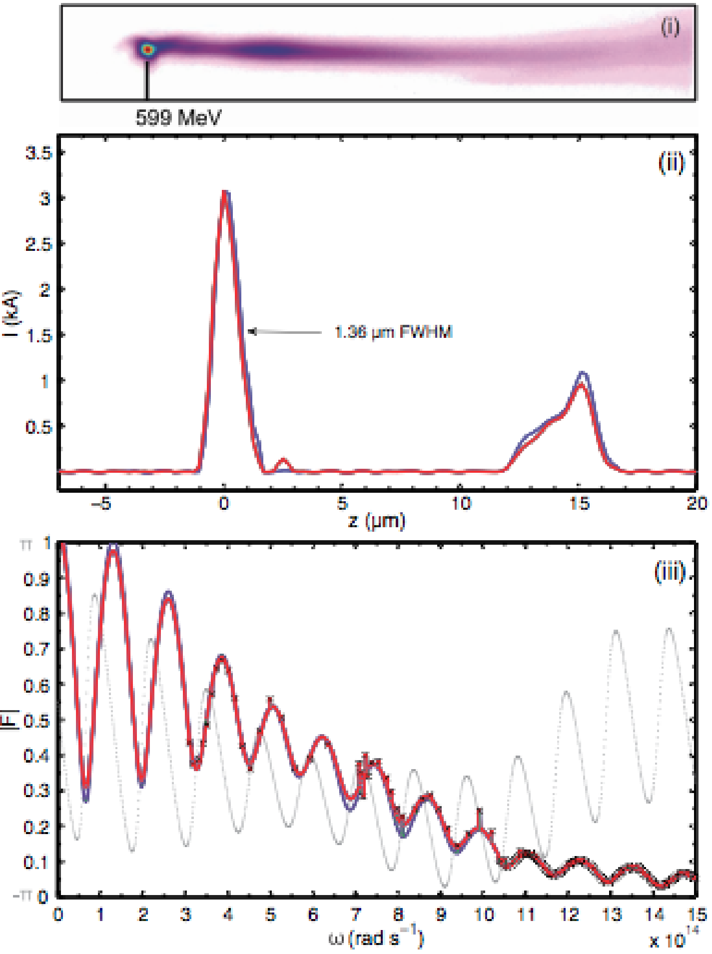

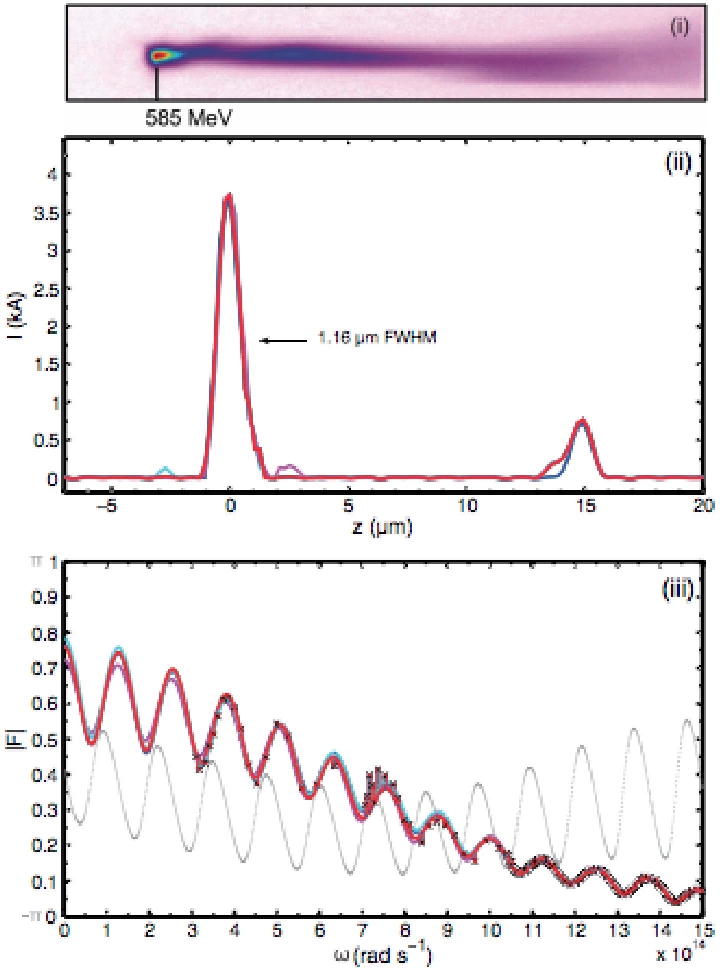

- Bunch length is smaller than the plasma period
- Typically few fs
- Linked to projected energy spectrum due to chirp
- Can also be controlled through injection process

1. Bajlekov, S. I. et al. Longitudinal electron bunch profile reconstruction by performing phase retrieval on coherent transition radiation spectra. Phys. Rev. Spec. Top. - Accel. Beams 16, 40701 (2013).

Electron beam properties: Emittance and transverse offsets

Single shot quadrupole method used to measure sub-micron emittance

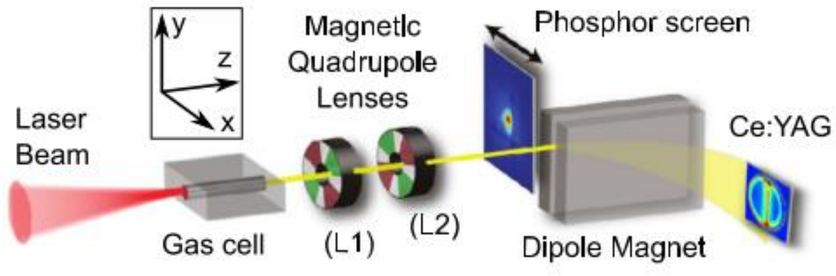

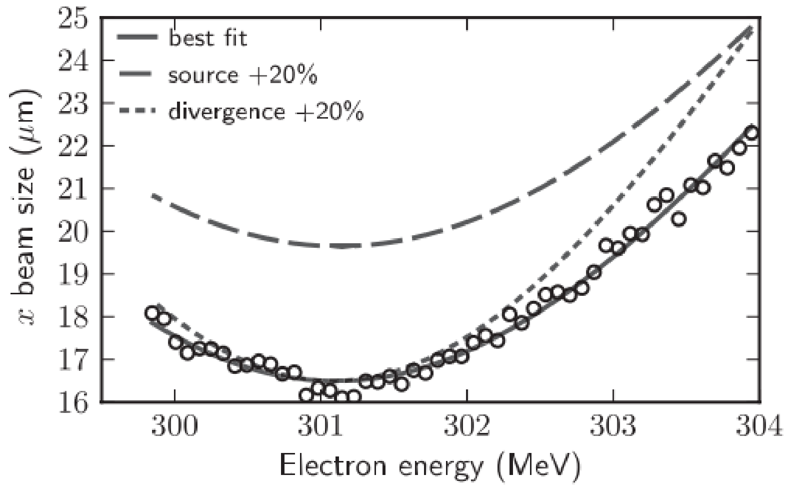

FIG. 3. The rms beam size vs beam energy for a single shot (circles). The solid fit line corresponds to a beam with normalized emittance of $0.14 \pm 0.01\pi$ mm mrad. The other lines show the expected functions for a 20% larger emittance by varying the inferred source size or divergence.

- Slice emittance of the electron bunch is due to variation in trapped electron orbits
- Projected emittance also includes head-to-tail correlations and beam offsets
- Focusing fields causes electrons to oscillate (betatron motion)
- Oscillation frequency and amplitude will vary between electrons

1. Weingartner, R. et al. Ultralow emittance electron beams from a laser-wakefield accelerator. Phys. Rev. Spec. Top. - Accel. Beams 15, 111302 (2012).

Electron beam properties: Stability and tunability

- Stability is affected by laser system stability and fluctuations in target parameters
- Non-linear process very sensitive to fluctuations
- Stability can be increased through use of controlled injection

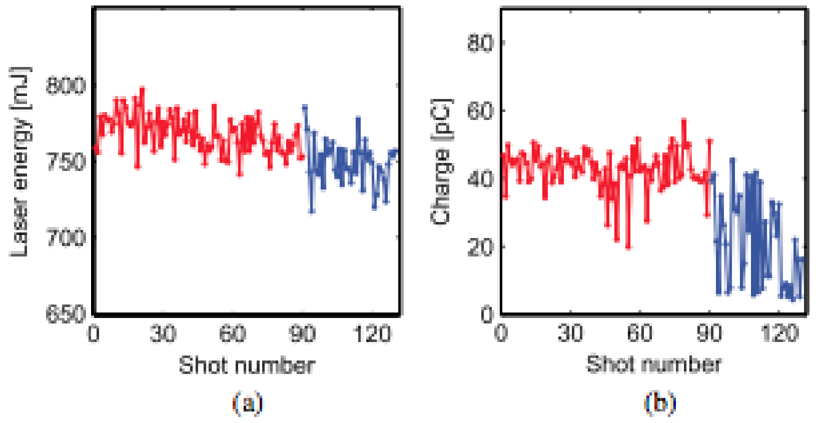

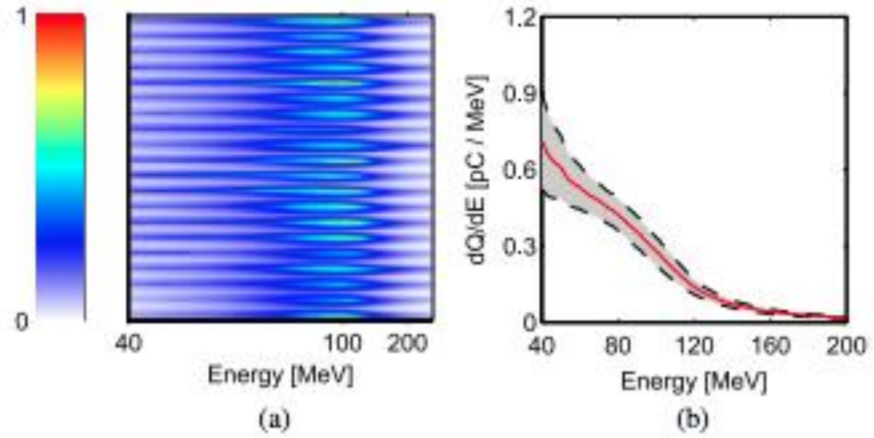

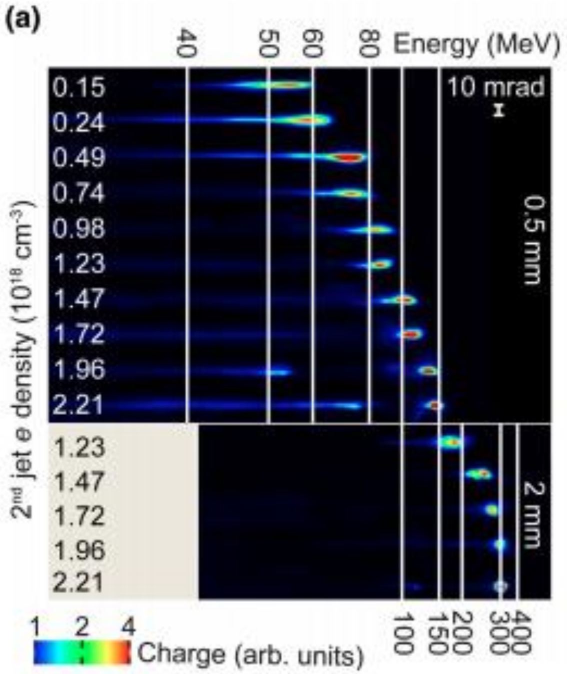

Separating injection and acceleration also allows control of the final beam energy by varying acceleration length or density

1. Hansson, M. et al. Enhanced stability of laser wakefield acceleration using dielectric capillary tubes. PRSTAB 17, 31303 (2014).
2. Golovin, G. et al. Tunable monoenergetic electron beams from independently controllable laser-wakefield acceleration and injection. PRSTAB 18, 11301 (2015).

Electrons oscillate transversely

Phenomenological[1] and kinetic[2] theories have examined the field structure and particle trajectories in the bubble/blowout regime

Simplest model is a sphere of positive charge with a thin sheath of electrons around the edge moving at the laser group velocity

$$E_x = \frac{k_p\xi}{2}E_{\text{crit}} \ , \ \ B_x = 0$$

$$E_y = -cB_z = \frac{k_p y}{4}E_{\text{crit}}$$

$$E_z = cB_y = \frac{k_p z}{4}E_{\text{crit}}$$

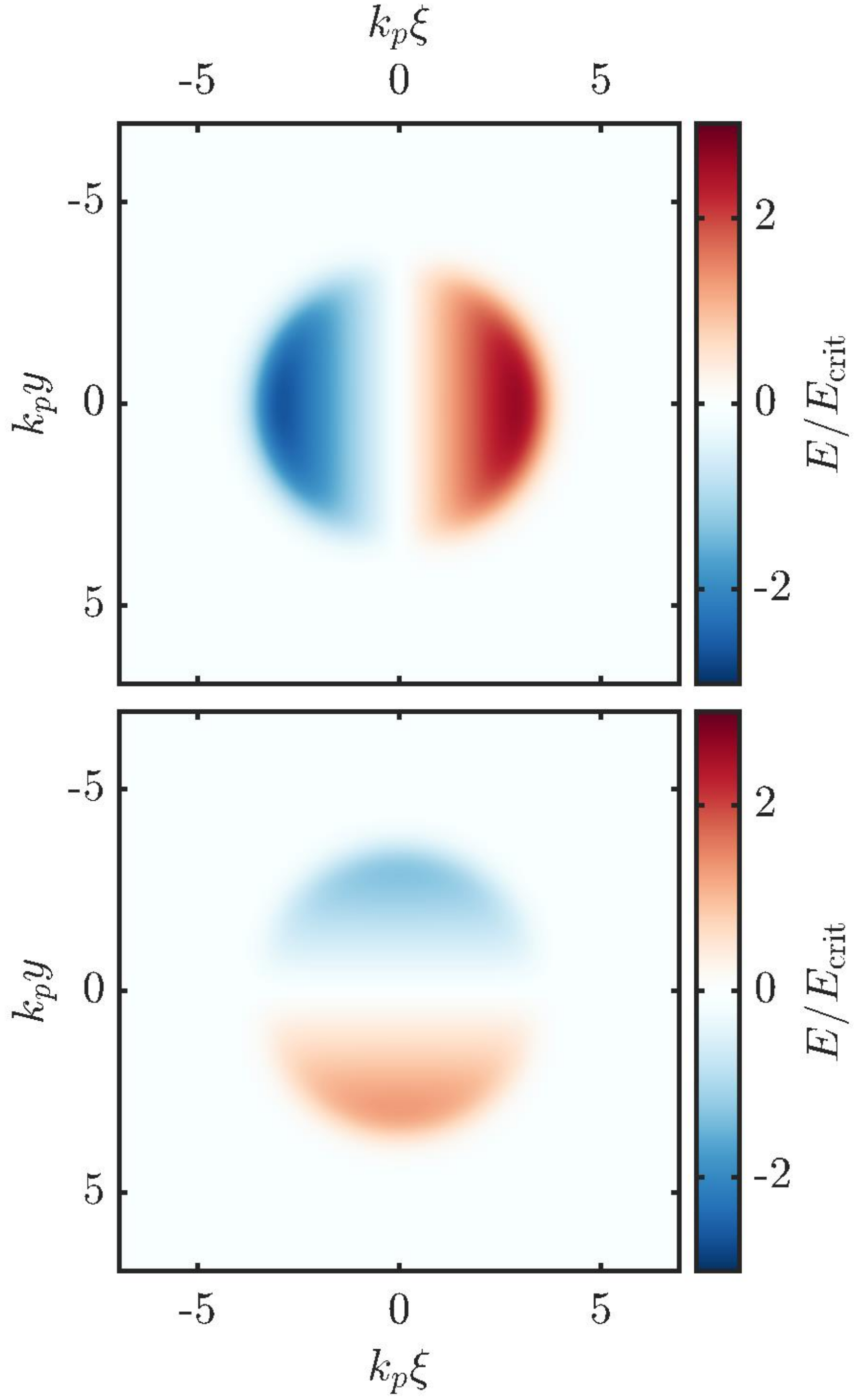

1. Kostyukov, I., Pukhov, A. & Kiselev, S. Phenomenological theory of laser-plasma interaction in 'bubble' regime. Phys. Plasmas 11, 5256 (2004).
Gordienko, S. & Pukhov, A. Scalings for ultrarelativistic laser plasmas and quasimonoenergetic electrons. Phys. Plasmas 12, 43109 (2005).
2. Lu, W. et al. A nonlinear theory for multidimensional relativistic plasma wave wakefields. Phys. Plasmas 13, 56709 (2006).

Betatron oscillations of electrons result in x-ray emission

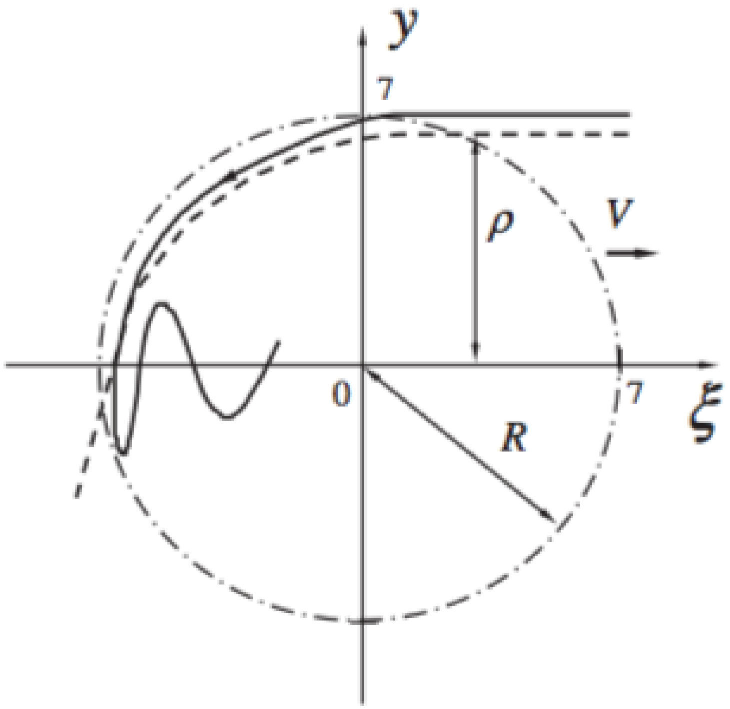

FIG. 1. Trajectory of the trapped (solid line) and untrapped electron (dashed line) calculated by numerical solution of Eqs. (1) and (2) and the bubble border (dashed circle). The coordinates are given in c/ω_p.

- Injected electrons typically have significant transverse momentum
- The strong focusing forces of the plasma wakefield cause the electrons to oscillate radially
- This oscillation leads to dipole emission which is Doppler shifted in the forward direction due to the longitudinal momentum

1. Kostyukov, I., Pukhov, A. & Kiselev, S. Phenomenological theory of laser-plasma interaction in 'bubble' regime. Phys. Plasmas 11, 5256 (2004).

Betatron oscillations of electrons result in x-ray emission

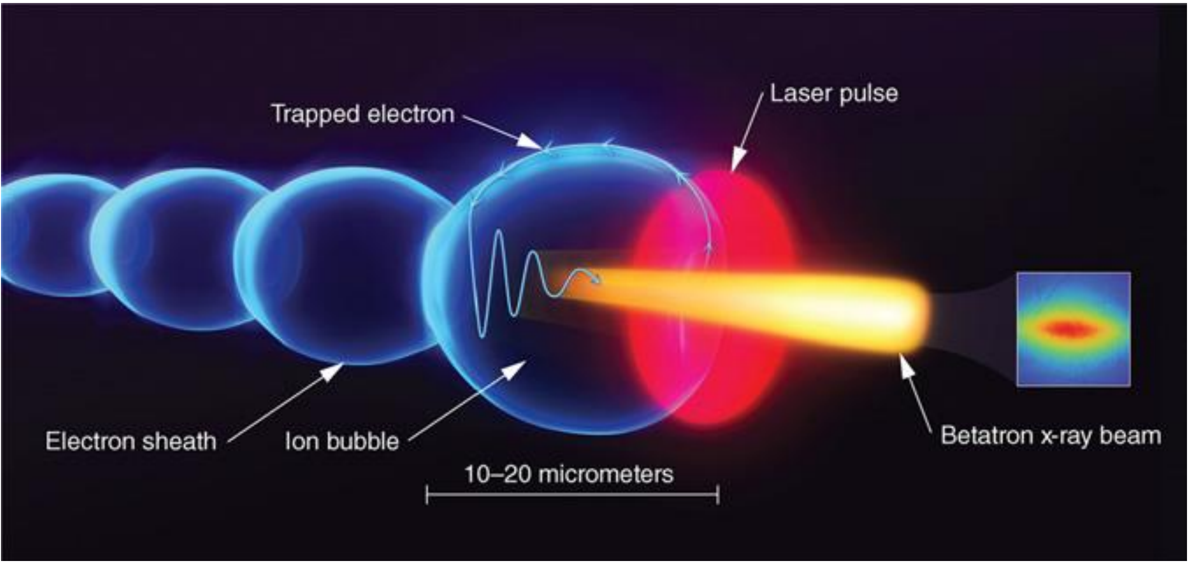

- The transverse motion of an electron in the bubble regime for

$$\gamma = \text{ constant}$$

$$F_{\perp} = -\frac{m_e {\omega_p}^2 r_{\perp}}{2}$$

$$\gamma m_e \frac{\mathrm{d}^2 r_{\perp}}{\mathrm{d}t^2} = -\frac{m_e {\omega_p}^2 r_{\perp}}{2}$$

$$\frac{\mathrm{d}^2 r_{\perp}}{\mathrm{d}t^2} = -\frac{{\omega_p}^2}{2\gamma} r_{\perp}$$

- And so oscillates with the betatron frequency

$$\omega_{\beta} = \frac{\omega_p}{\sqrt{2\gamma}}$$

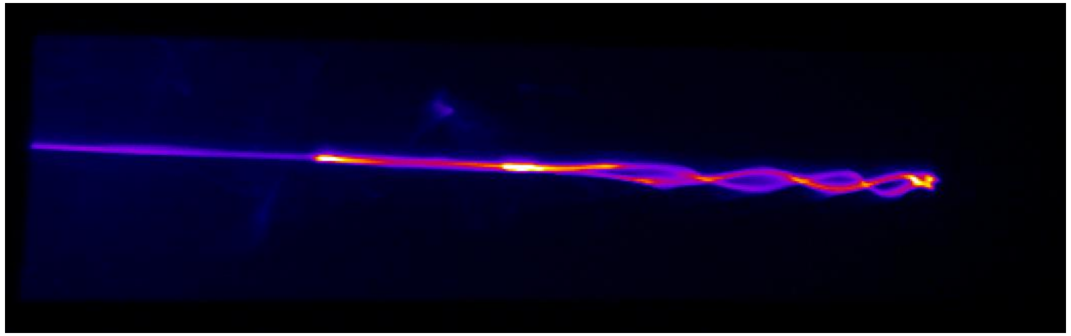

1. Albert, F., et al. Plasma Physics and Controlled Fusion, 56(8), 2014

Betatron oscillations of electrons result in x-ray emission

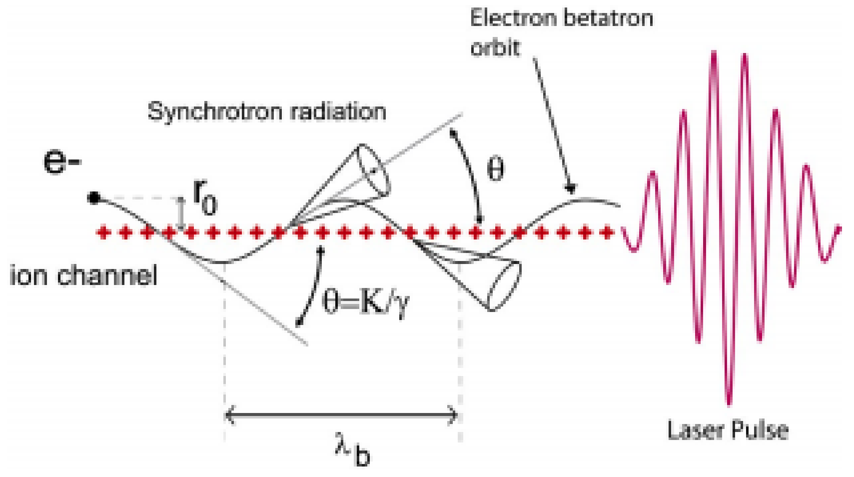

FIG. 1. (Color online). Betatron oscillation and radiation produced by a relativistic electron oscillating in an ion channel. θ is a scaled angle corresponding to the peak angular deflection of the electron. We define the parameter $K=\gamma\theta$ as the strength parameter associated to the channel. The produced synchrotron radiation is confined in a narrow cone of divergence θ.

- The *K* parameter which distinguishes the undulator regime from the wiggler regime is

$$K = \theta\gamma$$

$$K = \sqrt{\frac{\gamma}{2}}\omega_p r_\beta$$

$$K = \gamma\omega_\beta r_\beta$$

- At the maximum energy of an electron beam in the bubble regime with matched conditions [2]

$$K \simeq {\gamma_\phi}^{1/4} a_0$$

And so we are normally well into the wiggler regime

1. Phuoc, K. T. et al. Laser based synchrotron radiation. Phys. Plasmas 12, 23101 (2005).
2. Thomas, A. G. R. Scalings for radiation from plasma bubbles. Phys. Plasmas 17, 56708 (2010).

Betatron oscillations of electrons result in x-ray emission

- The electric and magnetic fields due to an electron in arbitrary motion is given by the Liénard-Wiechert potentials

$$\boldsymbol{E}(\boldsymbol{r},t) = -\frac{e}{4\pi\epsilon_0}\left[\frac{(\boldsymbol{n}-\boldsymbol{\beta})}{\gamma^2(1-\boldsymbol{n}\cdot\boldsymbol{\beta})^3R^2} + \frac{\boldsymbol{n}\times((\boldsymbol{n}-\boldsymbol{\beta})\times\dot{\boldsymbol{\beta}})}{c(1-\boldsymbol{n}\cdot\boldsymbol{\beta})^3R}\right]_{\mathrm{ret}}$$

$$\boldsymbol{B}(\boldsymbol{r},t) = [\boldsymbol{n}\times\boldsymbol{E}]_{\mathrm{ret}}$$

$$R = |\boldsymbol{x}-\boldsymbol{r}(\tau_0)|$$

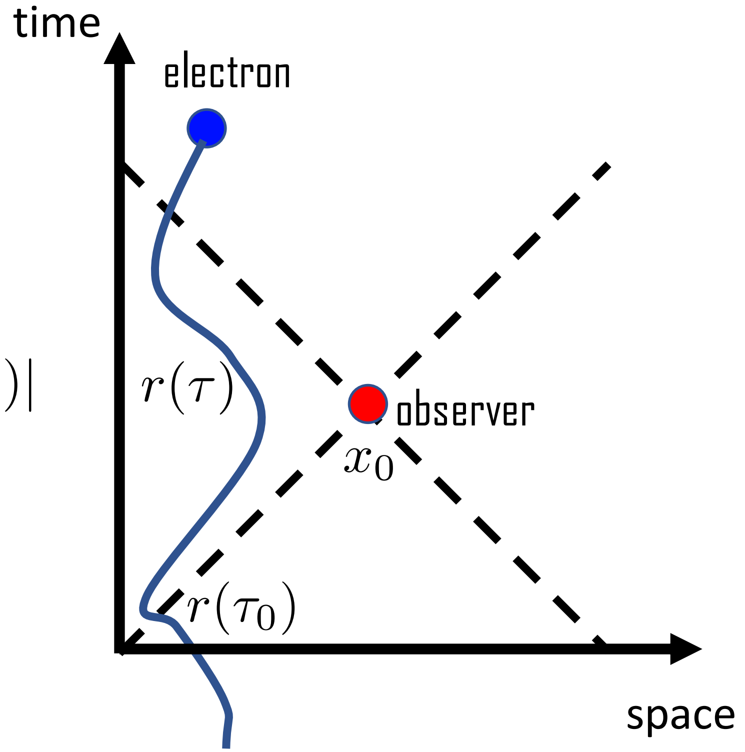

- Fields at a given point are calucated due to particle motion at the 'retarded time', to account for the information speed limit

1. J.D. Jackson, Classical Electrodynamics, Wiley, New York, 3rd Ed. (1999)

Betatron oscillations of electrons result in x-ray emission

Synchrotron spectrum

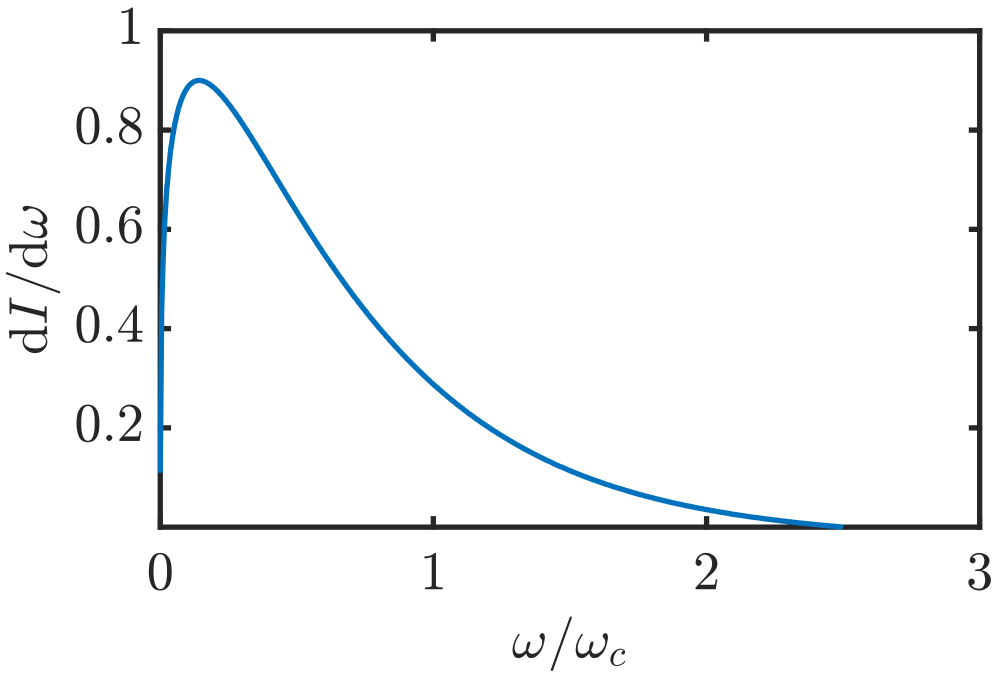

- The radiated spectrum is synchrotron-like

$$\frac{\mathrm{d}I}{\mathrm{d}\omega} \simeq \sqrt{3}\frac{e^2}{\pi\epsilon_0 c}N_\beta\gamma\frac{\omega}{\omega_c}\int_{2\omega/\omega_c}^{\infty}\mathrm{d}\xi\mathcal{K}_{5/3}(\xi)$$

with $\xi = \omega/\omega_c$ and $\omega_c \simeq 3\gamma^2\omega_\beta$

- The emission angle is $\Theta \simeq \omega_\beta r_\beta$

- The radiated power is $P_s = \dfrac{e^2}{12\pi\epsilon_0 c}\gamma^4{\omega_\beta}^4{r_\beta}^2$

- So you can get a lot of high energy photons from a short interaction length

$$\hbar\omega_c \sim 1 - 100\mathrm{keV}$$

1. Esarey, E., Shadwick, B. A., Catravas, P. & Leemans, W. P. Synchrotron radiation from electron beams in plasma-focusing channels. Phys. Rev. E 65, 56505 (2002).

Comparison of peak brightness of LWFA betatron x-ray sources

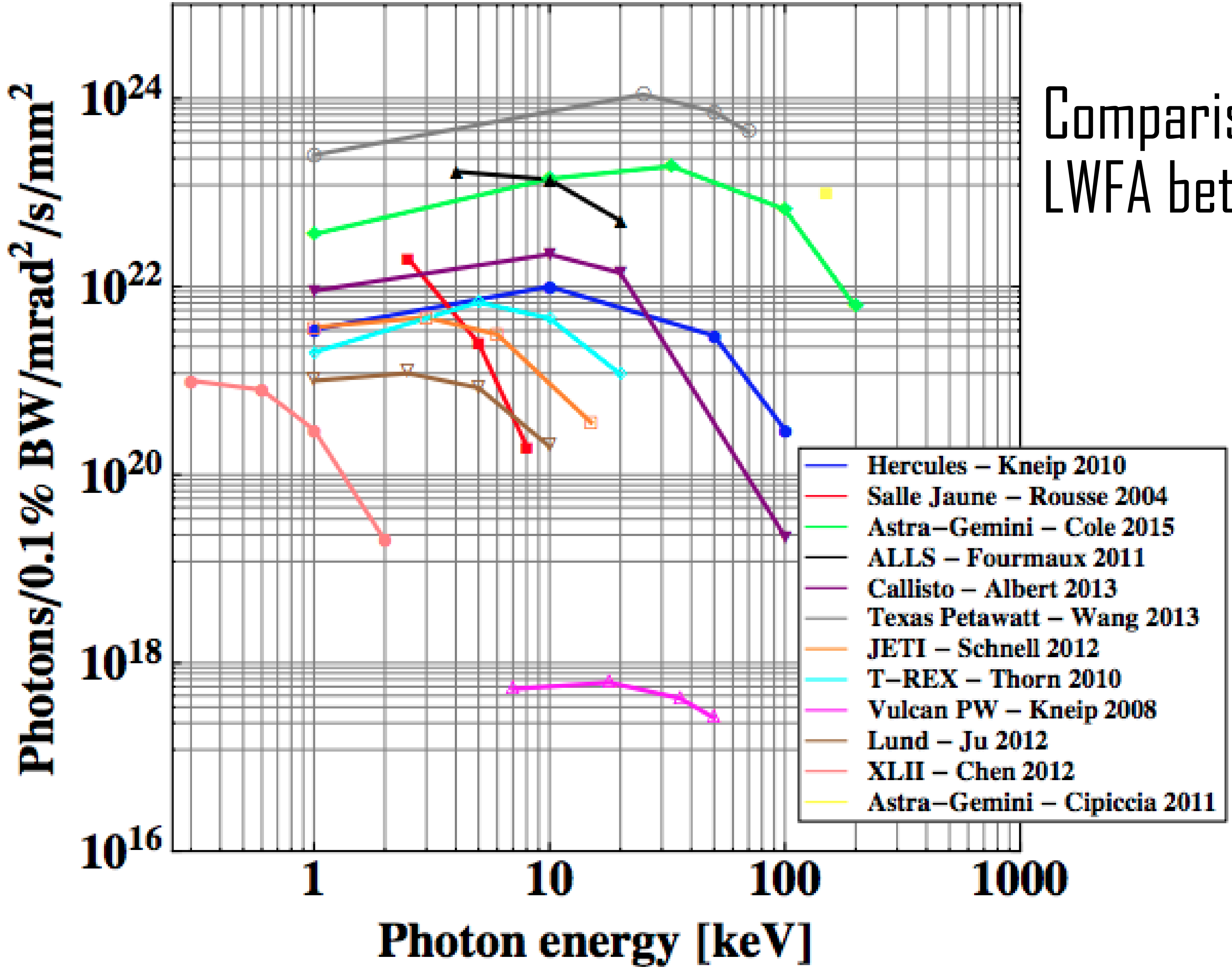

1. Albert, F. & Thomas, A. G. R. Applications of laser wakefield accelerator-based light sources. *Plasma Phys. Control. Fusion* **58,** 103001 (2016).

Imaging with plasma wiggler radiation

Micron scale source size capable of single shot phase contrast imaging and tomography

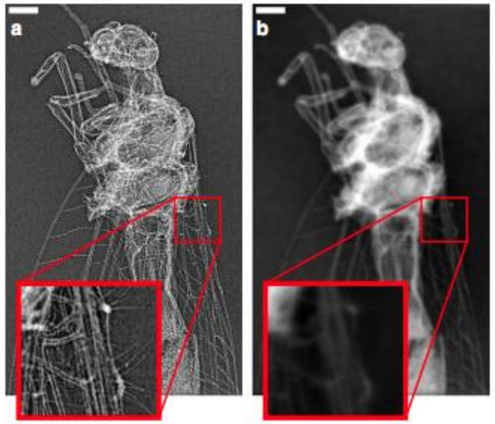

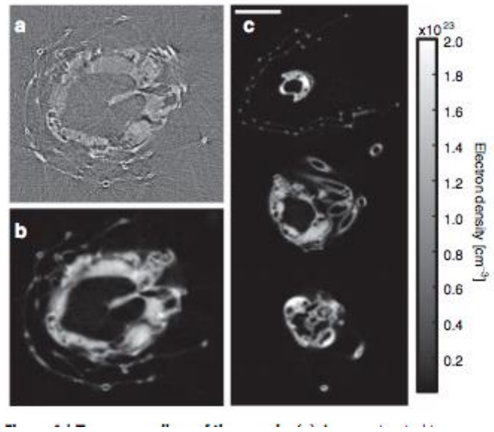

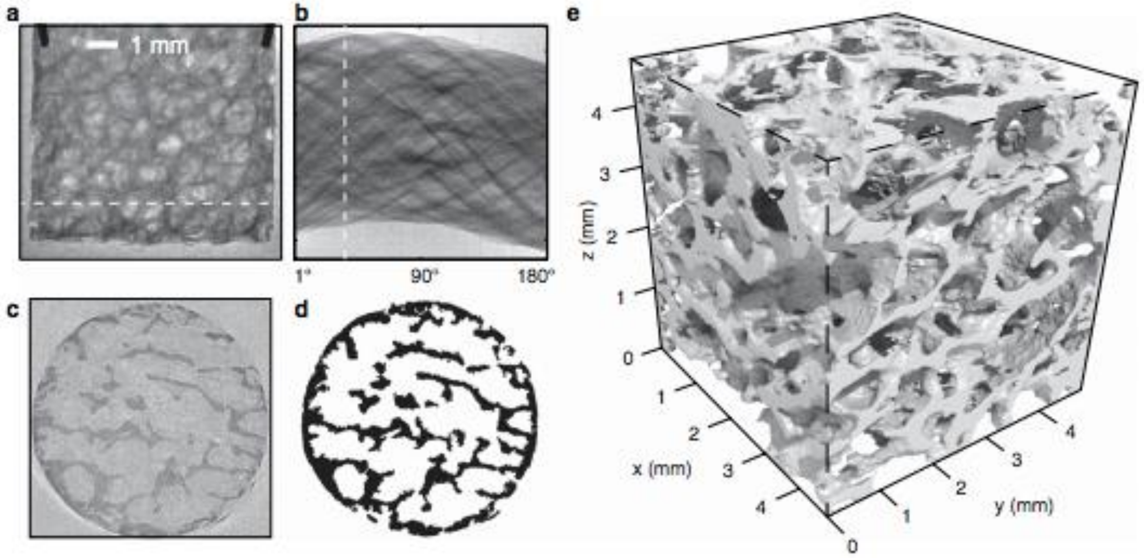

1. Wenz, J. et al. Quantitative X-ray phase-contrast microtomography from a compact laser-driven betatron source. Nat. Commun. 6, 7568 (2015).
2. Cole, J. M. et al. Tomography of human trabecular bone with a laser-wakefield driven x-ray source. Plasma Phys. Control. Fusion 58, 14008 (2016).

Betatron oscillations of electrons result in x-ray emission

Short temporal duration and synchronization to high power laser ideal for pump probe experiments

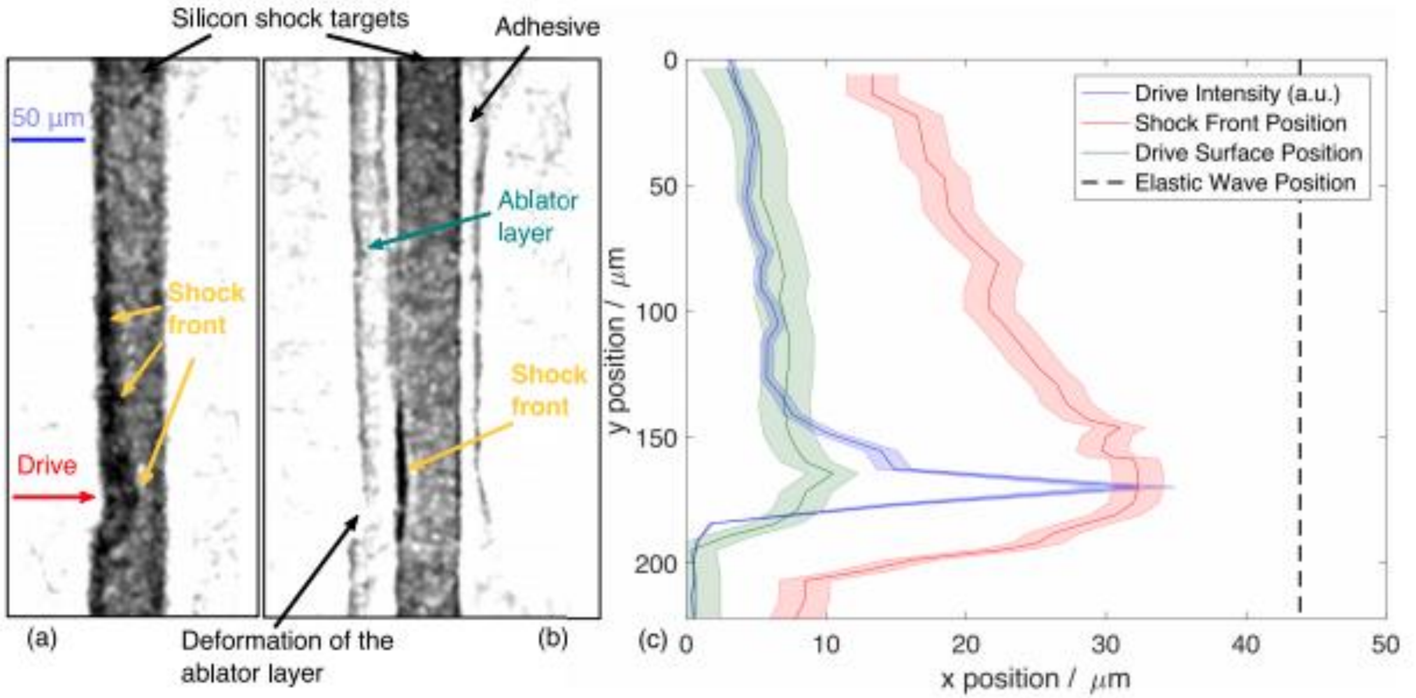

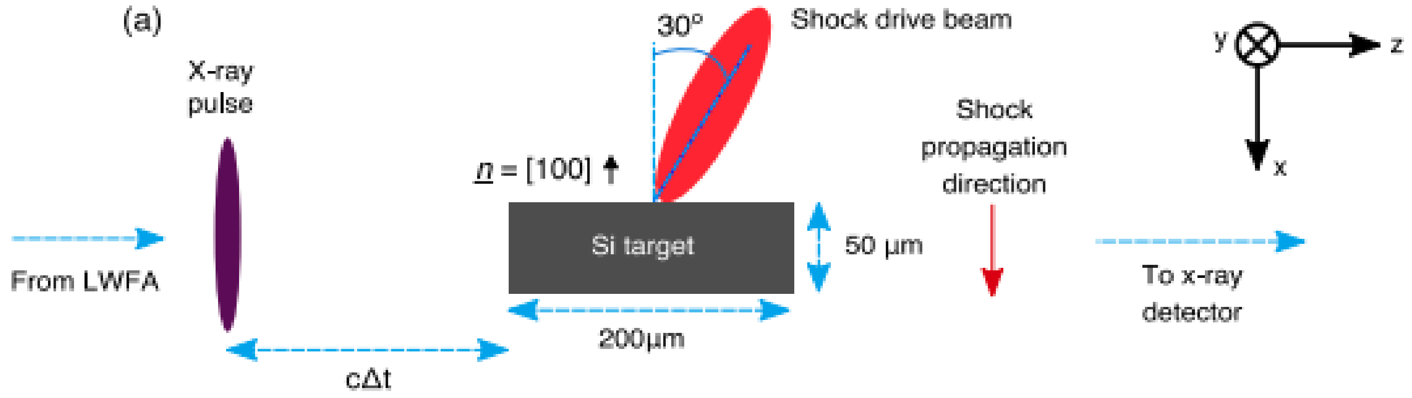

1. Wood, J. C. et al. Ultrafast Imaging of Laser Driven Shock Waves using Betatron X-rays from a Laser Wakefield Accelerator. (2018).

Alternative photon sources

- The accelerated electron bunch can be used to generate photons by several other methods
  - Magnetic undulator/wiggler -> free electron laser
  - Bremstrahhlung through collision with a static target
  - Thomson scattering or inverse Compton Scattering
- There is also considerable interest in using these methods for fundamental studies of quantum effects in radiation reaction and pair production via the Breit-Wheeler process

Inverse Compton scattering

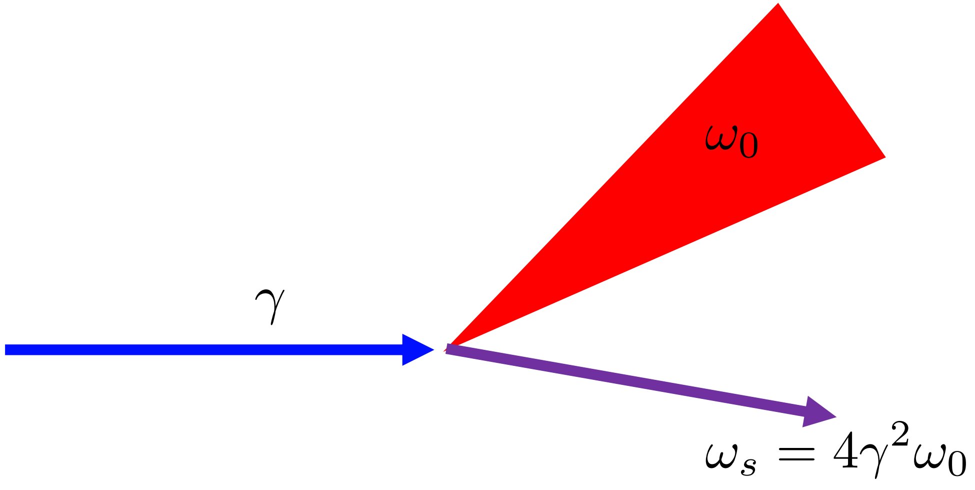

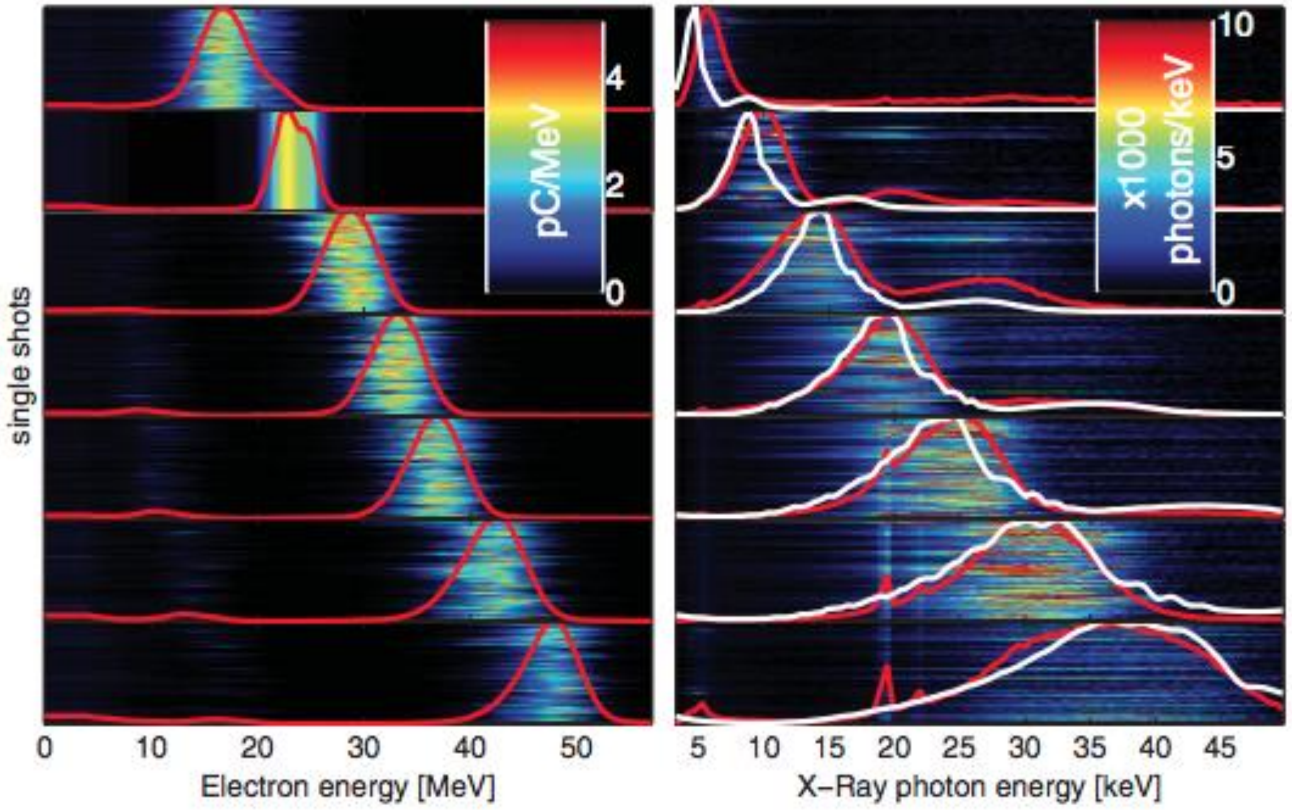

- Laser field causes the electron bunch to oscillate
- Laser frequency Doppler shifted up in rest frame of electron ar emission is Doppler shifted up again back in lab frame

1. Khrennikov, K. *et al.* Tunable All-Optical Quasimonochromatic Thomson X-Ray Source in the Nonlinear Regime. *Phys. Rev. Lett.* **114,** 195003 (2015).

Inverse Compton scattering

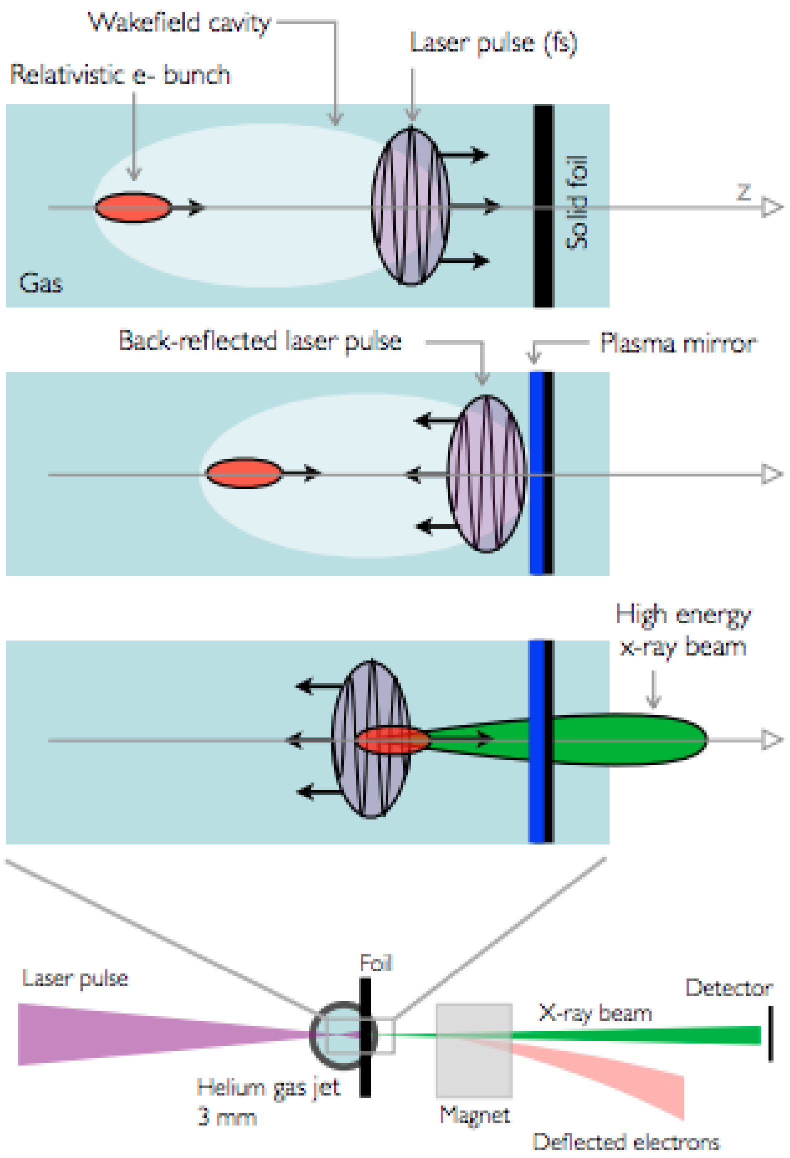

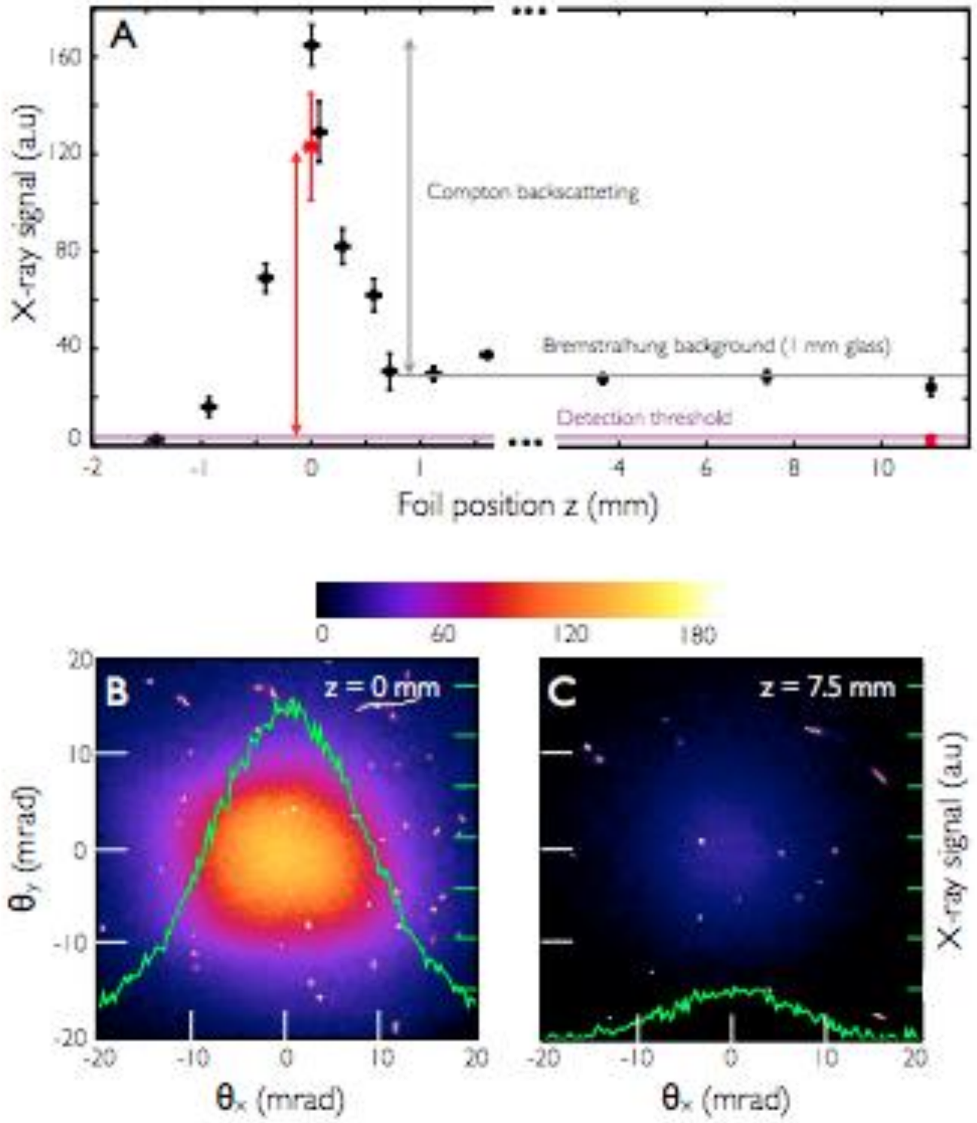

1. Ta Phuoc, K. *et al.* All-optical Compton gamma-ray source. *Nat. Photonics* **6,** 308–311 (2012).

Experimental tests of quantum radiation reaction

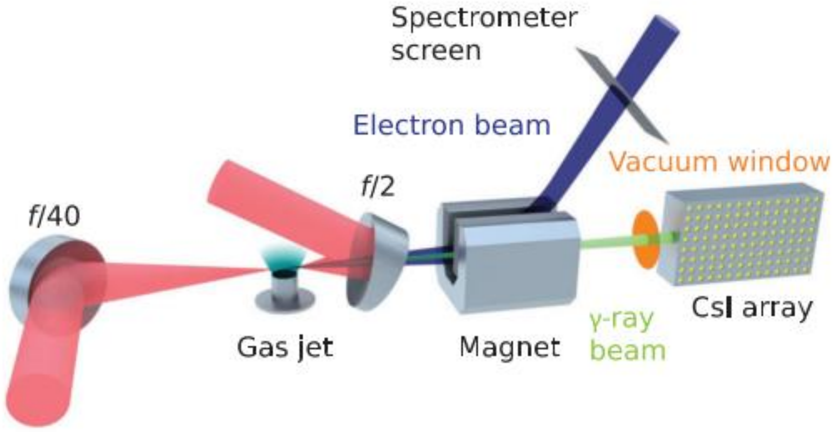

FIG. 1. Schematic of the experimental setup. All components are inside a vacuum chamber except for the CsI array.

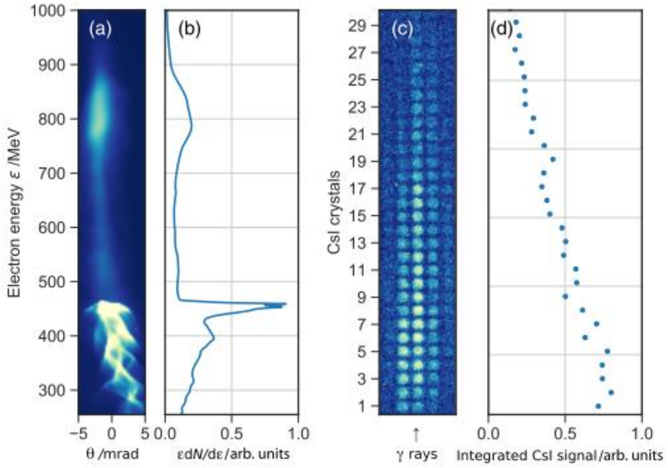

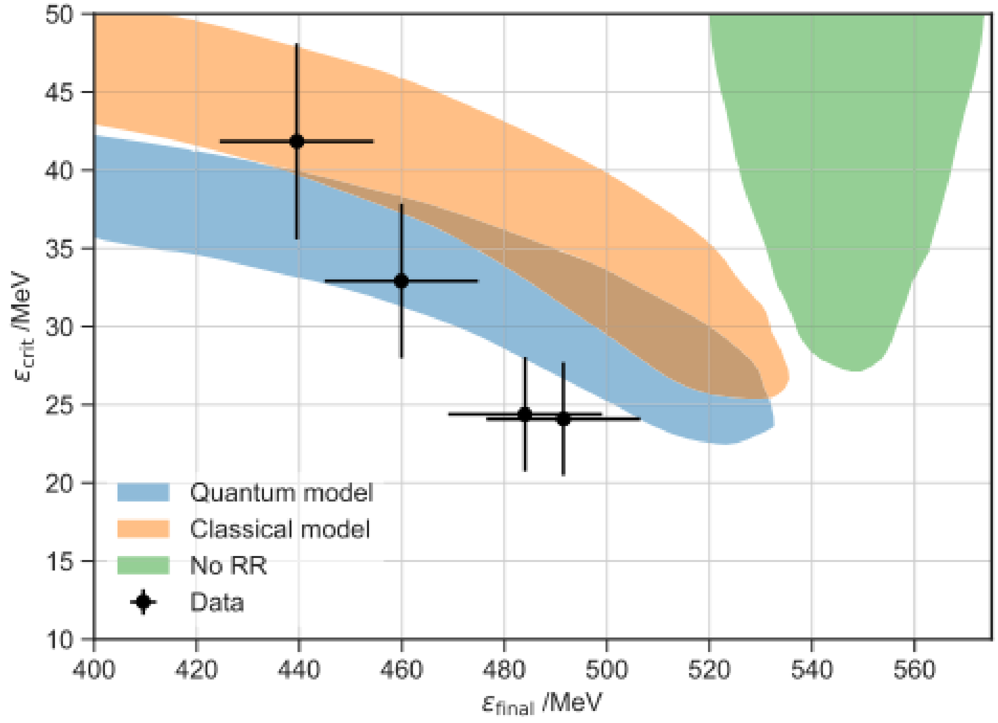

1. Cole, J. M. *et al.* Experimental Evidence of Radiation Reaction in the Collision of a High-Intensity Laser Pulse with a Laser-Wakefield Accelerated Electron Beam. *Phys. Rev. X* **8,** 11020 (2018).